THE TEMPERATURE DEPENDENCE OF THE ELECTRO-OPTIC KERR EFFECT IN SOLUTIONS

JOHN HENRY ROBSON BSc MSc

A THESIS SUBMITTED FOR THE DEGREE OF

DOCTOR OF PHILOSOPHY

THE UNIVERSITY OF ASTON IN BIRMINGHAM

OCT 1993

THE UNIVERSITY OF ASTON IN BIRMINGHAM

THE TEMPERATURE DEPENDENCE OF THE ELECTRO-OPTIC KERR EFFECT IN SOLUTIONS

A thesis submitted for the degree of Doctor of philosophy

by

JOHN HENRY ROBSON OCT 1993

SUMMARY

A novel Kerr cell of greater optical path length and temperature stability has been designed and built. The Kerr effect experimental has been substantially automated using an Apple IIe computer. Software has been written allowing the computer to partially control the Kerr effect equipment and to acquire and analyse the relevant data.

The temperature dependent electro-optic Kerr effect of 2-methyl-4-nitroaniline, p-nitroaniline, nitrobenzene, aniline, and toluene as solutions in 1,4-dioxane has been studied. The Kerr effect measurements combined with dipole moment, depolarisation ratio, dielectric, and electronic polarisation measurements have been used to calculate the first hyperpolarisability of the solute.

Although first hyperpolarisabilities for the compounds studied have been measured in various physical states using a variety of experimental techniques, it is gratifying to find that the values presented in this thesis have a linear relationship with values reported by other workers.

KEY WORDS : POLARISABILITY, 2-METHYL-4-NITROANILINE HYPERPOLARISABILITY,

To my girl friend Kim Read and especially to my Mum and Dad

ACKNOWLEDGEMENTS

I would like to express my thanks and gratitude to my supervisor, Dr. Martin S. Beevers for his help and support throughout this project.

My thanks are also extended to; Mr. R. Wheeler for his helpful suggestions and patience during the construction of the new Kerr cell, and to Mr David Bleby for the alteration and repair of various electrical equipment.

Finally I would like to especially thank my parents for their financial support and encouragement, and my girl friend Kim Read for putting up with me continually talking about my PhD course.

LIST OF CONTENTS

LIST OF FIGURES

LIST OF TABLES

CHAPTER 1

INTRODUCTION

1.1 INTRODUCTION.

When light passes through a medium the oscillating electric field, E, of the radiation polarises the material and induces an oscillating electric dipole in the material's molecules. For most materials the induced dipole per unit volume, P, is linearly proportional to the applied field, such that

$$P = \varepsilon_o \chi_1 E \qquad 1.1$$

where χ is the linear electric susceptibility and ε_o is the permittivity of free space. Non-linear optical responses are only possible for materials in which the non-zero second order or higher order electric susceptibilities, χ_2, χ_3,... contribute to the electric polarisability, P, where

$$P = \varepsilon_o \left(\chi_1 E + \chi_2 EE + \chi_3 EEE + ...\right) \qquad 1.2$$

The odd terms (χ_1 etc.) contribute to the polarisation of all materials, but the even coefficients only contribute if the material lacks a centre of symmetry. Non-zero even

order susceptibilities are only possible in crystals having a non-centrosymmetric space group and in liquids and gases whose molecules are non-centrosymmetric and have been partially oriented by the application of an external electric field.

Materials that exhibit non-linear optical properties are now commonly used in a wide variety of applications such as modulating waves carrying information, amplifying signals, and to providing fast switching etc. The complete range of applications are too numerous to discuss in this introduction but a brief explanation of two of the more interesting effects caused by the non-linear susceptibilities are mentioned below.

According to standard electro-magnetic theory the electric susceptibility and the refractive index of a material are related according to

$$n^2 = 1 + \chi \qquad 1.3$$

In the linear case χ is merely equivalent to χ_1 and the refractive index of the material remains constant upon the application of an electric field. However, if we consider the non-linear terms then we find that the refractive index of the material becomes field dependent, which is the requirement for a modulator.

Another effect caused by the non-linearity, which has practical applications, but is especially important as a diagnostic tool in the study of non-linear optical materials is the phenomenon commonly referred to as

second harmonic generation (SHG). If an intense laser beam of frequency f is incident on a non-linear crystal such that the field can be represented by

$$E \sin(2\pi ft) \qquad 1.4$$

then the second term in equation 1.2 will contribute to the overall polarisation according to

$$\varepsilon_o \chi_2 E^2 \sin^2(2\pi ft) \qquad 1.5$$

Utilising the well known trigonometric formula, $\cos 2\theta = 1 - 2\sin^2\theta$, the contribution to the polarisation then becomes

$$\frac{1}{2}\varepsilon_o \chi_2 E^2 (1 - \cos 4\pi ft) \qquad 1.6$$

The cosine term represents an oscillating polarisation at double the input frequency, which emits radiation at the doubled frequency. This effect of frequency doubling is what classifies second harmonic generation. If the intensity of the incident laser beam and the intensity of the resultant laser beam emerging from the crystal at double the input frequency can be measured, it is then possible to determine the susceptibility χ_2.

Finding new and more efficient non-linear materials is currently an important area of research as the materials currently in use require electric fields of around several thousand volts per centimetre before the

non-linear contributions to the polarisation become sufficiently large to be of use. In recent years interest has switched from the development of inorganic materials for non-linear applications to organic materials, which may have as much or more to offer than the more conventional inorganic materials. In general most current non-linear optical devices consist of rugged and easily processed inorganic materials. Organic materials have so far not gained as much popularity because they are generally fragile, less easily processed and less chemically and physically stable than their inorganic counterparts. However, some organic materials are already known which have second order non-linear properties that surpass those of inorganic materials. They also possess greater chemical and physical stability in the range of operation (i.e. over 1μm) than the best inorganic materials[120-123]. It is therefore likely that as research continues organic crystals will become used extensively in non-linear optical devices.

Research into the non-linear properties of an organic material can be performed using SHG experiments on a single crystal. However, this investigative technique is prohibitive because of the cost of growing, orienting, cutting, and polishing crystals of sufficient purity. Further, the analyses of the crystalline experiments requires an x-ray structural determination to obtain the magnitude and the absolute sign of the molecular non-linearity.

As the crystal properties of a molecular solid reflect primarily a combination of the molecular contributions, then if the molecular basis for the non-linear behaviour can be defined, materials with substantially greater non-linear properties can be predicted by quantum mechanical calculations or by chemical intuition.

At the molecular level the non-linear contribution to a material comes from the molecular dipole moment, μ, induced by the local electric field, according to

$$\mu = \alpha E + \beta EE + \gamma EEE + \ldots\ldots \qquad 1.7$$

where α, β, and γ are tensor quantities normally referred to as the polarisability, first hyperpolarisability, and second hyperpolarisability respectively; α, β, and γ are analogous to the bulk susceptibilities, χ_1, χ_2, χ_3. The crystal polarisation is then the sum of the molecular contributions moderated by contributions from the crystal structure. However, the molecular contributions dominate and so a material with a high value of β in the liquid or gas phase should in its solid phase have a high χ_2 value, provided that a non-centrosymmetric structure results.

This allows the first hyperpolarisability of a material to be determined by measuring the intensity of the second harmonic generation from a solution in which the molecules have been partly oriented (to produce an overall non-centrosymmetric distribution) by an electric field. SHG experiments can provide rapid and accurate

measurements on a wide range of molecules and in this way it is possible to screen potential materials for sufficiently high non-linear properties before a crystal of the material is grown. There are several reviews on the subject[1,2,3,4,5,6,7,35] of SHG theory and experiments that cover the above more than adequately.

Another method of determining the hyperpolarisability coefficients of a material is through the temperature dependence of the electro-optic Kerr effect. This method is technically simpler than SHG experiments and has the benefit of determining other molecular parameters. The absolute sign of the first hyperpolarisability is also determined directly from Kerr measurements whereas the squared term, β^2, is determined from SHG experiments.

The Kerr effect was first discovered in 1875 by John Kerr[8] who noticed that double refraction or birefringence could be induced in glass by the application of a sufficiently intense electric field. Kerr established that the magnitude of the birefringence δ depended on the electric field strength E and the length L of the optical path through the field by the relation

$$\delta = 2\pi BLE^2 = 2\pi L(n_p - n_s) / \lambda \qquad 1.8$$

where $n_{||}$ and $n_{\perp}$ are the refractive indices for the components of the light in the medium parallel and perpendicular to the field, and λ is the appropriate wave-length. B is commonly referred to as the "Kerr constant" of the substance under examination. Another

more commonly used quantity denoting the magnitude of the Kerr effect is the molar Kerr constant. This quantity was introduced by Otterbein, in analogy with the molar polarisation, to express the electrically induced optical birefringence by an additive quantity that is independent of concentration for single compounds.

The theory of the Kerr Effect was effectively developed over several years starting in 1910 with a paper written by Langevin[9] and then extended by Born[10] (1918), Peterlin and Stuart (1939)[11], and Stuart (1939)[12], on the basis of an orientation mechanism of the particles under the influence of the external electric field, through their permanent or induced dipole moment. The fundamental statements on the theory of electric birefringence, excluding non-linear effects, are concisely expressed by the formulae derived from the Langevin-Born orientation theory. The Kerr effect has been the subject of several reviews concerned with liquids (Le Fèvre and Le Fèvre 1955[13], 1960[14]; Smith 1960[15]), polymers (Peterlin and Stuart 1953[16]; Volkenstein 1963[17]; O'Konski 1968[18]) and proteins (Yoshioka and Watanabe 1969[19]).

The Langevin-born orientation theory allows birefringence measurements combined with light scattering, refractive index, and dielectric constant measurements to characterise the polarisability tensors of the molecules[20]. This led to the deduction of bond polarisabilities that can be used (assuming additivity[21,22]) to predict the polarisability tensors of

new molecules and their conformations. On the microscopic level the observed Kerr effect (i.e. Double refraction or Birefringence) in molecules is due to three distinct effects, discussed below.

(i) In a finite field the interaction between the electric field and the dipole moment (permanent or induced) will distort the orientationally averaged spatial correlation's of the molecules. This yields spatial anisotropy which therefore results in the medium becoming birefringent.

(ii) The polarisability of the molecules may already be anisotropic, such that in the presence of an electric field the axis parallel to the direction of maximum polarisability will tend to align itself in the direction of the electric field.

(iii) The electrostriction effect causes the fluid density to increase with increasing field strength, which increases the susceptibility of the fluid. This is only present when electric fields are applied to the medium at low frequencies because at optical frequencies the macroscopic motion of the medium cannot follow such frequencies.

In 1955 Buckingham extended the Langevin-Born orientation theory to include the distortion effects that can be seen in the molecular polarisability at high field strengths. This distortion is, as already mentioned, commonly referred to as the hyperpolarisability. It is a matter of debate whether the hyperpolarisability coefficients that contribute to the

molar Kerr constant are equivalent to the SHG coefficients. However, B.J Orr[23] concluded that for optical frequencies far from resonance, as is the case in this project, the hyperpolarisability contributions to both the molar Kerr constant and the SHG should be approximately equal.

As the Langevin-Born theory is only strictly applicable to gases at very low pressures much of the early work in the Kerr effect was done in the gaseous form at atmospheric pressure. This faced researchers with the basic problem that the Kerr effect in gases and vapours at atmospheric pressures is comparatively small and hard to determine. At higher pressures the molar Kerr constant is larger and therefore easier to determine but analysing the results is complicated by the molecular interactions that occur at higher densities. To circumvent this problem, it is possible, as suggested by Buckingham, to develop the molar Kerr constant as a series in the density. Thus, if measurements of the molar Kerr constant are taken over a series of pressures (up to several hundred atmospheres) the results can be extrapolated back to zero pressure[24-27] to obtain a value for the molar Kerr constant that should be equivalent to the dilute gas value. Using this extrapolation technique a lot of the early work concerning the Kerr effect was carried out on simple molecules such as substituted methane's, but as researchers turned their attention to larger molecules the temperatures involved to vaporise

these molecules made measurements of the Kerr effect in the gaseous form prohibitive.

Attention then turned to the measurement of molecules, particularly the aromatic species such as benzene and substituted benzene's, as solutes in non-dipole solvents, usually at 298 K. The analysis of such results is however seriously complicated by the effects of solute-solvent and solute-solute interactions[28] and lack of information as to the precise relationship between the optical and static polarisability tensor.

In an attempt to compensate for the solvent effect, birefringence measurements are conducted over a series of solute concentrations and then extrapolated back to what is known as the infinite dilution molar Kerr constant. This extrapolation can be accomplished in much the same way as apparently first devised by Briegleb[29] and followed by Stuart and Volkmann[30], Otterbein[31], Sachsse[32], and Friedrich[33] or by a more direct method devised by Le Fèvre and Le Fèvre[13]. The expression for the infinite dilution molar Kerr constant is identical to the corresponding expression for the dilute gas except for the use of *effective* values of μ, α, and β instead of those for the isolated molecule. This makes it possible to determine the coefficients of the molar Kerr constant from dilute solution data using the same methodology as applied to low pressure gases.

In 1921 Gans[34,38] suggested a method in which the static polarisability could effectively be removed from the Langevin-Born orientation theory. Gans' theory

although working well for some molecules proved to be totally inaccurate for others. Le Fèvre achieved the same end as Gans by assuming that the ratios of the polarisability tensors (atomic and electronic) are equal to P_D/P_E. Where P_D is the dispersion polarisation and P_E is the electronic polarisation.

By making observations of the birefringence in molecules over a range of temperatures it is possible to separate the temperature coefficients that contribute to the molar Kerr constant. These temperature coefficients combined with measurements of dipole moments, molar refraction and depolarised Rayleigh scattering allow the polarisability and hyperpolarisability coefficients of the material to be determined. Measurement of the temperature dependence of the Kerr effect in gases and vapours has, over the past few decades, provided fairly accurate polarisability anisotropies and Kerr hyperpolarisabilities for several small molecules (particularly substituted methane's). However, since the arrival of the laser the Kerr effect method of determining the hyperpolarisability has not proved as popular as the SHG method for larger molecules in solution.

One of the simplest ways in which an organic molecule can have a large optical non-linearity is by possessing a conjugated system of bonds that lead to a strong π-electron de-localisation. Whereas the linear polarisability increases as the cube of the length of the conjugation[124], the higher order polarisabilities increase

even faster[120,125]. The de-localisation of the π-electrons can be further enhanced by the addition of donor and acceptor groups at opposite ends of the conjugated system. The strong charge transfer between such groups operating across the entire extended system markedly adds to the optical non-linearity of the structure[126].

The aim of this project is to investigate the hyperpolarisability properties of a benzene ring containing donor groups conjugated with electron attracting groups through primarily the temperature dependence of the electro-optic Kerr effect in solutions. If this experimental method proves successful it is hoped, ultimately, that this will allow selection criteria or a bond addivity model to be used when designing materials for non-linear applications. As already mentioned it is essential that the molecule is able to crystallise in a structure lacking a centre of inversion, for all components of the second-order hyperpolarisability χ vanish for a centrosymmetric crystal. However, crystallisation of a molecule into a noncentrosymmetric structure can be achieved by attaching to it a suitable substituents that causes steric hindrance[122,127].

A major part of the work undertaken in the project was the design and manufacture of the equipment necessary to make accurate electro-optic Kerr effect measurements over a range of temperature. The most significant part of this work was the design and manufacture of a longer optical path length, temperature stabilised, Kerr cell.

Much of the Kerr effect measurement process was automated using an Apple IIe computer and a stepper motor to rotate the analyser during the measurement of the birefringence. The computer can control the application of a square-wave voltage across the Kerr cell, record and then analyse the resultant optical signals for known orientations of the analyser. In this way it is hoped that Kerr constant measurements would be obtained to a higher degree of accuracy than previously possible. All the electro-optic data aquired for dilute solutions employed 1,4-dioxane as the solvent. As the latter freezes at 11.8^{o}C and boils at 101^{o}C temperature dependence measurements of the molar Kerr constant were conducted over the temperature range 15-70^{o}C in 5^{o}C intervals.

CHAPTER 2

THE KERR EFFECT

2.1 INTRODUCTION

This chapter is primarily concerned with the theory of linear polarisation, the concept of the principal axes of polarisation and the relationship between polarisability and the induced dipole moment. The orientation of a molecule upon the application of an electric field is discussed in terms of the induced and permanent dipole moments. The orientation of a molecule by an electric field is the basis of the Langevin-Born orientation theory used to describe the magnitude of the Kerr effect. The linear Kerr effect is then described using the Langevin-Born theory and is later extended to include the hyperpolarisability terms proposed by Buckingham[36]. The means by which the hyperpolarisability coefficients can be separated from the molar Kerr constant are then discussed for the ideal gas situation followed by a description of the extrapolation techniques to obtain the infinite dilution molar Kerr constant - analysed using the techniques employed for low pressure gases. Finally, the reader is introduced to the bond-addivity model for molecular hyperpolarisabilities

proposed by Buckingham. The frequency dependence of the Kerr effect is also discussed.

2.2 MOLAR POLARISATION (THE POLARISABILITY α)

When a molecule is subjected to an electric field there is a small displacement of electrical centres which induces a dipole in the molecule. The difference between the dipole moment before and during the application of an electric field E_o is called the induced dipole moment μ. If there is a net increase in the dipole moment during the application of an electric field E_o then the molecule is said to be polarisable.

In most cases polarisable molecules are polarised linearly, that is, the induced moment μ is proportional to E_o. In such a case we have

$$\mu = \alpha.E_o \qquad 2.1$$

where α is the polarisability of the molecule and is either electro-static or electro-optic.

However this is only the case when the molecule is completely spherical. Generally the molecule is elliptical and the induced dipole moment μ does not have the same direction as the applied field E_o. In this case it is necessary to use a polarisability tensor α, such that

$$\begin{bmatrix} \mu_x \\ \mu_y \\ \mu_z \end{bmatrix} = \begin{bmatrix} \alpha_{11} & \alpha_{12} & \alpha_{13} \\ \alpha_{21} & \alpha_{22} & \alpha_{23} \\ \alpha_{31} & \alpha_{32} & \alpha_{33} \end{bmatrix} . \begin{bmatrix} E_{ox} \\ E_{oy} \\ E_{oz} \end{bmatrix} \qquad 2.2$$

However, it is more convenient to write equation 2.2 in the form

$$\underline{\mu} = \underline{\alpha} . \underline{E}_o \qquad 2.3$$

If a Cartesian co-ordinate system (x,y,z) is chosen with its axes in the direction of the principal axes (1,2,3) of the ellipse of polarisability then the polarisability tensor will be in diagonalised form:

$$\underline{\alpha}_{principal-axes} = \begin{bmatrix} \alpha_1 & 0 & 0 \\ 0 & \alpha_2 & 0 \\ 0 & 0 & \alpha_3 \end{bmatrix} \qquad 2.4$$

Since in all cases where the external field acts at an angle to 1,2 or 3 the induced dipole moment will itself lie at an angle to the field direction, it is then easy to understand why non-polar molecules tend to align themselves with their axis of greatest polarisability parallel to the field. Since permanent molecular dipole moments are about 10^5 times greater than induced moments, the orientative action of a field on a polar molecule is overwhelmingly controlled by the disposition of the resultant moment in the molecular structure.

2.3 LINEAR KERR EFFECT THEORY

In 1910 Langevin[9] assumed that the orientation of a molecule by the induced dipole of a molecule (when it is subjected to an electric field) resulted in an electrostatic and optical anisotropy in the molecule. Born[10] in 1918 extended the theory of Langevin to include the effect of an electric field to molecules which posses a possible permanent electric doublet. It is therefore necessary to consider both the Langevin and Born hypothesis for the orientation of polar molecules.

The Langevin-Born orientation theory expresses the Kerr constant, *B*, by the formula (in e.s.u.)

$$B = \pi N_m \left(n^2 + 2\right)^2 (\varepsilon + 2)^2 (\theta_1 + \theta_2) \Big/ 27 n \lambda \qquad 2.5$$

where, N_m, is the number of molecules cm^{-3}, ε the static dielectric constant, θ_1 the so called anisotropy term, and θ_2 the so called dipole term. The terms θ_1 and θ_2 are expanded as

$$\theta_1 = (1/45kT)\left[(a_1 - a_2)(\alpha_1 - \alpha_2) + (a_2 - a_3)(\alpha_2 - \alpha_3) + (a_3 - a_1)(\alpha_3 - \alpha_1)\right] \qquad 2.6$$

and

$$\theta_2 = \left(1/45k^2T^2\right)\left[\left(\mu_1^2 - \mu_2^2\right)(\alpha_1 - \alpha_2) + \left(\mu_2^2 - \mu_3^2\right)(\alpha_2 - \alpha_3) + \left(\mu_3^2 - \mu_1^2\right)(\alpha_3 - \alpha_1)\right] \qquad 2.7$$

A full formal treatment of equation 2.5 is given by Le Fèvre and Le Fèvre[13] in a review paper written in 1955.

In 1921 Gans[37,38,39] suggested that the electrostatic polarisabilities (a_1, a_2, and a_3) and the electro-optic polarisabilities (α_1, α_2, and α_3) are related by

$$a_1/\alpha_1 = a_2/\alpha_2 = a_3/\alpha_3 = \frac{(\varepsilon - 1)}{(n^2 - 1)} \qquad 2.8$$

thus allowing the static polarisability tensor to be removed from equation equation 2.7. Le Fèvre and Le Fèvre[13] have achieved the same end by assuming

$$\underline{a}_i/\underline{\alpha}_i = P_D/P_E \qquad 2.9$$

where P_D and P_E are the distortion and electronic polarisation respectively. Similarly, if we make the approximation

$$\alpha_1/a_1 = \alpha_2/a_2 = \alpha_3/a_3 = \alpha/a \qquad 2.10$$

where

$$a = \frac{1}{3}(a_1 + a_2 + a_3) \qquad 2.11$$

and

$$\alpha = \frac{1}{3}(\alpha_1 + \alpha_2 + \alpha_3) \qquad 2.12$$

Then, if we define an anisotropy parameter δ by

$$\delta_a^2 = \left[(a_1 - a)^2 + (a_2 - a)^2 + (a_3 - a)^2\right]/6a^2 \qquad 2.13$$

and

$$\delta_\alpha^2 = \left[(\alpha_1 - \alpha)^2 + (\alpha_2 - \alpha)^2 + (\alpha_3 - \alpha)^2\right]/6\alpha^2 \qquad 2.14$$

Using the assumption made in equation 2.10 one then has $\delta_a^2 = \delta_\alpha^2 = \delta^2$ and equation 2.6 reduces to

$$\theta_1 = \frac{18}{45kT}\delta^2 a\alpha \qquad 2.15$$

The approximation on which equation 2.15 is based is rather arbitary, since there is no *a priori* reason why the components of the atomic polarisability $\underline{a}$ should be proportional to those of the electronic polarisability. Infrared absorption calculations have shown that for many molecules the ratio between the components of $\underline{a}$ may differ widely from that for $\underline{\alpha}$, and in some cases with $\underline{\alpha}_{||} > \underline{\alpha}_{\perp}$ one nevertheless has $\underline{a}_{||} < \underline{a}_{\perp}$ (where $||$ and $\perp$ refer to the components of the polarisation parallel and perpendicular to the applied electric field). This means that instead of the approximation mentioned, one can also make the approximation that, $\underline{a}$, is isotropic[91] yielding:

$$\theta_1 = \frac{18}{45kT}\delta_\alpha^2\alpha^2 \qquad 2.16$$

It is worth noting that equation 2.16 holds exactly when the electric field inducing the birefringence is of optical frequency.

Otterbein[31] in analogy with the molar polarisation $[_mP]$, expressed the electrically induced optical birefringence by an additive quantity that is independent of concentration for single compounds. This expression for the magnitude of the optical birefringence is known as the molar Kerr constant, denoted by $_mK$ and defined by

$$_mK = \frac{6nN_m}{(n^2+2)^2(\varepsilon+2)^2} \operatorname{Lim}_{E\to 0} \frac{n_p - n_s}{E^2} \qquad 2.17$$

$$= \frac{6\lambda nBM}{(n^2+2)^2(\varepsilon+2)^2 d} \qquad 2.18$$

where M is the molecular weight, n the refractive index, ε the dielectric constant, d the density of the medium, and λ the wave-length of the light used to determine B. Stuart[40] defines the molar Kerr constant differently, i.e., smaller by a factor six according to equation 2.18. The physical significance of $_mK$ may be regarded as the difference between the molecular refraction per unit field taken parallel and perpendicular to the direction of the applied field E.

Inherent in equation 2.18 is the classical assumption that the effective macroscopic local field acting on a molecule when in an external field, E, is given by the relation[41]

$$E = 3E_o/(\varepsilon + 2) \qquad 2.19$$

Technically equation 2.18 lacks a factor of 9 on the RHS of the equation which arises from the local field approximation shown in equation 2.19. However as the local field approximation is uncertain some workers[29,30] have taken ${}_mK$ as one-sixth that shown in equation 2.18, only few other workers have included the multiplication factor of 9. In general most workers[31,32,42,43] have preferred to express ${}_mK$ as that shown in equation 2.18 and that practice will be continued throughout this thesis.

An alternative approach would have been to use the Onsager cavity theory for the local field instead of the Lorentz theory i.e.

$$E = (2\varepsilon + 1)E_o/3\varepsilon \qquad 2.20$$

The difference in the results obtained from using either equation 2.19 or equation 2.20 have (for dilute solutions of a solute in a non-polar solvent) generally proved indistinguishable for many workers[44]. However the same cannot be said for pure polar solvents. When dealing with a polar liquid it is then necessary to consider the Onsager field model for polar liquids[45].

2.4 NON-LINEAR KERR EFFECT THEORY

According to the Langevin-Born orientation theory molecules which are spherically symmetric and non polar should not become birefringent in the presence of an electric field. However experimental evidence confirmed that these molecules did exhibit a small but distinct birefringence.

The unexpected Kerr constant for spherically symmetric molecules led Buckingham[36] in 1955 to extend the Langevin-Born orientation theory to include the distortion effects seen in the molecular polarisability at high field strengths. This distortion is commonly referred to as the hyperpolarizability and results in the induced dipole moment of a molecules in an electric field being no longer directly proportional to the applied electric field. A full mathematical derivation of Buckingham and Pople's modification to the Langevin-Born orientation theory can be seen in reference 36. Here, it is only necessary to state that the modified equation for ${}_{m}K$ was derived by Buckingham and Pople in the limit of low densities for a uniform electric field, E, neglecting dispersion, electronic and vibration states of the molecule and molecular interactions. The modified equation in SI units using Cartesian tensor suffix notation[46] is defined by

$$ {}_mK = \frac{N}{910\varepsilon_o}\left\{2\gamma_{\alpha\alpha\beta\beta} + \frac{1}{kT}\left[4\mu_\alpha^{(0)}\beta_{\alpha\beta\beta} + 3\left(a_{\alpha\beta}\alpha_{\alpha\beta} - 3a\alpha\right)\right] + \frac{1}{k^2T^2}\left[\alpha_{\alpha\beta}\mu_\alpha^{(0)}\mu_\beta^{(0)} - \alpha\left(\mu^{(0)}\right)^2\right]\right\} \qquad 2.21 $$

where ε_o is the permittivity of free space, N is Avogadro's number and k is the Boltzmann factor. Equation 2.21 is therefore only strictly applicable to low density gases/vapours, but good agreement with equation 2.21 can be obtained for measurements of ${}_mK$ for solutes that are extrapolated to infinite dilution in non polar solvents[47], either directly or by the method described by Le Fèvre and Le Fèvre[13] or by Buckingham[48] (See Section 2.6). It is worth noting that the hyperpolarisabilities under consideration only describe the influence exerted on the electronic polarisability by a static field and do not consider contributions due to atomic polarisation.

2.5 DISCUSSION OF THE VARIOUS ELEMENTS CONTRIBUTING TO THE MOLAR KERR EFFECT EQUATION

The molecular Kerr constant ${}_mK$ consists of four terms: a part dependent on T^{-1} that is solely due to the anisotropy of the polarisability, a part dependent on T^{-2} due to the orientation of the anisotropic molecules by the permanent dipoles, a part dependent on T^{-1} due to the orientation of the first hyperpolarizability by the dipole, and a temperature independent part that is due to the second

hyperpolarizability. These parts will be denoted by $[K_1]$, $[K_2]$, $[K_3]$, and $[K_4]$, respectively, where

$$ {}_mK = [K_1] + [K_2] + [K_3] + [K_4] \qquad 2.22 $$

If the axes of the molecular co-ordinate system are chosen to be co-directional to the principal axes of the polarisability tensor then the term $[K_1]$ is, according to equation 2.21, given by (SI)

$$ \begin{aligned} [K_1] &= \frac{N}{270kT\varepsilon_0}\left(a_{\alpha\beta}\alpha_{\alpha\beta} - 3a\alpha\right) \\ &= \frac{N}{910kT\varepsilon_0}\left[(a_1 - a_2)(\alpha_1 - \alpha_2) + (a_2 - a_3)(\alpha_2 - \alpha_3)\right. \\ &\qquad \left. +(a_3 - a_1)(\alpha_3 - \alpha_1)\right] \end{aligned} \qquad 2.23 $$

By using the anisotropy parameter, δ, defined by equation 2.14 and the same assumption made to simplify equation 2.6 to equation 2.16, then equation 2.23 may be rewritten as

$$ [K_1] = \frac{N}{45kT\varepsilon_0}\delta_\alpha^2\alpha^2 \qquad 2.24 $$

Term $[K_2]$, which is due to the orientation of the anisotropic polarisabilities by the permanent dipoles, is, according to equation 2.21, given by

$$ [K_2] = \frac{N}{270k^2T^2\varepsilon_0}\left[\alpha_{\alpha\beta}\mu_\alpha^{(0)}\mu_\beta^{(0)} - \alpha\left(\mu^{(0)}\right)^2\right] \qquad 2.25 $$

which can be rewritten as

$$[K_2] = \frac{N}{910k^2T^2\varepsilon_0}\left[\left(\mu_1^2 - \mu_2^2\right)(\alpha_1 - \alpha_2) + \left(\mu_2^2 - \mu_3^2\right)(\alpha_2 - \alpha_3) + \left(\mu_3^2 - \mu_1^2\right)(\alpha_3 - \alpha_1)\right] \qquad 2.26$$

where the molecular co-ordinate system is again taken to be coincident with the principal axes of polarisability. For molecules where the dipole is along one of these axes, which by convention is then taken as the z-axis, equation 2.26 reduces to

$$[K_2] = \frac{N\mu^2}{270k^2T^2\varepsilon_0}(\alpha_3 - \alpha) \qquad 2.27$$

For symmetric top molecules this can also be written as:

$$[K_2] = \frac{N\mu^2}{90k^2T^2\varepsilon_0}\alpha\delta_\alpha \qquad 2.28$$

For the $[K_3]$ term the z-axis of the molecular co-ordinate system is generally chosen so that it lies along the direction of the permanent dipole moment and is therefore independent of the principal axes of the polarisability. $[K_3]$ is then given by

$$[K_3] = \frac{N}{910kT\varepsilon_0}\left[4\mu^{(0)}\beta_{\alpha\beta\beta}\right] = \frac{2N\mu}{405kT\varepsilon_0}(\beta_{113} + \beta_{223} + \beta_{333}) \qquad 2.29$$

Following Buckingham[47] a mean first hyperpolarizability can be defined by

$$\beta = \frac{3}{5}(\beta_{113} + \beta_{223} + \beta_{333}) \qquad 2.30$$

and a first hyperpolarizability anisotropy by

$$\Delta\beta = \beta_{333} - \frac{3}{2}(\beta_{113} + \beta_{223}) \qquad 2.31$$

equation 2.29 can then be rewritten as

$$[K_3] = \frac{2N\mu\beta}{243kT\varepsilon_0} \qquad 2.32$$

Finally, the term $[K_4]$ is considered. According to equation 2.21 $[K_4]$ is defined by

$$[K_4] = \frac{2N}{910\varepsilon_0}\gamma_{\alpha\alpha\beta\beta} \qquad 2.33$$

Again it is generally more convenient and customary to define a mean second hyperpolarizability using the nomenclature of Buckingham[47]. Thus

$$\begin{aligned}\gamma &= \frac{1}{5}\gamma_{\alpha\alpha\beta\beta} \\ &= \frac{1}{5}(\gamma_{1111} + \gamma_{2222} + \gamma_{3333} + 2\gamma_{1122} + 2\gamma_{2233} + 2\gamma_{3311})\end{aligned} \qquad 2.34$$

which also permits equation 2.33 to be rewritten as

$$[K_4] = \frac{N}{405\varepsilon_0}\gamma \qquad 2.35$$

2.6 INFINITE DILUTION MOLAR KERR CONSTANT, ${}_{\infty}K_2$

As already mentioned above, equation 2.21 for the molar Kerr constant, ${}_{m}K$, is only strictly applicable to low density gases/vapours. Generally, equation 2.21 may not be satisfactorily used to determine ${}_{m}K$ for a solute. Instead the molar Kerr constant of a solution, ${}_{m}K_{12}$, is determined from experimental measurement of Kerr constant, B_{12}, refractive index, n_{12}, dielectric constant, ε_{12}, and density, d_{12}. The subscripts 1,2, and 12 indicate solvent, solute, and solution respectively. The molar Kerr constant of the solute can then be determined using the colligative relationship

$${}_{m}K_{12} = {}_{m}K_1 f_1 + {}_{m}K_2 f_2 \qquad 2.36$$

where f_1 and f_2 are expressed as molar fractions and it is assumed that ${}_{m}K_1$, the molar Kerr constant of the solvent, is independent of f_1. Values of ${}_{m}K_2$ calculated in this way usually show a marked variation with f_2 and therefore need to be extrapolated to infinite dilution (i.e. ${}_{\infty}K_2$). This can be accomplished by plotting ${}_{m}K_2$ against f_2 and taking the intercept with the y-axis as the value of ${}_{\infty}K_2$ or by using the expression[49]

$$ {}_{\infty}K_2 = {}_{m}K_1 + \left(\frac{\partial C}{\partial f_2} {}_{m}K_{12} \right)_{f_2 = 0} \qquad 2.37 $$

However, Le Fèvre and Le Fèvre proposed that the application of equation 2.37 caused uncertain estimates in ${}_{m}K_2$. This was not surprising as every ${}_{m}K_2$ value depends on the independent measurement of (B, ε, n, and d) the errors in which can combine unpredictably to affect the value of ${}_{m}K_2$. Le Fèvre and Le Fèvre therefore devised a method in which the individual observations were smoothed and the ${}_{\infty}K_2$ was then directly calculated. The argument used followed that for dielectric polarisation (i.e. the following equations were assumed to apply at high dilution)

$$ \begin{aligned} \varepsilon_{12} &= \varepsilon_1(1 + \alpha\omega_2) \\ d_{12} &= d_1(1 + \beta\omega_2) \\ n_{12} &= n_1(1 + \gamma\omega_2) \\ B_{12} &= B_1(1 + \delta\omega_2) \end{aligned} \qquad 2.38 $$

where ω_2 is the concentration expressed as the weight fraction of solute. Occasionally B_{12}, ε_{12}, and d_{12} do not show a linear relationship with ω_2. In such an instance measurements are fitted to an equation of the type

$$ (B_{12} - B_1) = (\text{first constant})\omega_2 + (\text{second constant})\omega_2^2 $$

where

$$ \delta B_1 = \text{first constant} \qquad 2.39 $$

The infinite dilution molar Kerr constant, ${}_{\infty}K_2$, is then derived from

$$ {}_{\infty}K_2 = \left(1 - \beta + \gamma + \delta - H\gamma - J\alpha\varepsilon_1\right){}_{s}K_1M_2 \qquad 2.40 $$

where, ${}_{s}K_1$ is the specific Kerr constant of the solvent, defined by

$$ {}_{s}K_1 = \frac{6\lambda n_1 B_1}{\left(n_1^2 + 2\right)^2\left(\varepsilon_1 + 2\right)^2 d_1} \qquad 2.41 $$

where

$$ H = 4n_1^2/\left(n_1^2 + 2\right) \qquad 2.42 $$

and

$$ J = 2/\left(\varepsilon_1 + 2\right) \qquad 2.43 $$

The quantities H, J, and ${}_{s}K_1$ are constants for the chosen solvent at a particular temperature.

With the introduction of the infinite dilution molar Kerr constant expressions for $[K_1]$, $[K_2]$, and $[K_3]$ are obtained which are identical to the corresponding expressions for the dilute gas except for the use of *effective* values of μ, α, and β instead of those for the isolated molecules. This makes it possible to analyse values of ${}_{\infty}K_2$ in the same way as for dilute gases. The use of effective values for μ, α, and β requires that measurements of the dipole moment, molar refraction and

Rayleigh depolarisation ratio are calculated from dilute solution data and not from data obtained for the low density gas.

2.7 RESOLVING THE EXPERIMENTAL VALUES OF $_{\infty}K_2$ INTO $[K_1]$, $[K_2]$, $[K_3]$, AND $[K_4]$

Molecular symmetry can greatly simplify the constituents making up the molecular Kerr constant[50]; however for polar molecules with low symmetry it is necessary to employ more than one technique in solving for the components of $_{\infty}K_2$. In general the measurements of the depolarisation ratio of Raleigh light scattering, dipole moment, and the electronic polarisation are required.

Simplification of equation 2.21 because of the presence of symmetry, is particularly significant for spherical-top molecules, where the dipole moment, μ, and the anisotropy parameter, δ, are equal and zero due to spherical, tetrahedral, or octahedral symmetry. Thus, it can be seen from equation 2.21 that for spherical-top molecules the only term left in $_{\infty}K_2$ is $[K_4]$ and therefore the value of γ can be determined from direct measurements of the Kerr effect. In general, values of γ are about 10^{-35} e.s.u.

For non-polar molecules possessing lower degrees of symmetry to those just discussed, $[K_2]$ and $[K_3]$ are equal and zero. It is therefore necessary to separate the

values of $[K_1]$ and $[K_4]$, which can be accomplished by taking Kerr effect measurements over a wide range of temperature. According to equation 2.21 if ${}_{\infty}K_2$ is plotted as a function of 1/T then $[K_4]$ can be determined from the intersection of the straight line with the axis and $[K_1]$ can be determined from the gradient. Then, from equation 2.35, γ can be calculated. An alternative to the temperature analyses of ${}_{\infty}K_2$ employed in the determination of γ is to utilise depolarisation Raleigh scattering and electronic polarisation which enables $[K_1]$ to be calculated directly. Also subtraction of $[K_1]$ from ${}_{\infty}K_2$ yields $[K_4]$ and therefore γ.

For polar molecules, with low degrees of symmetry, the splitting of ${}_{\infty}K_2$ into its coefficients is extremely difficult, but should be possible by combining temperature analysis of the Kerr effect, depolarisation ratio of Rayleigh light scattering, and electronic polarisation. For symmetric top molecules $[K_1]$ and $[K_2]$ can be calculated from equations 2.24 and 2.28. A plot of ${}_{\infty}K_2-[K_1]T-[K_2]T^2$ against 1/T should, according to theory, result in a straight line. The mean second hyperpolarizability, γ, can then be calculated from the intersection of the straight line the ordinate axis and the first hyperpolarizability, β, from the gradient of the line. For molecules of lower symmetry it is theoretically possible to plot ${}_{\infty}K_2$ against 1/T and to fit the corresponding curve to a polynomial of degree three and thus determine the coefficients making up ${}_{\infty}K_2$. However, due to the number of experimental techniques

involved in calculating ${}_{\infty}K_2$ and the large extrapolations involving $(1/T)\rightarrow 0$, this method is often extremely inaccurate. It is therefore more common to either ignore the second order hyperpolarisability entirely or to use a value determined from the low density gas or to use a value calculated using bond additivity techniques. Thus, if $T\left({}_{\infty}K_2 - [K_4]\right)$ is plotted against 1/T the first hyperpolarisability can be determined from the intersection of the resulting straight line and $[K_1]$ from the gradient of the line.

2.8 BOND ADDITIVITY APPROXIMATION

Since a bond-additivity scheme for molecular polarisability is already well established it would seem to be reasonable and advantageous to develop an analogous approximation for hyperpolarisabilities. Following Buckingham[47], the approximation for β for a molecule with N bonds can be written as

$$\beta_{\alpha\beta\gamma} = \sum_{i=1}^{N} \beta^{(i)}_{\alpha\beta\gamma} \qquad 2.44$$

If the ith bond is symmetric about its axis, $\beta^{(i)}_{\alpha\beta\gamma}$ can be expressed in terms of its mean and its anisotropy

$$\beta^{(i)}_{\alpha\beta\gamma} = \left(\frac{1}{3}\beta^{(i)} - \frac{1}{5}\Delta\beta^{(i)}\right)\left(l^{(i)}_{\alpha}\delta_{\beta\gamma} + l^{(i)}_{\beta}\delta_{\gamma\alpha} + l^{(i)}_{\gamma}\delta_{\alpha\beta}\right) \qquad 2.45$$

$$+ \Delta\beta^{(i)} l^{(i)}_{\alpha} l^{(i)}_{\beta} l^{(i)}_{\gamma}$$

$$\beta^{(i)}_{\alpha\beta\gamma} = \left(\frac{1}{3}\beta^{(i)} - \frac{1}{5}\Delta\beta^{(i)}\right)\left(l^{(i)}_{\alpha}\delta_{\beta\gamma} + l^{(i)}_{\beta}\delta_{\gamma\alpha} + l^{(i)}_{\gamma}\delta_{\alpha\beta}\right) \qquad 2.45$$

$$+ \Delta\beta^{(i)} l^{(i)}_{\alpha} l^{(i)}_{\beta} l^{(i)}_{\gamma}$$

where $l^{(i)}_{\alpha}$ is the cosine of the angle between the axis of the ith bond and the α-direction. The kronecker delta $\delta_{\alpha\beta}$ is unity if $\alpha=\beta$ and is zero otherwise.

Since γ is independent of the bond directions the second order hyperpolarizability of a molecule is a straight addition of the second hyperpolarizability of each bond making up the molecule.

In the above bond additivity approximation[47], all components of the first hyperpolarizability tensor β of an arbitrary molecule can be obtained from the mean first hyperpolarisabilities and the first hyperpolarizability anisotropies of the bonds by adequate linear superposition using the bond angles involved. This bond additivity approximation has limited uses particularly for molecules that have highly polar bonds, as the model proposed by Buckingham ignores induced dipole moments caused by bond-bond interactions. The effect of bond-bond interactions is particularly considerable for halogenated methane's and therefore the bond additivity approximation proposed by Buckingham gives only moderate results for these molecules. However an interacting segment model (I.S.M.)[51,52] has proved fairly successful in providing a bond additivity model for the halogenated methane's that takes into account bond-bond interactions. Additional information about the components of the first

hyperpolarizability tensor, β, can be obtained from second-harmonic light-scattering (S.H.L.S.)[53]. Results obtained from S.H.L.S. have indicated that in many cases $\Delta\beta << \beta$[54,55], thus

$$\beta_{333} \approx \frac{3}{2}(\beta_{113} + \beta_{223}) \approx \beta \qquad 2.46$$

2.9 FREQUENCY DEPENDENCE OF THE KERR CONSTANT, B

In section 2.39 the equation for the evaluation of the molar Kerr constant of a solute at infinite dilution developed by Le Fèvre and Le Fèvre was introduced. Equations 2.47 and 2.48 which expand ${}_sK_1$ and H, show that these quantities, and therefore ${}_\infty K_2$, must in some way depend on the wavelength

$$({}_sK_1)_\lambda = \frac{6\lambda n_\lambda B_\lambda}{\left(n_\lambda^2 + 2\right)^2 (\varepsilon + 2)^2 d_1} \qquad 2.47$$

$$H_\lambda = 4n_\lambda^2 \Big/ \left(n_\lambda^2 + 2\right) \qquad 2.48$$

In the literature there is little experimental results describing the wavelength dependence of the Kerr effect. However, there are a number of relationships between B_λ and λ, and the refractive index, n_λ. The oldest of these relationship's (equation 2.49) is due to Havelock,[56]; others are equation 2.50 by Quarles[57], and equation 2.51 by Powers[58].

$$B_\lambda = h\left(n_\lambda^2 - 1\right)^2 / \lambda n_\lambda \qquad 2.49$$

$$B_\lambda = k\left(n_\lambda^2 - 1\right)\left(n_\lambda^2 + 2\right) / \lambda n_\lambda \qquad 2.50$$

$$B_\lambda = K\left(n_\lambda^2 + 2\right)^2 / \lambda n_\lambda \qquad 2.51$$

where h, k, and K are constants determined at a particular wavelength. Equations 2.49, 2.50, and 2.51 do not consider inflections or discontinuities in the B_λ-λ relationship as λ approaches or becomes an absorption wavelength. However, the formulae of the Drude or Sellmeier[59] type avoid this problem.

Le Fèvre and Solomons[60] have reported some experimental investigations concerning the wavelength dependence of the Kerr constant for benzene and carbon tetrachloride. Their results indicate a slight preference for the use of equation 2.49 by Havelock when extrapolating the Kerr constant over wavelength for benzene and carbon tetrachloride.

CHAPTER 3

MEASUREMENT OF THE EXPERIMENTAL KERR CONSTANT, B

3.1 INTRODUCTION

This study involves the measurement of a number of experimentally observable quantities, using various physical techniques; the most important of these being the Kerr constant, B. All measurements of the Kerr constant used in this thesis were made using the nulled intensity method[65], which involves applying short duration electric fields across the Kerr cell. This technique reduces the effect of electrophoresis, conductivity, electrode polarisation and heating effects that hindered earlier studies of the Kerr effect that used a.c. or d.c. electric field methods.

Much of the necessary equipment required to measure the Kerr constant had previously been assembled by other researchers, and was mostly suitable for the experiments carried out in this thesis. However, to obtain more accurate results than was currently possible some parts of the apparatus were altered or completely replaced. In particular a new large optical path length (15cm) Kerr cell was designed and built with a sample volume of $\approx 30cm^3$.

The major part of this chapter is concerned with the experimental technique used for the measurement of the Kerr constant along with a description of the equipment used and designed for that purpose. The preparation of the solutions used and the Kerr constant results obtained are also presented.

3.2 KERR EFFECT EQUIPMENT

A diagram of the apparatus used to measure the electrically induced phase difference, δ, is shown in Figure 3.1. All the optical components were mounted on a two metre length of optical bench enclosed in a light-proof cabinet. A plane-polarised beam of monochromatic light is passed through the Kerr cell polarised at 45^{o} to the direction of the applied pulsed electric field, E. The light emerging from the Kerr cell is then passed through a quarter wave retarder, oriented with its principal optic axis at 45^{o} to the Kerr cell electrodes and the direction of the applied field. The light then passes through a polariser (analyser) which can be rotated via a stepper motor and a series of gears. The intensity of the light passing through this polariser is then detected by a photomultiplier. The output of the photomultiplier is connected to a transient recorder which in turn is connected to an oscilloscope and an Apple II computer, using an Xcalibur VIA board. In this way the electrically induced optical pulse can be

effectively displayed and analysed by the computer. The voltage applied across the Kerr cell was monitored using a Tektronix probe (model P6013A) which attenuated the voltage by a factor of approximately 10^3. The voltage from the probe could then be measured using a Thurlby (1503-HA) digital multimeter.

3.2.1 Light source

A plane-polarised beam of monochromatic light was generated by a Spectra Physics helium/neon laser emitting at a wavelength of 632.8nm and with a power rating of 5mW. The laser was polarised at 45° relative to its direction of propagation and was mounted on the optical bench such that the beam of light propagated parallel to the bench. The beam of light produced by the laser had a working diameter of 1mm, therefore the electrode separation in the Kerr cell was set to just over 1mm to allow the light beam to pass unhindered through the cell.

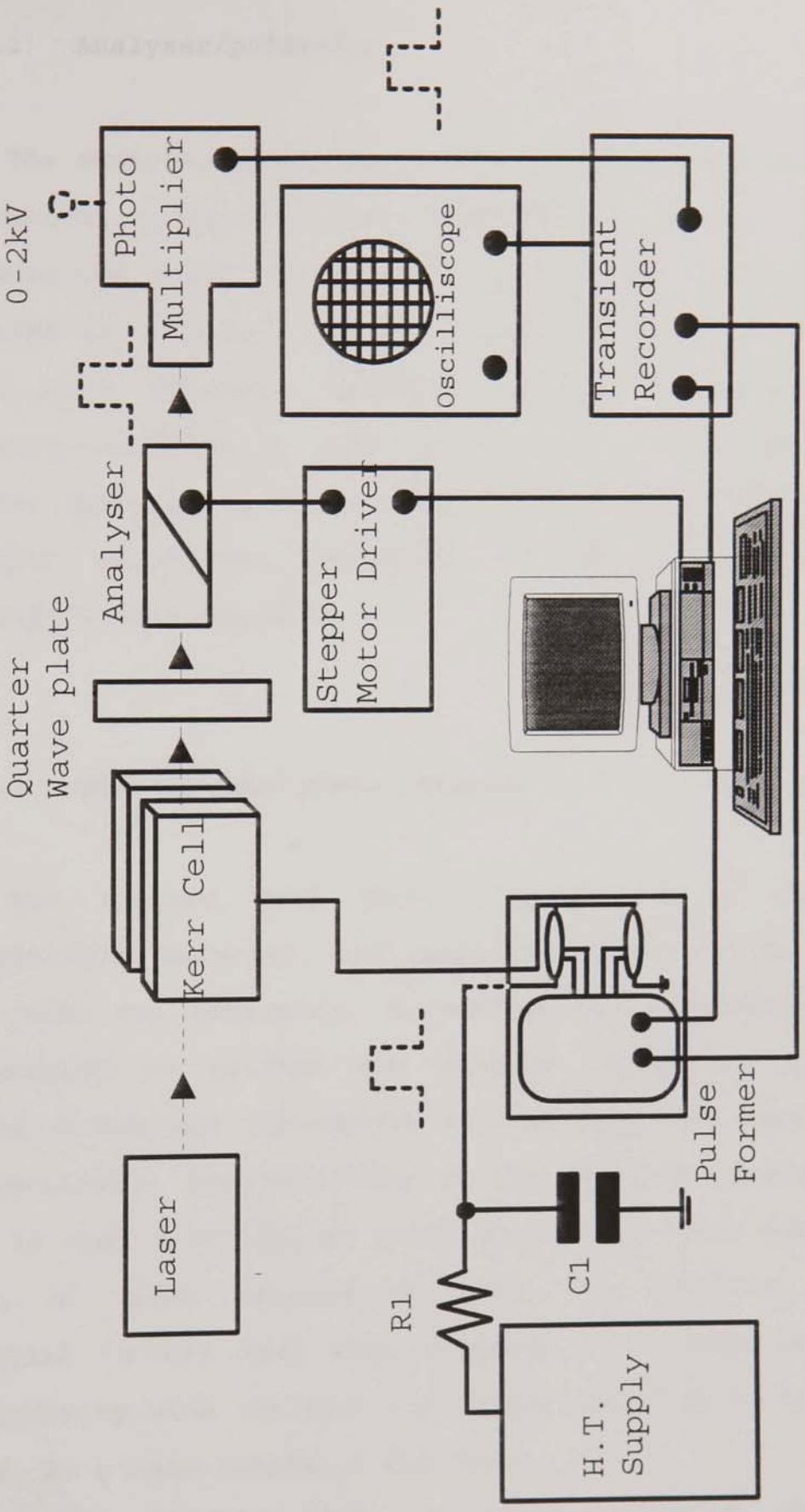

Figure 3.1 Kerr effect equipment

3.2.2 Analyser/polariser

The analyser in Figure 3.1 was a Glan-Thompson double refraction polariser of commercial origin. It was constructed from two calcite prisms glued together and mounted in a hollow brass cylinder. The brass tube was held in a rotatable graduated circle, which could be rotated clockwise or anti-clockwise via a set of gears, either manually or by a stepper motor. Each step of the stepper motor was equivalent to moving the analyser through 0.0045 degrees.

3.2.3 Quarter-wave plate retarder

The quarter wave plate consists of a disc of birefringent material, and therefore, there exists within the disk two orthogonal directions of propagation that correspond to maximum and minimum refractive indices. These directions correspond to the slow and fast axes, respectively. The thickness of the disk is specifically cut so that a 90° degree phase shift will occur between a beam of light propagating with its electric vector parallel to the fast axes compared to a beam of light propagating with its electric vector parallel to the slow axes, at a wave-length of 632.8nm.

If an incident beam of plane polarised light is incident on the disk such that its electric vector propagates parallel to either the fast or slow axis of

the disk, then there will be no effect on the beams polarisation. However, if the incident beam is elliptically polarised then the emerging beam will be converted into plane polarised light.

The advantages of using a quarter wave plate in the optical arrangement has been emphasised by several authors (O'Konski and Haltner 1956[62]; Houssier and Fredericq 1966[63]): it gives a greater sensitivity than without the plate; it enables the sign of the birefringence to be determined, and it allows higher accuracy in the measurement of relaxation times.

3.2.4 Positioning the optical axes of the quarter-wave plate.

The Kerr cell was filled with HPLC grade toluene and the quarter-wave plate was removed from the equipment set-up shown in Figure 3.1. The polariser was then crossed with respect to the polarisation of the laser beam, such that the intensity of light reaching the photo-multiplier was at a minimum. When the retarder was re-introduced a light-signal was detected by the photomultiplier. This light signal is then extinguished by rotating the quarter-wave plate. It is possible for the quarter-wave plate to extinguish the light when either the slow or fast axis of the plate is at 45° to the applied electric field. Toluene has a positive Kerr effect and if this is to correspond to a positive

rotation of the analyser in order to null the birefringent optical square wave pulse the slow axis of the retarder must be at 45° to the applied electric field. Therefore to check that the retarder is correctly oriented a square wave electric field is applied across the Kerr cell and it is checked that a positive (clockwise) rotation of the analyser does indeed null the optical signal.

3.2.5 Photomultiplier

The electrical configuration of the electrodes of the photomultiplier tube (E.M.I 9816B) are set for high gain usage. The gain and/or smoothing of the photomultiplier output can be adjusted by two switches that vary the resistance and capacitance (and therefore the time constant) of the output circuit. The photomultiplier was mounted in a brass tube that had a 20mm aperture near the window of the photomultiplier. Interference from stray light was minimised by the addition of a collimating aluminium barrel, 80mm long, with a 2mm diameter aperture placed in front of the aperture. The HT driving potential was supplied by a Brandenberg model 472B generator that could be varied between 0 and -2kV. In general the operating driving potential applied to the photomultiplier was constantly adjusted so that the output from the photomultiplier never exceeded two volts. This was considered to be the upper output voltage of the

photomultiplier before saturation of the photomultiplier tube occurred.

3.3 EQUIPMENT DESIGN AND MODIFICATIONS

It can be seen from Chapter 2 that the first hyperpolarisability β is determined from the y-intercept of a plot of $[_{\infty}K_2]T - [K_4]T$ against $1/T$. The experimental values of β reported in the literature have, in general, large standard errors associated with them. These errors are mainly due to the small variation of $_{\infty}K_2$ with temperature and the range of measurable temperatures involved in the extrapolation of T^{-1} to zero required to compute β. Therefore to reduce the errors involved in determining β, measurements of the temperature dependence of the Kerr constant, B, must be obtained as accurately as possible. Three main approaches were taken in an attempt to obtain Kerr constant measurements of sufficient accuracy. These approaches can be characterised by

1) Modifications of the high voltage pulse former[64] to provide high quality square wave pulses up to 10kV. The equipment was previously only capable of producing square wave pulses up to 5kV before multiple triggering of the pulse former occurred and/or arcing of the high voltage lines to ground.

2) Computer aided control of the measurement and the analyses of the Kerr effect.

3) The design and building of a new Kerr cell that had a longer optical path length and improved temperature stability.

3.3.1 Modifications to the high voltage pulse former

As the birefringence induced in the molecules of a sample increases as E^2 (see equation 1.8) a doubling of the electric field will increase the resultant birefringence by a factor of four. The electric field produced between the electrodes in a Kerr cell is determined from

$$E = V/d \qquad 3.1$$

where V is the voltage and d is the distance between the electrodes. Therefore, it can be seen from equation 1.8 and equation 3.1 that even a small increase in the pulse voltage can provide more accurate birefringence measurements by increasing the signal to noise ratio.

The circuit diagram of the high voltage pulse former used by S.Mumby[64] is shown in Figure 3.2. The schematic diagram of how the high voltage pulse former produces the high voltage pulse that is applied across the Kerr cell

is shown in Figure 3.3. The complete description of how the circuit operates can also be found in reference 64.

The maximum voltage that the high voltage generator in Figure 3.1 was capable of producing was 10kV. Unfortunately the quality of the pulse produced by the H.T. pulse former became seriously degraded at voltages approaching 5kV. These degradations in the pulse took the form of

1) Multiple pulse triggering,
2) h.t. tracking,
3) shortened pulse widths,
4) noise spikes, and
5) decay of the H.T. voltage over the pulse width.

According to the parts list in Table 3.1 the value of the resistor R10 is 820kΩ. However, on inspection of the circuit board it was found that a section of the circuit had been incorrectly constructed and that the value of R10 was in fact 100kΩ. As the product of R10 and C9 determine the upper limit to the H.T. pulse width it can be seen that the upper limit was in fact 1ms instead of 8.2ms as expected. The removal and subsequent replacement of resistor R10 with a 820kΩ resistor permitted the circuit to provide H.T. pulses with duration up to 8.2ms.

Investigation of the 15V supply line in Figure 3.2 showed that as the reed switches closed the current drawn by the switches was such that the capacitors C12 and C13 could not maintain the supply voltage at 15V.

also the reference voltage for IC1, IC2, and IC3 it was considered that the drop in the supply voltage, combined with noise spikes on the trigger lines, might be responsible for multiple triggering. The capacitors C12 and C13 where consequently increased to the current 5700μF and decoupling capacitors (10nF) where placed on all the trigger inputs to the monostable 555s'

To reduce H.T. sparking and electromagnetic radiation all exposed H.T. wires where wrapped in Teflon tape and the copper mesh on all coaxial connection cables were stripped down to at least 1cm from the exposed H.T. wire.

It was found that the reed switches in Figure 3.1 and Figure 3.2 instead of closing directly on the application of a magnetic field, "bounced" before closing. This "bouncing" produced high voltage spikes on the trailing edge of the H.T. pulse. To reduce these spikes the current limiting resistor R1 shown in Figure 3.2 was reduced to 11.1kΩ.

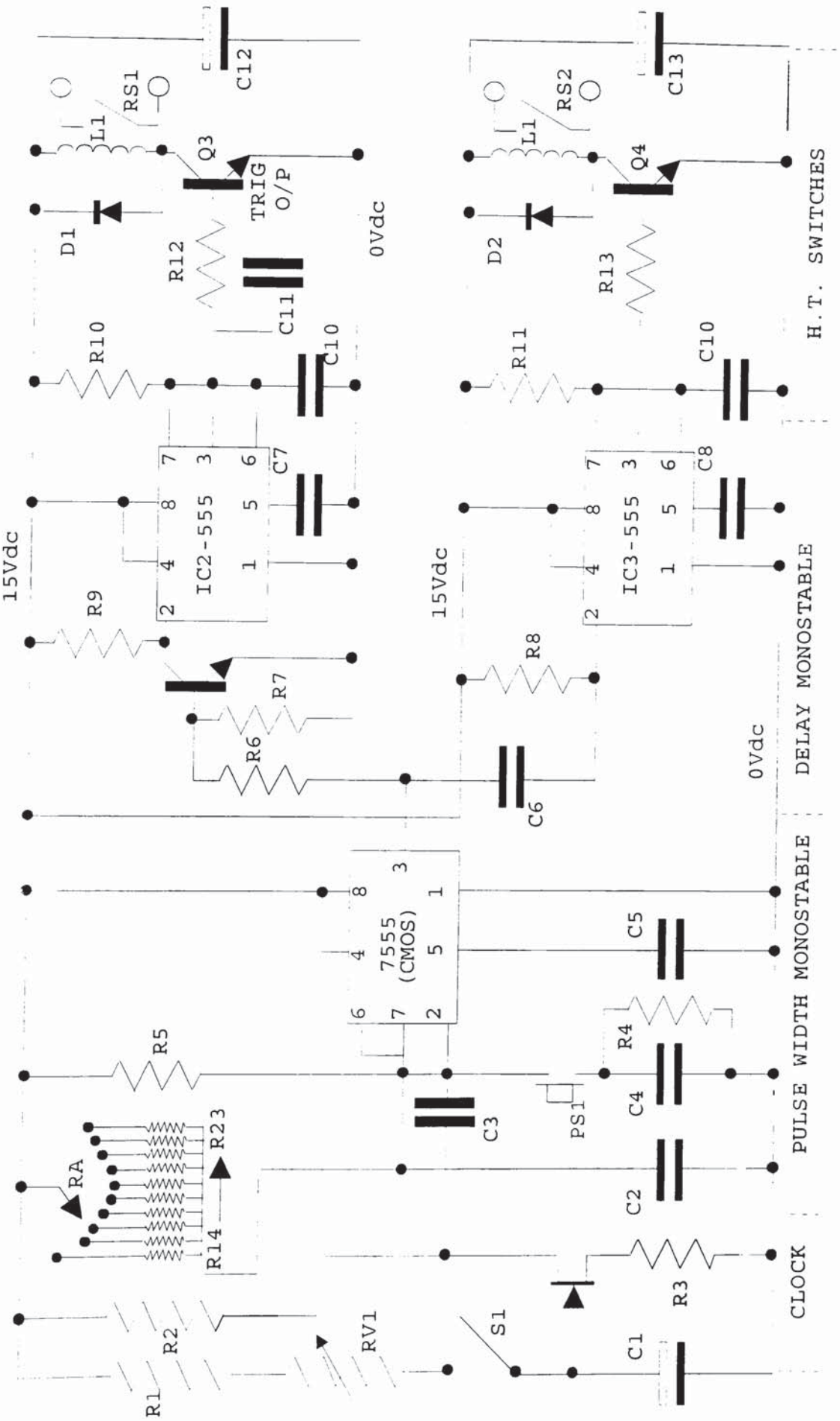

Figure 3.2 Circuit diagram of the H.T. pulse former

Table 3.1 Parts list for circuit shown in Figure 3.2

Resistors

R1	220kΩ
R2	2.2kΩ
R3	10Ω
R4	12MΩ
R5	39kΩ
R6	4.7kΩ
R8	15kΩ
R9	10kΩ
R10	820kΩ
R11	820kΩ
R12	1.0kΩ
R13	1.0kΩ
RV1	1MΩ potentiometer
RA	Twelve switched values
R14	1.0kΩ
R15	1.6kΩ
R16	4.7kΩ
R17	15kΩ
R18	39kΩ
R19	100kΩ
R20	160kΩ
R21	390kΩ
R22	1.0MΩ
R23	4.3MΩ

Capacitors

C1	1μF/25V	tantalum
C2	0.1μF	disc ceramic
C3	0.047μF	disc ceramic
C4	0.01μF	disc ceramic
C5	0.047μF	disc ceramic
C6	0.047μF	disc ceramic
C8	0.047μF	disc ceramic
C9	0.01μF	disc ceramic
C10	0.01μF	disc ceramic
C11	0.005μF	disc ceramic
C12	5700μF/25V	electrolytic
C13	5700μF/25V	electrolytic

Semiconductors

Q1	2N2646
Q2	BC108
Q3,Q4	2N3053
D1,D2	1N4001
IC1	7555CMOS
IC2,IC3	555

Switches

PS1 Press switch
RS1,RS2,DTA 812
10kv reed switches normally open,tungsten contacts

Inductances
L1,L2 90-130 ampere turns wound on P.T.F.E. former

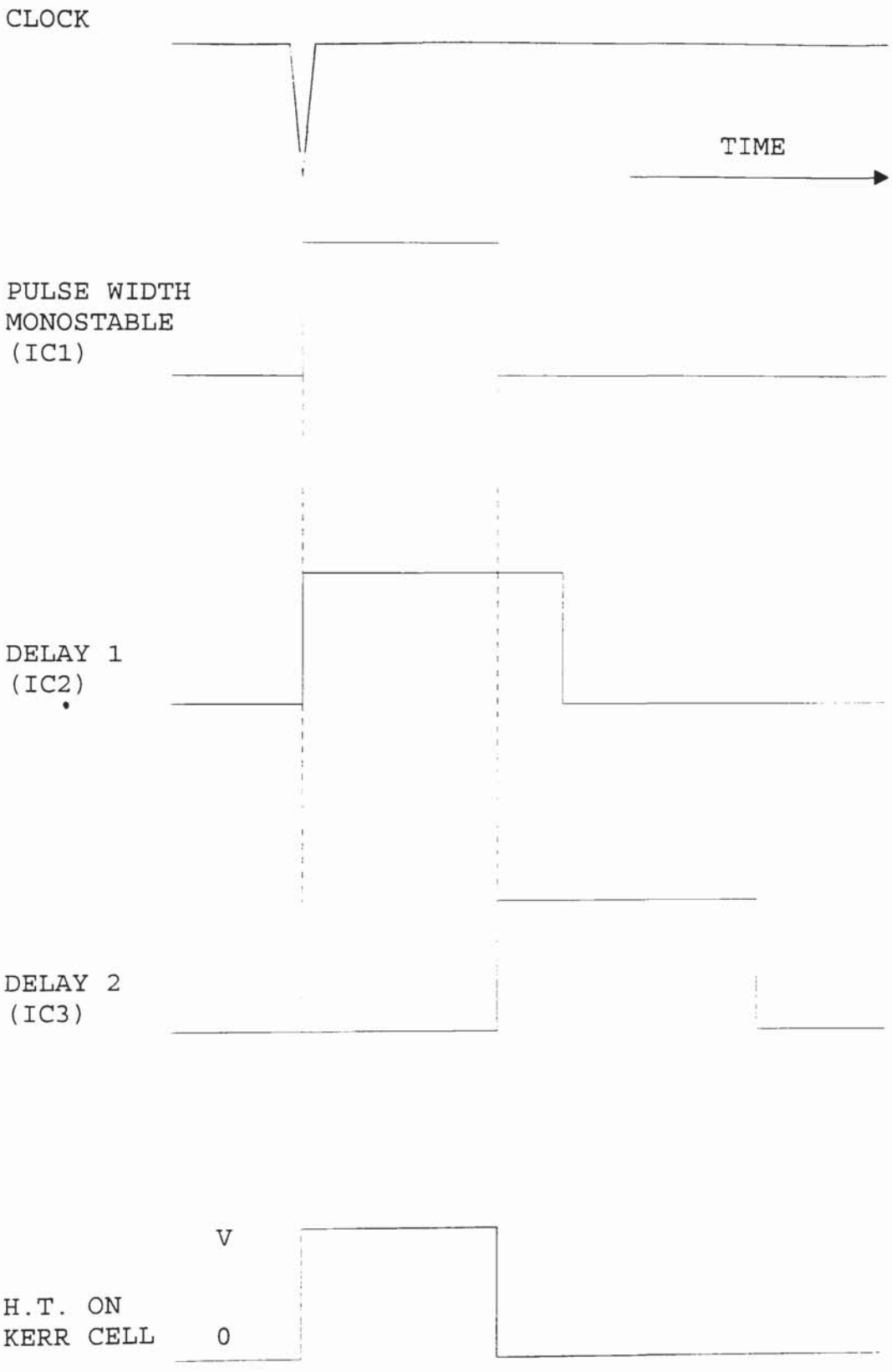

Figure 3.3 Timing diagram of the clock and three monostables in the high voltage pulse former.

.3.2 Computer connections

On the application of an electric field to the Kerr ell the pulse of light detected by the photomultiplier as recorded using a Datalab model DL905 transient ecorder. The transient recorder was triggered by the igh voltage pulse former as the electric field was pplied across the Kerr cell. The high voltage pulse ormer could be triggered either manually or by the Apple Ie computer. The triggering signal from the high voltage ulse former was arranged so that a short delay occurred etween the electric field being applied across the Kerr ell and the receipt of the optical signal. This rrangement allowed a portion of the optical baseline field-off light-level) to be recorded immediately receding the transient change in the light intensity pon the application of the electric field. The optical ignal captured by the transient recorder was displayed ontinuously on an oscilloscope that was set in the X,Y ode, the two channels acting as the X and Y inputs. The ptical signal could also be transferred to the Apple IIe omputer using an Xcalibur Via interface board and a imple machine code program. The optical signal could hen be analysed immediately or stored onto a floppy disk or later analysis. The connection from the computer to he transient recorder not only allows the transfer of he optical signal but also permits the computer to re-rm the transient recorder.

Two relay switches have been added to the interface oard that are opened and closed via the interface board nd are connected to the stepper motor driver and switch 1 (figure 3.2) of the H.T. pulse former. In this way the omputer is capable of applying an H.T. pulse to the Kerr ell, rotating the second polariser, and transferring the eceived optical signal to its memory for either mmediate analysis or to a floppy disk. The Via interface oard was inserted into slot 5 of the Apple II computer. he control commands to arm the transient recorder, otate the analyser, trigger the high voltage pulse ormer, and to transfer the received optical signal to he computer are given in Appendix A.

.3.3 Protecting the computer from the H.T.

Due to the electromagnetic radiation emitted by the .T. equipment the apple II computer had to be shielded y enclosing it in an aluminium box. Although the luminium box normally provided adequate protection, it as not sufficient to prevent the computer malfunctioning t voltages greater than 6kV. Consequently a 410Ω esistor was placed on the output of the H.T. supply reed witch to reduce the emission of electromagnetic adiation. Although the inclusion of the 410Ω resistor oes reduce the rise-time of the H.T. on the Kerr cell, : does not seriously affect the optical signal because ie rise-time (ca μs) of the H.T. is much longer than the

natural orientational relaxation times (ca 10^{-9}s) of the dipoles in the solution.

3.3.4 Stepper motor

A stepper motor has been attached to the gears and rods controlling the orientation of the analyser. This allows the analyser to be rotated clockwise/anti-clockwise in incremental steps of 0.0045 degrees, which is an improvement on the minimum rotation previously available (0.05 degrees). The stepper motor can be driven manually or by the Apple IIe computer. The use of a step motor allows partial automation of the Kerr effect equipment and significantly reduces any errors in the analyser angle due to backlash in the gear train, human limitations, and error.

3.4 NEW LONGER OPTICAL PATH LENGTH KERR CELL

3.4.1 System requirements

In order to perform accurate measurements of the Kerr constant, B, over a temperature range it was necessary to design and build a new Kerr cell which met the following requirements:

1) Good optical stability,

2) sufficiently long optical path length,

3) good temperature stability, and

4) easy to fill and empty

A considerable amount of time and experimentation went into perfecting the design of the Kerr cell. The major design changes made to the final version of the Kerr cell can be seen in section 3.2.

3.4.2 Description of the new longer optical path length Kerr cell

Shown in figures 3.4, 3.5, 3.5, and 3.6 are the diagrams for the final version of the Kerr cell. The Kerr cell consists of two tubes (one of glass and the other Perspex) with the glass tube placed inside the Perspex tube. Two Teflon end caps hold the tubes in place, see Figure 3.5 and Figure 3.7. A specially built frame consisting of aluminium plates and steel bolts ensures a seal between the glass tube and the Teflon by compressing the whole arrangement together. Compression and a silicon based sealant (Dow Corning 732 RTV) creates a seal between the Perspex tube and the Teflon. Each Teflon end cap has a hole drilled through its' centre over which is placed a high quality optical quartz disk which acts as a window. Both quartz disks were carefully selected for their freedom from strain birefringence.

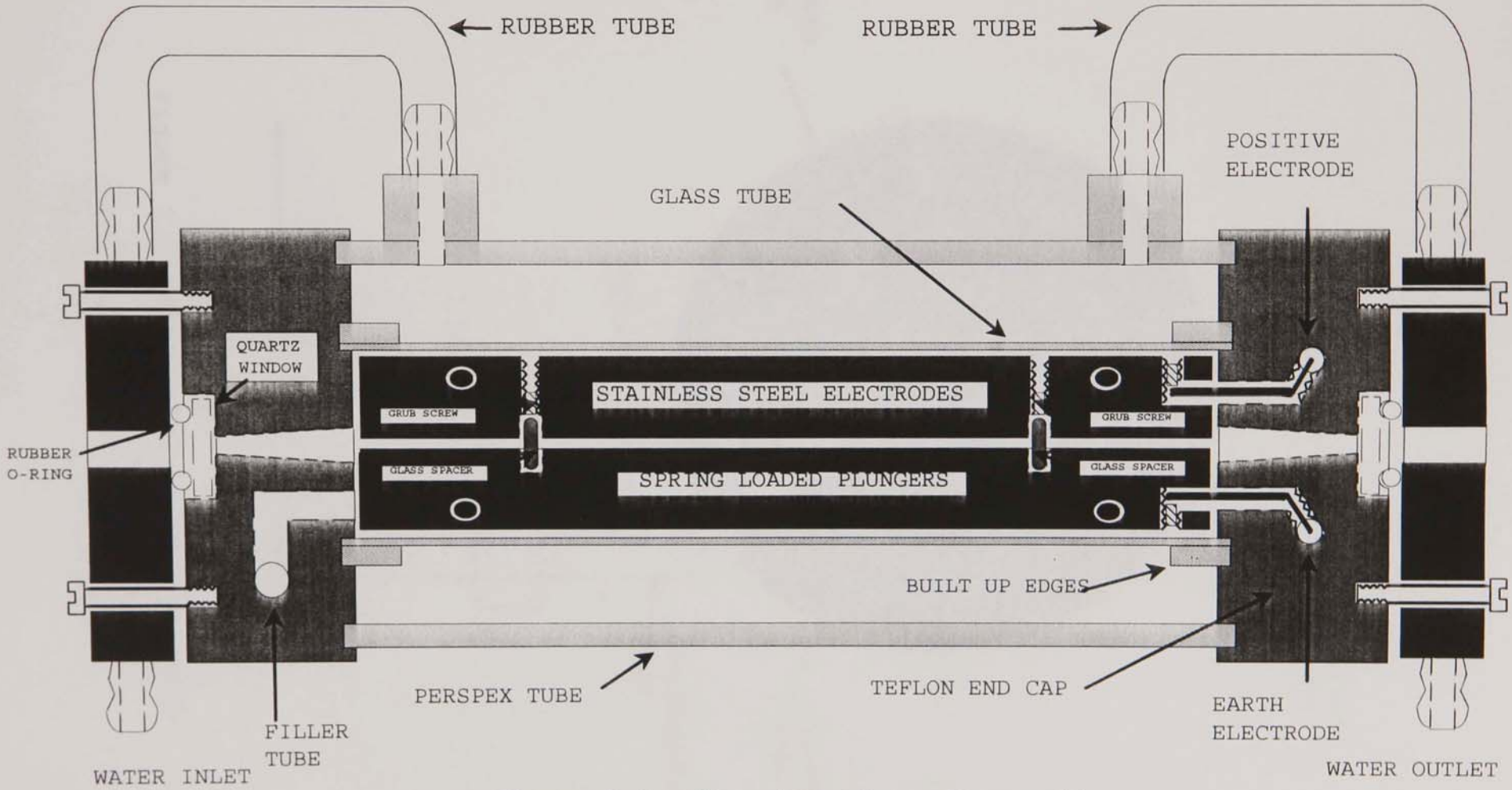

Figure 3.4 Top view of new Kerr cell

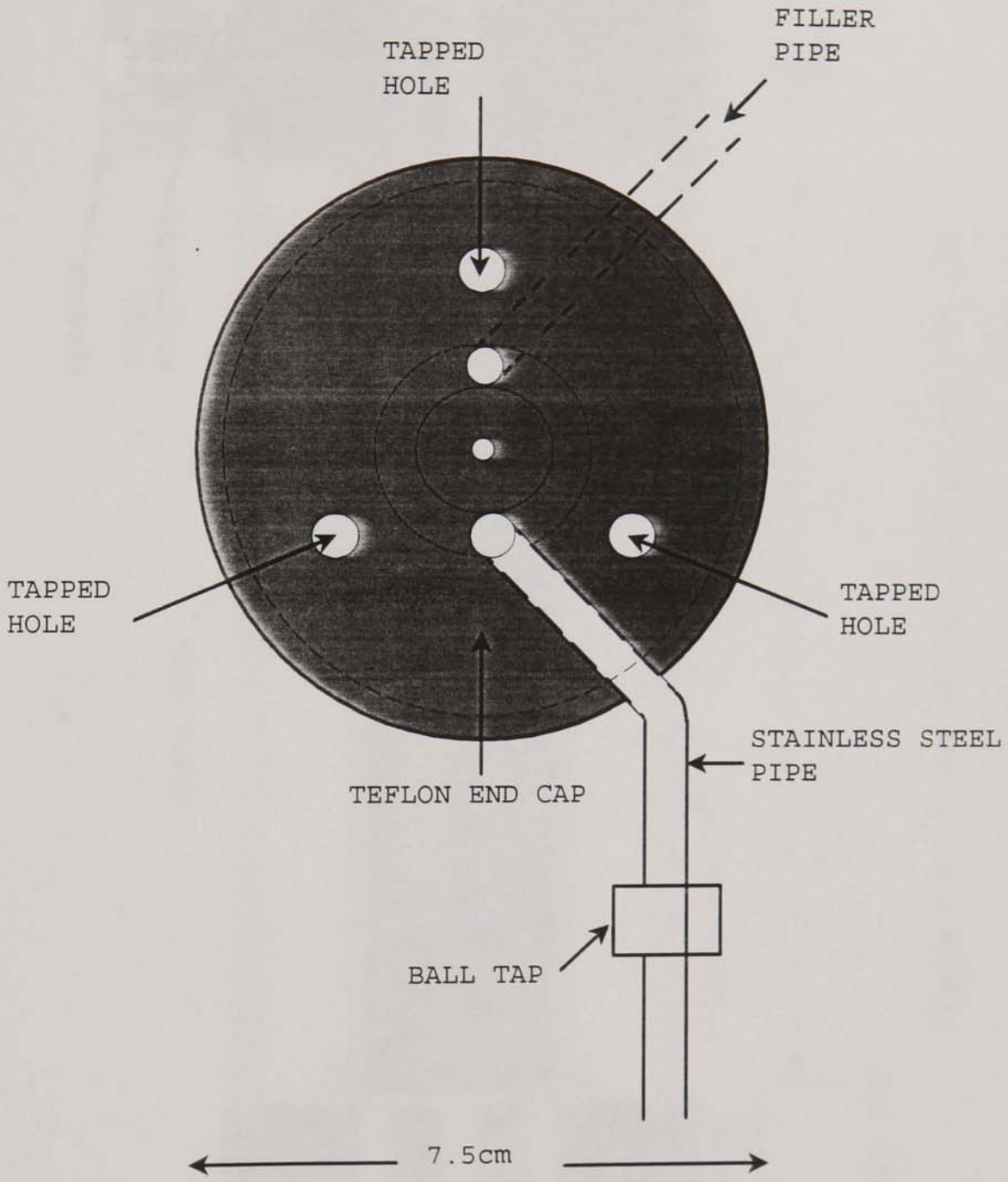

Figure 3.5 Front view of new Kerr cell

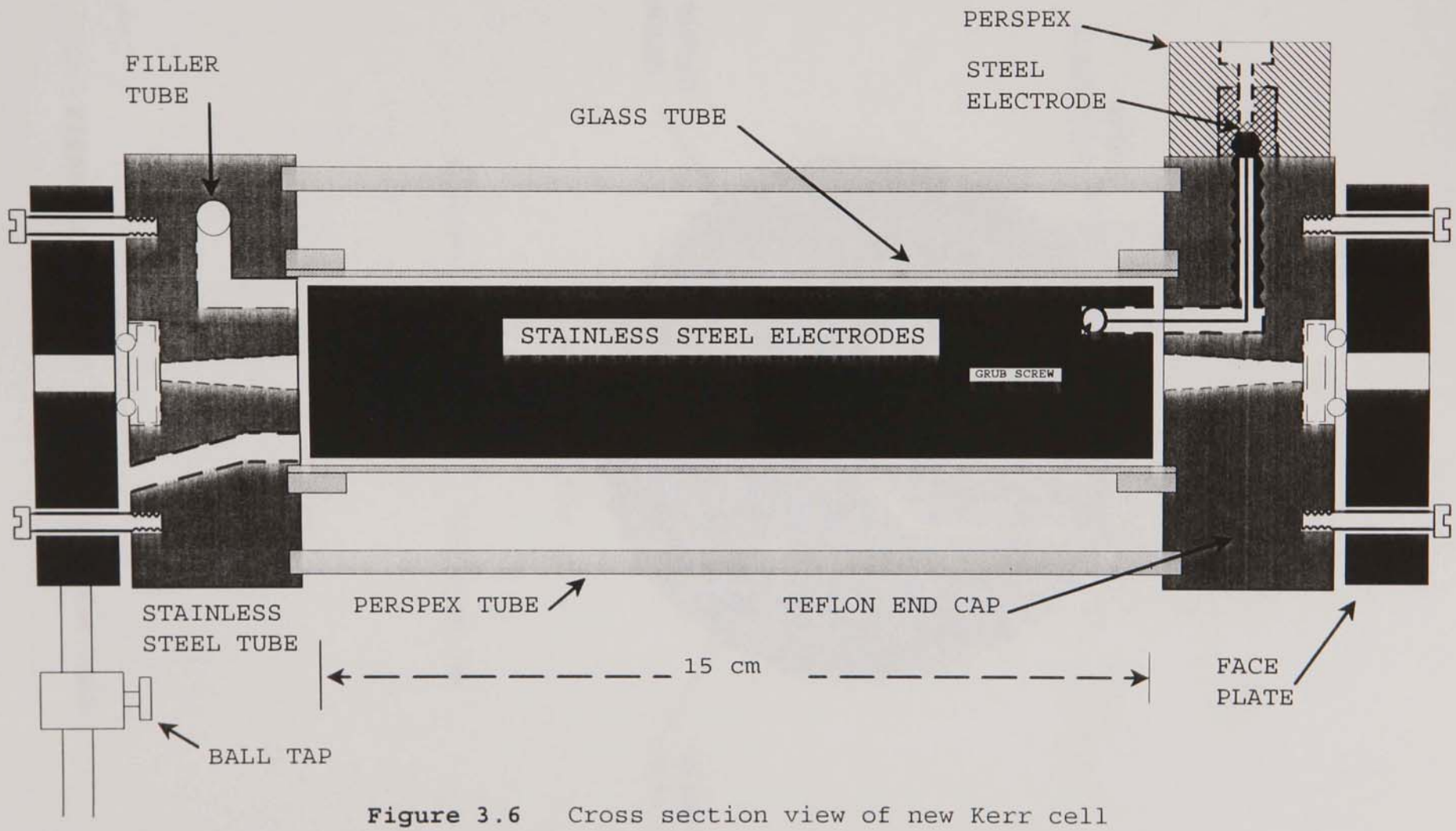

Figure 3.6 Cross section view of new Kerr cell

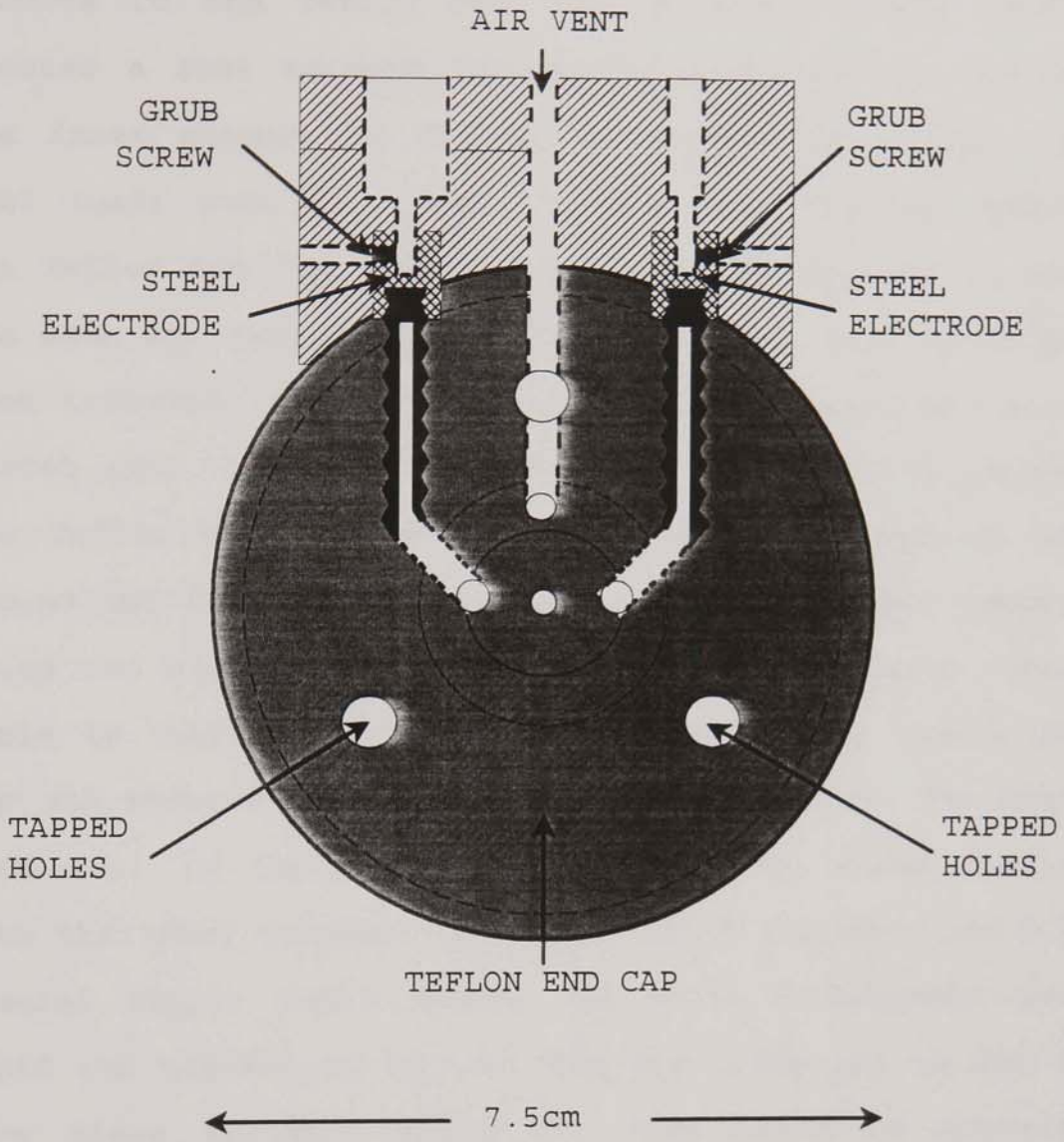

Figure 3.7 Back view of new Kerr cell

A brass retaining ring, through which heated/cooled water is passed, and a rubber 'O' ring secures the quartz windows to the Teflon end cap. A simple paper washer creates a seal between the quartz disk and the Teflon. The inner chamber is filled via a stainless-steel tube that leads into the chamber via a hole drilled through the Teflon end cap. The inner chamber is emptied in much the same way except that a stainless-steel ball valve has been included. Electrodes, also of stainless-steel, where placed into the inner chamber. Two wires passing through the Teflon end cap into the inner chamber provide the ground and H.T. supply to the electrodes and are secured using two Allen-key grub screws. The H.T. coaxial supply cable is connected to two brass rods on the Teflon end cap and secured using an Allen-key grub screw. The brass rods are, in turn, connected to the two wires leading into the inner chamber. A Perspex block supports the H.T. coaxial supply cable making the whole arrangement more rigid and preventing arcing. The electrode gap is set by five glass spacers, which fit into pairs of opposing holes drilled into the electrodes. The depth of the holes in the ground electrode may be varied by adjusting five Allen-key grub screws, and in this way the electrode gap may be varied.

The electrodes are supported in the inner glass chamber by four glass pegs and four spring loaded plungers. These spring loaded plungers also supply the force required to prevent the electrode gap from varying. Both electrodes were highly polished and rounded at their

extremities to prevent arcing between them. A K-type thermocouple was fed into the inner chamber through a hole that allowed air to escape from the chamber during filling. The thermocouple allowed the temperature of the inner chamber to be measured to $\pm 0.1^{o}C$. Two connections to the outer chamber make it possible to pass water through the outer chamber thus heating/cooling the inner chamber.

The aluminium end plates (connected together with three brass rods) are fixed to a base plate in such a way as to allow the Kerr cell to be tilted. This tilting action aids the filling and emptying of the Kerr cell. Two optical mounts attached to the base plate allow the Kerr cell to be rotated horizontally and moved perpendicular with respect to the laser beam.

3.4.3 Sealing the inner chamber

Initially the glass and Perspex tubes were sealed to the Teflon end caps using a Dow Corning water resistant silicon sealant (Type 732 RTV). When the cell was filled with toluene the sealant swelled and broke apart blocking the light path through the Kerr cell. The cell was therefore dismantled and resealed using only the minimum quantity of sealant required to successfully reseal the cell. The cell was then baked for forty-eight hours at $50^{o}C$ in an attempt to improve the cross-linking density of the sealant. However these methods proved unsuccessful. On the recommendation of Dow Corning the cell was then

resealed using Dow Corning 730 solvent resistant sealant. The 730 solvent resistant sealant proved more successful than the previous sealant since it did not break apart on the application of a solvent. However, over time even this sealant degenerated and finally allowed water to pass from the outer chamber to the inner. A new glass inner tube was then specially constructed with optically ground flanged edges and heat treated to remove any stress/strain caused by the grinding. A thin layer of Teflon tape was wound onto the end of the glass tube and the whole arrangement compressed between the two end caps. This method successfully sealed the cell.

3.4.4 Grub screws

All solutions prepared for electro-optic examination are filtered using 0.22μ Millipore Fluoropore filters. The solutions are filtered to reduce light scattering and therefore increase the signal-to-noise ratio (S-N ratio). However, when the cell was filled with carbon tetrachloride the S-N ratio decreased. The decrease in the S-N ratio was caused by rust particles released from the Allen-key grub-screws and floating in the cell, due to the high density of the carbon tetrachloride. The Allen-key grub-screws were therefore replaced with stainless-steel grub-screws.

3.4.5 Sealing the quartz windows

Initially the quartz windows were mounted straight onto the Teflon end cap and were secured in place using a rubber O-ring. This method proved unsuitable because it was not possible to machine a sufficiently flat surface on the Teflon to allow the windows to be sealed using only minimal pressure. A flat disk of solvent-resistant rubber (Viton) was then placed between the quartz window and the Teflon. This allowed the window to be sealed using only minimal pressure. However, the solvent-resistant rubber had a tendency to swell with some solvents and thus induce strain birefringence in the quartz windows. A successful seal between the quartz window and the Teflon was achieved using a high quality paper washer.

3.5 TEMPERATURE CONTROL AND STABILISATION OF THE KERR CELL

Initial experiments to determine the temperature stability of the Kerr cell resulted in refraction of the laser beam passing through the cell. For even small changes in the temperature (approx. 5°C) the beam was refracted to such an extent that it completely missed the far window of the cell. It was proposed that this refraction was caused by a temperature gradient through the cell, consequently a second thermocouple was inserted

into the far end of the cell. As expected the thermocouples at either end of the cell did not give the same temperature reading, thus proving that a temperature gradient did exist. The exact explanation why such a gradient should exist is not fully understood but it did seem likely that it was caused by unsymmetric heat loss through the Teflon end caps.

To overcome the heat loss through the Teflon end caps the system of heating/cooling the cell by passing water through the outer chamber was abandoned in favour of enclosing the cell in an insulated box through which hot/cold air was passed. The above method did solve the refraction problem but meant that changing the temperature of the Kerr cell was considerably slower than the water method.

As the heated/cooled air method proved to be to slow for practical purposes it was decided to return to the water controlled method. Initially the plates holding the quartz windows in place were simple disks of aluminium and not the hollow brass plates currently used. Small resistors and a thermistor were placed on the aluminium plates so that the plates could be heated and maintained at the same temperature as the water temperature in the hope that this would help reduce the heat loss through the Teflon end caps. Essentially this method was successful but it was considered to be somewhat impractical. The aluminium plates were therefore replaced by two hollow brass plates through which water may pass. The water passing through the brass plates is the same as

the water passing through the outer chamber of the Kerr cell. In this way the heat loss through the Teflon end caps was corrected while still allowing the Kerr cell to be heated/cooled at a reasonable rate.

3.6 EXPERIMENTAL METHOD-THE NULLED PULSE TECHNIQUE

One of the most successful methods of measuring the birefringence of a sample is the nulled pulse technique[65,66] which involves the application of a square wave electric field of short duration (≈10ms) to the sample.

When there is no electric field applied across the Kerr cell the light remains unaffected by the Kerr cell and the quarter-wave retarder. The light arriving at the second polariser is therefore still polarised at 45° to the Kerr cell electrodes and can therefore be completely extinguished by the second polariser. When the two polarisers are oriented by an angle, α_N, such that no light will pass through them, then they are said to be "crossed".

When an electric field is applied across the Kerr cell a phase difference, δ, is introduced between the parallel and perpendicular vector components of the light beam. The phase retardation, δ, results in the light emerging from the cell being elliptically polarised. The quarter-wave retarder converts this elliptically polarised light into plane polarised light rotated by an

angle, α, (see Appendix B). The light emerging from the quarter-wave retarder can then be extinguished by rotating the second polariser by an angle α from the crossed position. The quarter-wave plate between the Kerr cell and the analyser enables a distinction to be made between positive and negative birefringences.

When no electric field is applied the intensity of light detected by the photomultiplier is given by

$$I_{E=0} = I_0 \sin^2 \alpha \qquad 3.2$$

where α is the rotation of the analyser with respect to the nulled position of the two polarisers (Malus' law). When an electric field is applied to the Kerr cell the detected light intensity is given by

$$I_{E>0} = I_o \sin^2(\alpha + \delta/2) \qquad 3.3$$

If the analyser is then rotated in discrete steps the difference between the optical intensities $I_{E=0}$ and $I_{E>0}$ will reduce until an angle α_1 is reached, such that the intensity $I_{E=0}$ and $I_{E>0}$ are equal (see Figure 3.8) the system is then said to be at the null-point. It can be shown (see Appendix C) that at the null-point when the angle α_1 is less than 20^o that

$$\alpha_1 = -\frac{\delta}{4} \qquad 3.4$$

Thus, for a pulsed mode of operation, equation 3.4 describes the relationship between the angular rotation of the analyser, required to equate the optical intensities, and the electronically induced phase retardation, δ. The Kerr constant, B, is then readily calculated form

$$B = \delta/2\pi lE^2 \qquad 3.5$$

However, this method requires exact measurements of the electrode length, the distance between the electrodes, and the voltage applied. Errors can also be introduced because of field effects at the end of the electrodes. Instead a graph of α_1 for various applied voltages was plotted against V^2, and the gradient, m_x, found. The Kerr cell was previously calibrated with a liquid of known Kerr constant, B_s. The graph of α_1 against V^2 for the standard liquid then gave a gradient, m_s. The Kerr constant, B_x, of the unknown liquid is then found from

$$B_x = B_s m_x/m_s \qquad 3.6$$

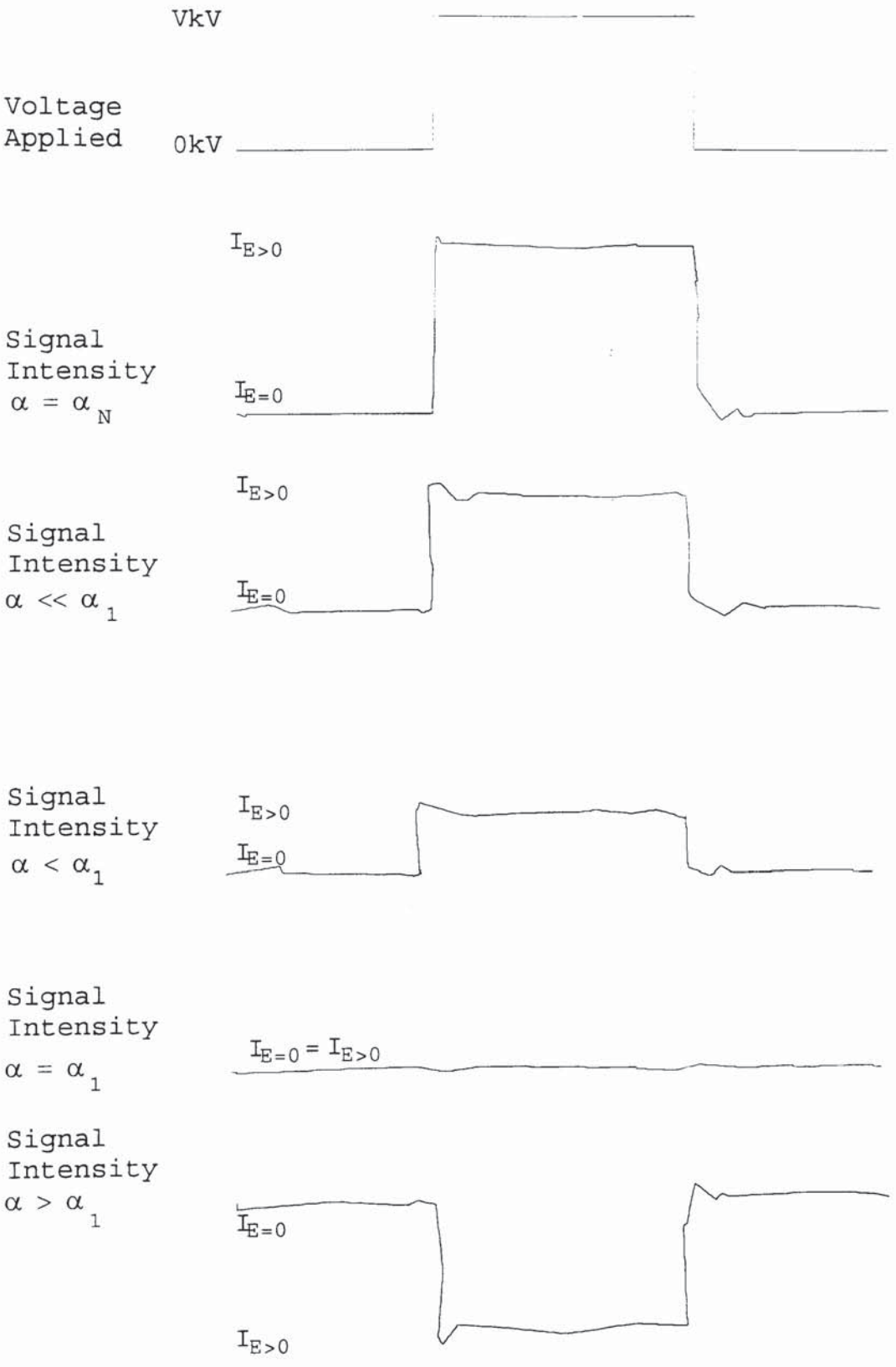

Figure 3.8 Schematic diagram of typical optical pulses.

3.6.2 Procedure for measuring the Kerr constant using the nulled pulse technique

The slow axis of the quarter-wave was manually set at 45° with respect to the direction of the applied electric field. The solution/solvent was placed in the Kerr cell at room temperature and it was checked that no air bubbles had formed at the quartz windows of the Kerr cell. If air bubbles do form these can usually be easily removed by tipping the Kerr cell. The water bath was then set to the desired temperature and the system was then left to reach temperature equilibrium. When the system had reached temperature equilibrium and a clear optical beam could be seen emerging from the cell the analyser was manually rotated to the crossed position. For a solution/solvent with a positive Kerr constant the analyser is then rotated manually a half turn anticlockwise and then a quarter turn clockwise. This is done to compensate for backlash in the gearing system. For a negative Kerr constant this process is reversed. The stepper motor control box can now be switched on (making sure that the rotation of the motor is set to clockwise) and the computer program listed in Appendix E can now be loaded. Once the computer program has been loaded the user is presented with the main-menu screen shown in Figure 3.9.

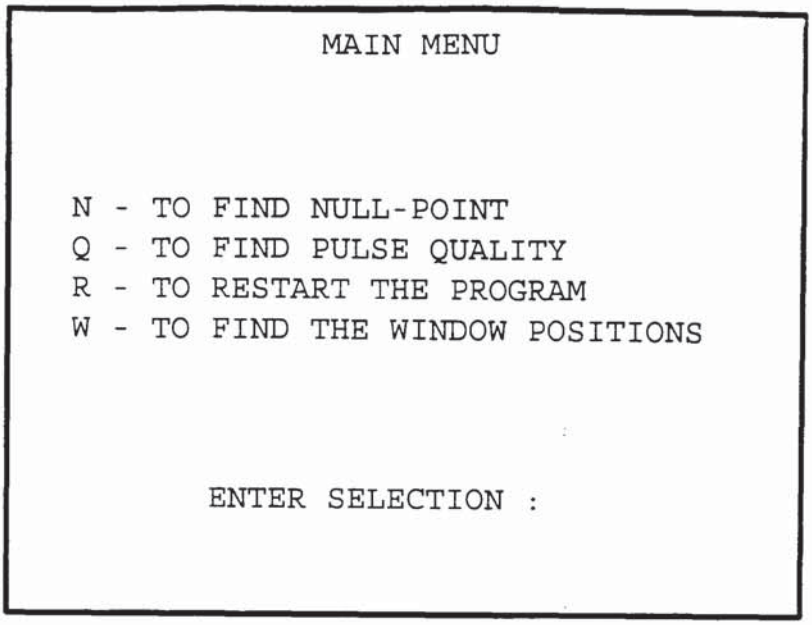

Figure 3.9 Computer program main menu

The user can now determine the quality of the optical pulse received by the photomultiplier by pressing 'Q' then 'RETURN' on the computer keyboard. It is important here to ensure that the transient recorder is set to the single pulse mode of operation. A sample of the crossed position optical signal being received by the photomultiplier will then be transferred to the computer. The average intensity level and standard deviation of the optical signal is then determined. If the deviation is greater than 3% the optical signal will be classed as noisy. If the pulse is 'noisy' this could indicate that the system has not reached temperature equilibrium or that the sample has not been filtered sufficiently. If the optical signal received by the transient recorder exceeds the transient recorder window limits the user will be informed of the situation by the program. The signal can be made to fall within the transient recorder

window limits by adjusting the offset voltage and/or voltage scale on the transient recorder. If the pulse is within the window limits and is 'clean' the user can now proceed to determining the zero applied voltage null point. This is accomplished by pressing 'N' and then 'RETURN' at the main menu. The user must then enter the stepper motor increment value (normally one) and the number of pulses to average over (normally one for a clean pulse). The program will then automatically find the null point.

In order for the computer program to determine the difference between the intensity levels of the on/off electric field state the program must be given four discrete windows positions. This is done by selecting the "find window positions" on the computer program menu i.e. press 'W' then 'RETURN'. The user is then required to transfer an optical pulse from the transient recorder to the computer. Manually increase the voltage applied to the Kerr cell until an optical square wave signal can be seen on the oscilloscope using the 'DISPLAY PULSE ON OSCILLOSCOPE' option in the sub-menu. Now transfer the optical signal to the computer using the 'TRANSFER PULSE TO COMPUTER' option in the sub-menu. This optical signal will then be displayed on the computer monitor see Figure 3.10. The solid white line running vertically from the bottom of the screen to the top is simply a marker position. The marker can be moved from the left of the screen to the right of the screen by pressing any key on the computer key board. By pressing the 'S' key on the

keyboard the window positions s1, s2, s3, and s4 can the be set (see Figure 3.11).

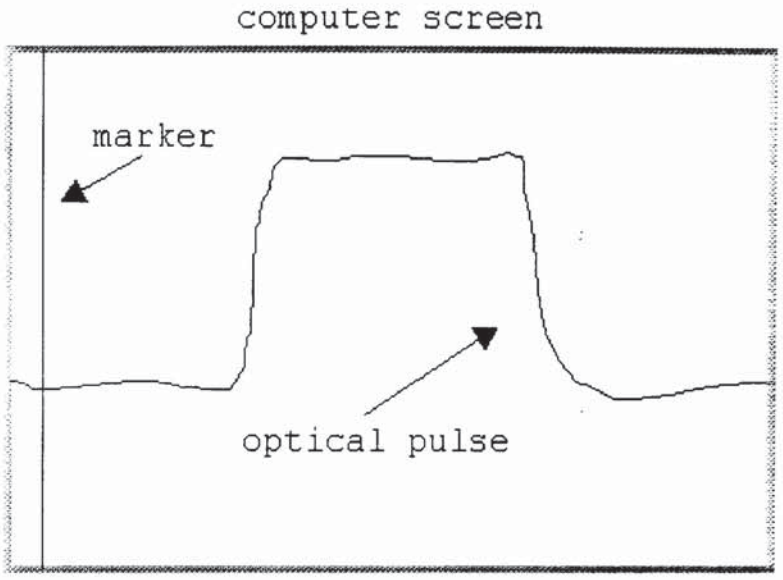

Figure 3.10 Computer program screen-typical optical pulse.

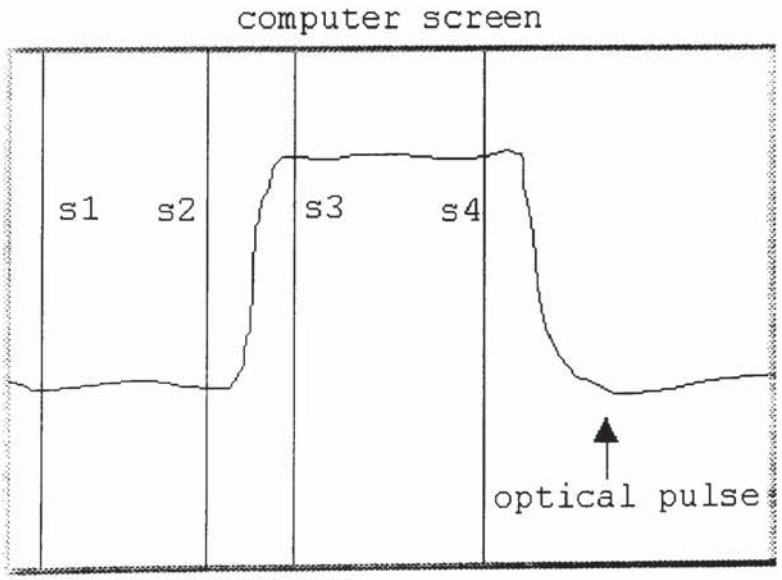

Figure 3.11 Computer program screen-setting window limits.

It is possible using this setting of the window positions to do relaxation measurements. This is possible because as the marker line scans across the optical pulse the time position of the marker and the intensity of the pulse at that time is displayed on the computer screen.

After setting the window positions the user will automatically proceed to determining the Kerr gradient of the sample. The user will then be required to enter the current operating voltage and the number of times the optical pulse should be averaged over. The user will also be required to enter the analyser step value at this point. The step value is effectively the number of degrees the analyser will move between analysing the optical signals. This value obviously changes according to the Kerr constant of the sample, the temperature, and the applied voltage. As a rough guide pure HPLC grade toluene at 25^{o}C and with an applied voltage of 1.5kV requires an increment value of 1. The computer program is set-up to suggest an increment value but this is entirely optional. The computer program will then automatically apply an electric field across the Kerr cell and record the received optical signal. The difference between the on/off electric field light intensity is then calculated and recorded. The computer will then move the analyser by the step value set by the user and repeat the above process until the pulse has become inverted (see Figure 3.8). It is important that the voltage scale on the transient recorder and the supply voltage to the photo-multiplier is not altered during this process. If the

optical pulse at some point exceeds the transient recorder window limits this can be corrected by adjusting the voltage offset on the transient recorder. It is suggested that the user set the step value such that 15-20 pulses are analysed before the pulse becomes inverted. The computer will then calculate the null-point for that voltage according to the method outlined in Appendix D. The whole process should then be repeated for at least seven further incremental applied voltages. Once sufficient null-points have been calculated the user enters '0' as the applied voltage and the computer will automatically calculate the Kerr gradient, m_x and its 68% confidence limit after the analyser has been returned to the zero voltage null point by the computer program. The results can then be printed to the computer screen and/or a printer. The gradient is expressed as stepV^{-2} but this can be converted to degrees by remembering that each step of the stepper motor is equivalent to moving the analyser by 0.0045 degrees. The temperature of the Kerr cell can now be altered and the whole process repeated.

3.7 MATERIALS

3.7.1 1,4-Dioxane and toluene

The 1,4-dioxane and toluene used throughout this thesis were HPLC grade bought from Aldrich. The compounds were tested using a glc and found to be more than 99%

pure. The compounds were stored over sodium wire to prevent contamination with water.

3.7.2 Nitrobenzene and aniline

When pure, nitrobenzene and aniline are colourless liquids. However, the nitrobenzene and aniline bought from Aldrich was found to have a distinctive brown colour. Consequently, the nitrobenzene and aniline were both distilled using standard techniques. The distilled liquids were colourless and a glc test confirmed both of these liquids to be greater than 99% pure. The distilled nitrobenzene and aniline were each stored in a dark flask under a nitrogen atmosphere to minimise any chemical reactions caused by light and/or oxygen.

3.7.3 2-Methyl-4-nitroaniline and p-nitroaniline

2-Methyl-4-nitroaniline and p-nitroaniline should be long needle shaped crystals with a light yellow colour. However, the compounds bought from Aldrich had a distinctive brown colour similar to that found for the nitrobenzene. It was therefore decided to re-crystallise both compounds. A saturated solution of the solute was prepared by dissolving the compound in a solution of 50% methanol and 50% water. The saturated solution was then boiled for 30 minutes with a small amount of activated

charcoal. After 30 minutes the solution was filtered to remove the activated charcoal and any insoluble impurities and then allowed to stand for two days. The solution was filtered to remove the 2-methyl-4-nitroaniline (or the p-nitroaniline) crystals that had formed. The filtrate was washed with water and allowed to dry for two days in an oven set at 40°C. The melting point of the crystals was then checked and was found to agree with literature values for both compounds (p-nitroaniline[75] m.p. 148.5-9.5°C and 2-methyl-4-nitroaniline[75] m.p. 152°C). Similar to nitrobenzene and aniline the p-nitroaniline and 2-methyl-4-nitroaniline crystals were stored in a dark flask under a nitrogen atmosphere.

3.7.4 Preparation of solutions

Solutions were prepared by weighing out accurately 2.5g, 2g, 1.5g, 1g, and 0.5g of solute in $50cm^3$ volumetric flasks and then making up to $50cm^3$ with 1,4-dioxane. The solutions were stored under nitrogen in a refrigerator. Approximately, $50cm^3$ of solution was sufficient for the measurement of the Kerr effect, refractive index, depolarisation ratio, dielectric constant, and density measurements. In this way there was minimal discrepancy in the solution concentration between the measurements. Before use the solutions were filtered using a Millipore Fluoropore 0.22μ filter.

3.8 KERR CONSTANT RESULTS

The Kerr gradient m_x was determined over a voltage range of 0.5-6kV for the solutions and 1.5-8kV for the solvents. The gradient was then converted into the Kerr constant B using equation 3.7. For the large volume cell the relevant values were (in SI)

$$B_x = \frac{0.79 \times 10^{-14} m_x}{5.544 \times 10^{-4}} \qquad 3.7$$

where 0.79×10^{-14} $V^{-2}m$ is taken as the Kerr constant of toluene[67] at 25°C (λ=632.8nm) and 5.544×10^{-4} is the gradient measured for toluene at 25°C. Taking 0.79×10^{-14} as the Kerr constant of toluene at 25°C was an arbitrary choice as literature values do vary, it would therefore have been just as acceptable to use the value 0.81×10^{-14} $V^{-2}m$ reported by Aroney *et al*[68]. Measurements on solutions were performed over a concentration range of 1-5% by weight, with increments of 1%. The solvent used being HPLC grade 1,4-dioxane (Aldrich). The cell was rinsed using filtered 1,4-dioxane following a change of solution. All solutions and solvents were filtered using a 0.22μm Millipore Fluoropore filter and dried before filling the Kerr cell. Temperature measurements were taken over the range 15-70°C inclusive in 5°C intervals. Following each change of temperature the system was allowed to stand until it had reached thermal equilibrium. This was generally evident by a clear round laser beam emerging from the cell and a low-noise optical

signal received by the photo-multiplier. The system generally took at least thirty minutes after a 5°C temperature change before a temperature equilibrium had been achieved. The null-point was independently determined at each temperature setting.

Graphs of the various Kerr constant measurements taken can be seen on the following pages. Tables of the results can also be seen in Appendix F.

Gradient measurements at each temperature for the compounds used initially appear to be very accurate, with errors about ±1% for a 68% confidence limit. However, graphs of the temperature dependence of the Kerr constant show that larger more significant errors do occur. It is proposed that these random errors are a result of the system not having truly achieved a thermal equilibrium and/or an incorrect determination of the null-point.

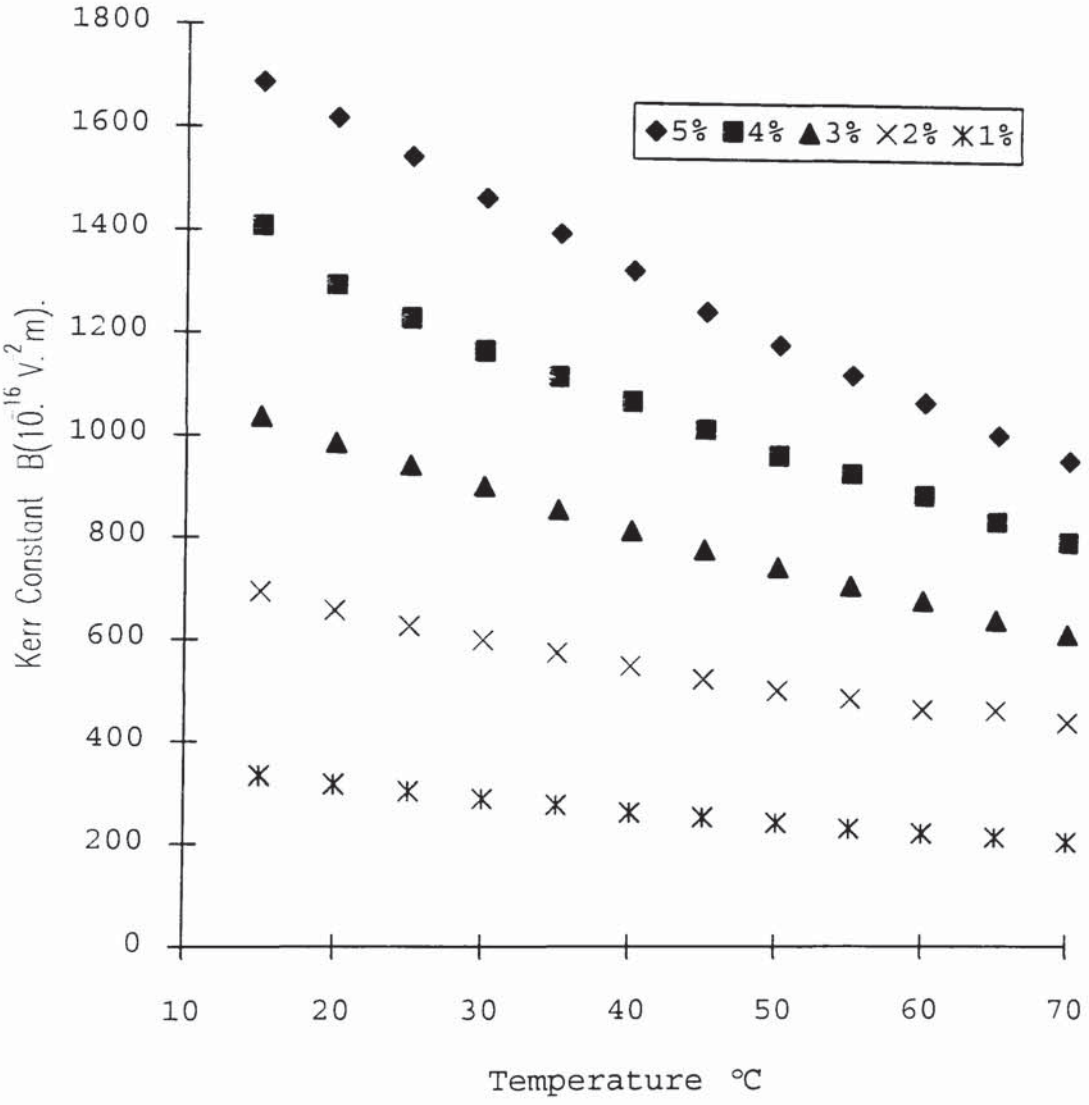

Figure 3.12 Kerr constant for solutions of 2-methyl-4-nitroaniline in 1,4-dioxane plotted as a function of temperature.

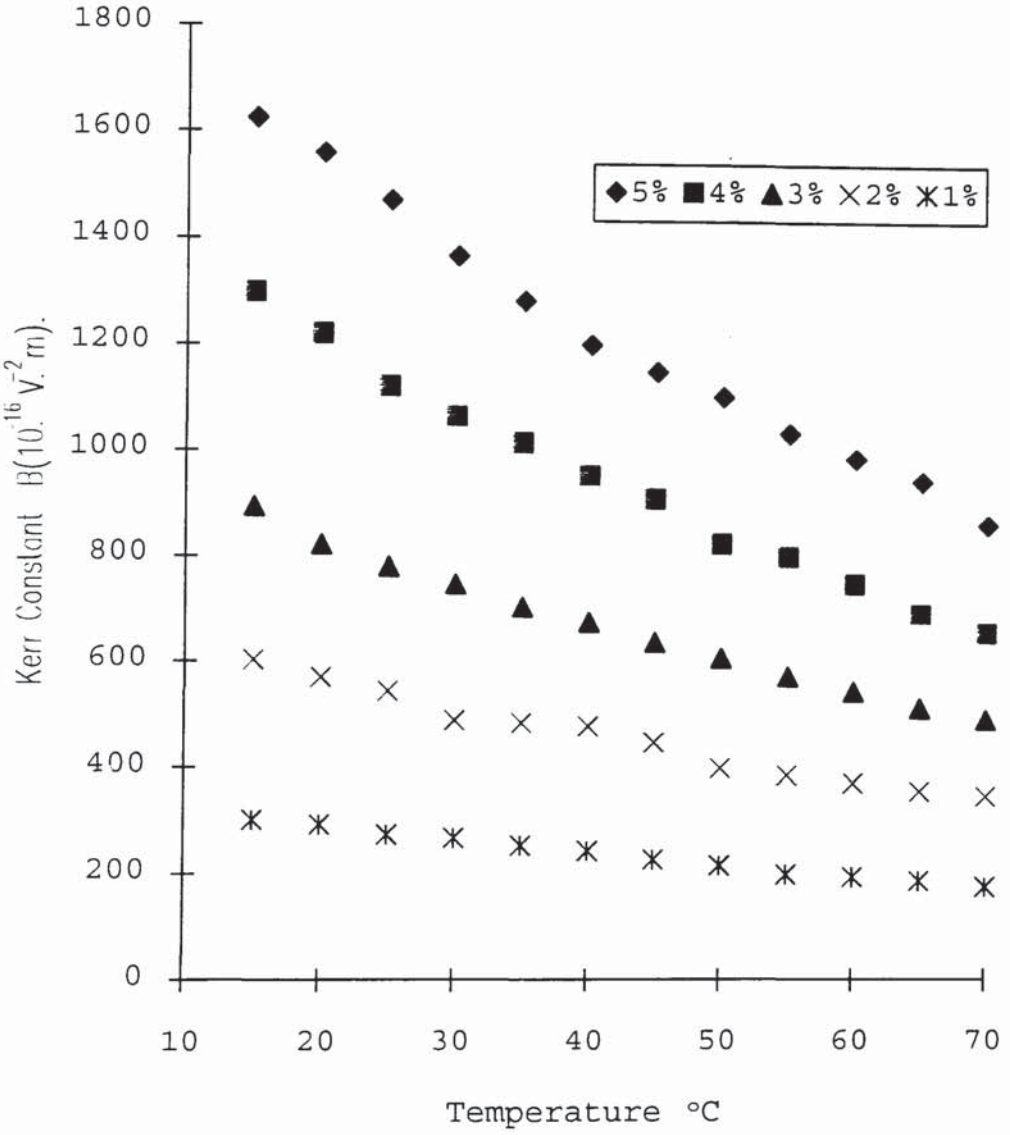

Figure 3.13 Kerr constant for solutions of p-nitroaniline in 1,4-dioxane plotted as a function of temperature.

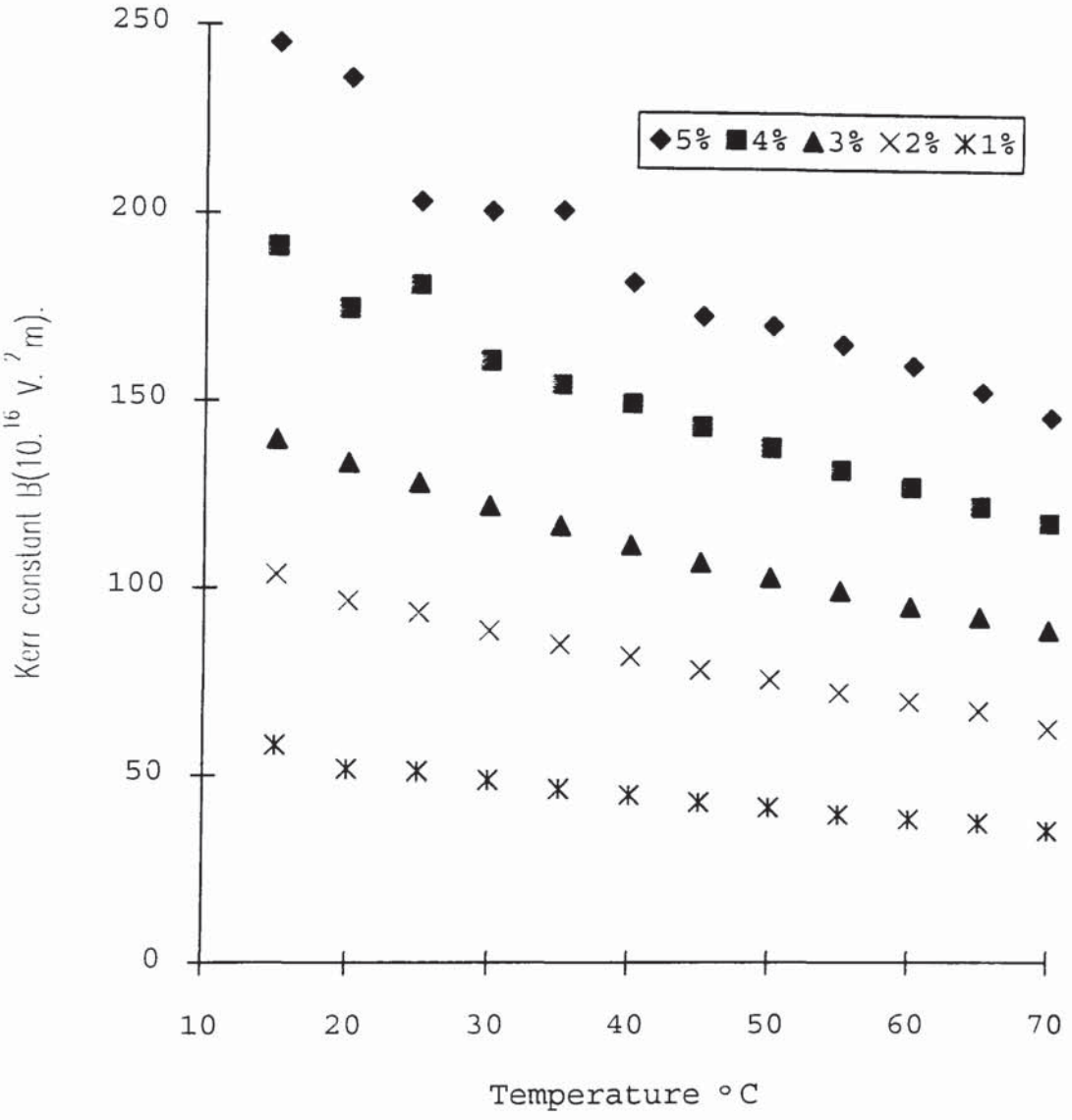

Figure 3.14 Kerr constant for solutions of nitrobenzene in 1,4-dioxane plotted as a function of temperature.

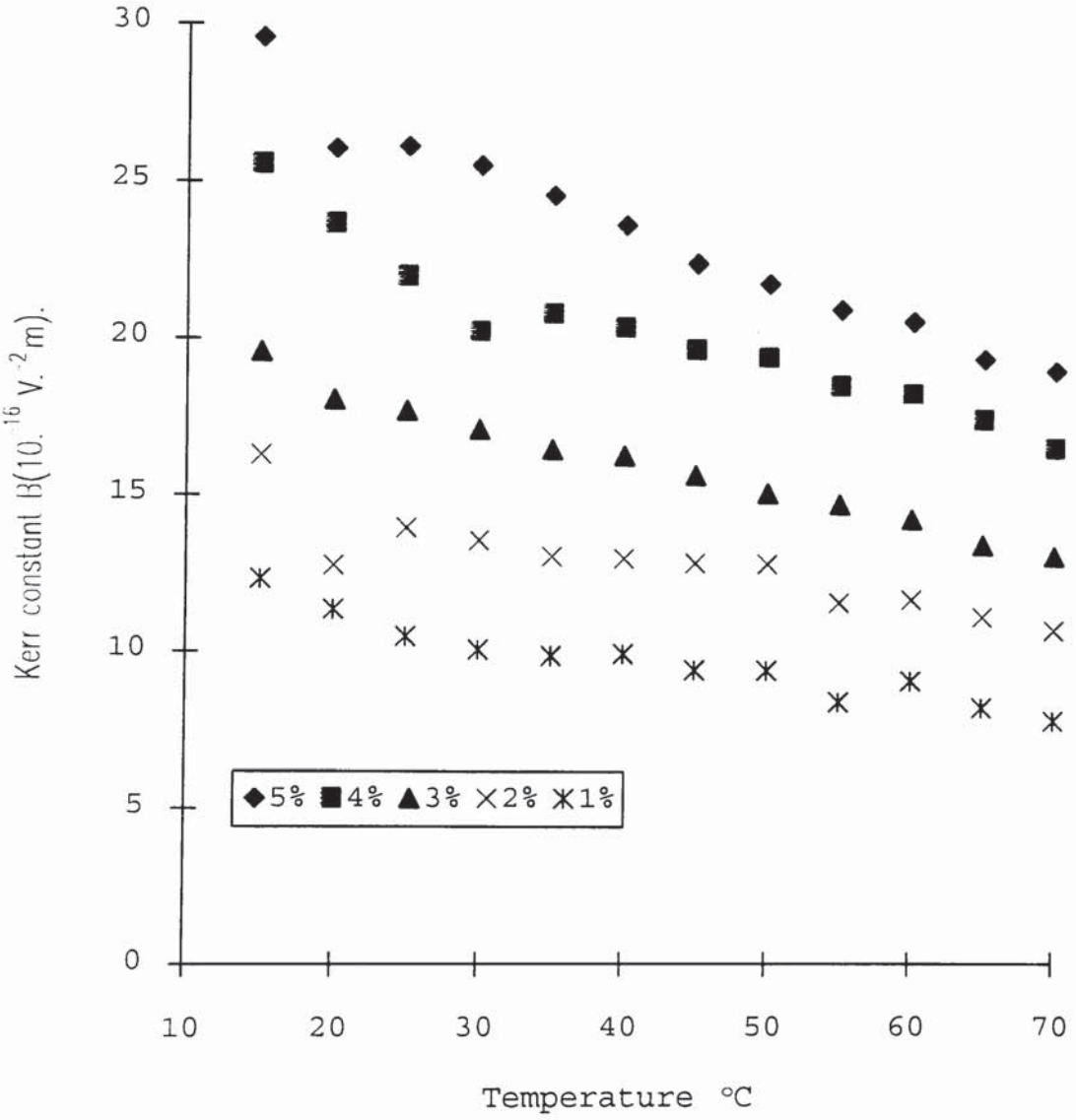

Figure 3.15 Kerr constant for solutions of aniline in 1,4-dioxane plotted as a function of temperature.

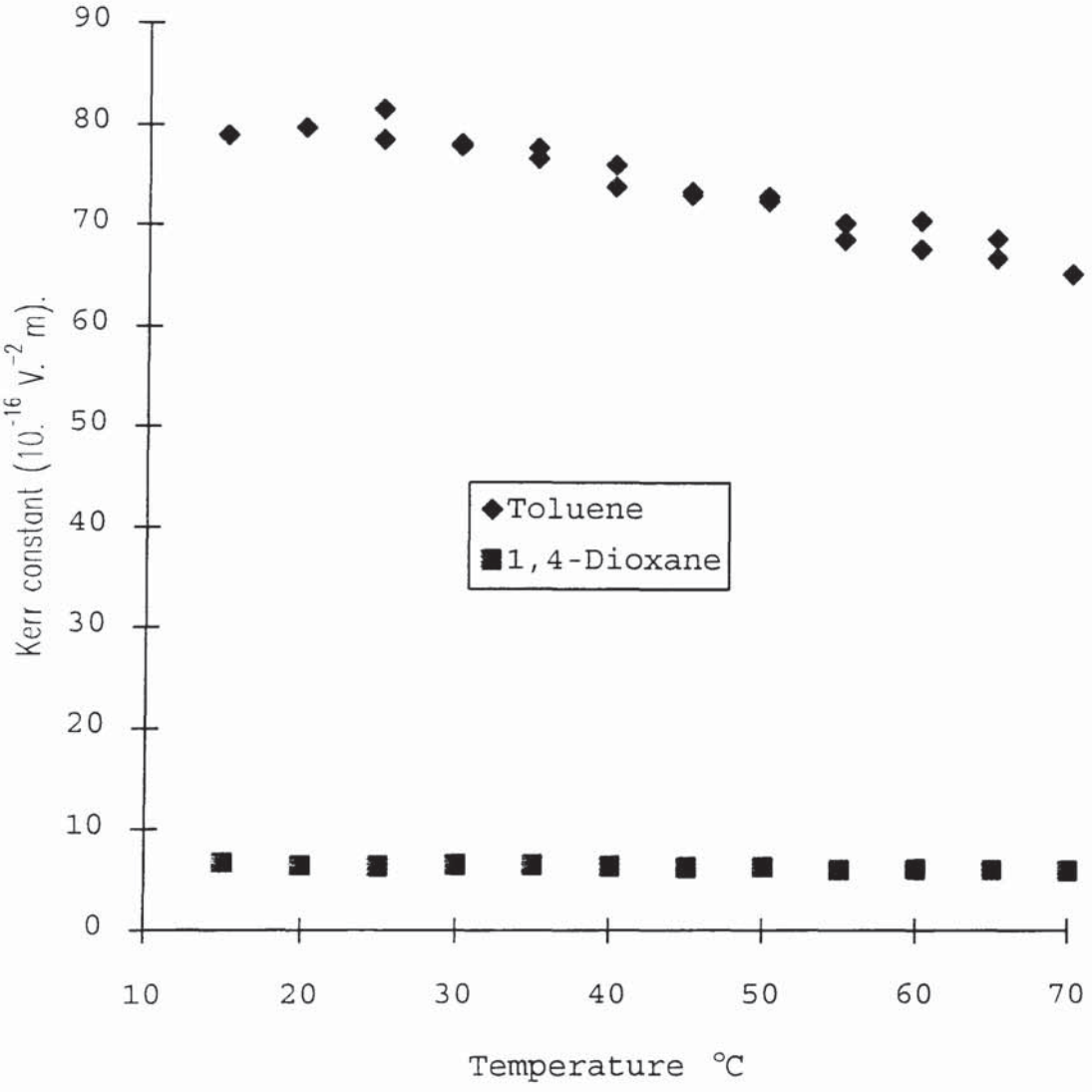

Figure 3.16 Kerr constant for HPLC grade toluene and 1,4-dioxane plotted as a function of temperature.

CHAPTER 4

DENSITY MEASUREMENT

4.1 INTRODUCTION

Density measurements were performed using a PAAR DMA Density Meter, in combination with two DMA 602 remote cells, used with the kind permission of Dr Jenkins of Aston University. Both cells were initially calibrated and used to perform all density measurements in this thesis. The cells were heated/cooled by circulating water through a jacket surrounding the cells.

4.2 THEORY OF DENSITY MEASUREMENTS

The measuring principal of the PAAR DMA Density Meter is based on the change of the natural frequency of a hollow oscillator when filled with different liquids. The mass, and thus the density, of the liquid changes this natural frequency due to a gross change of the oscillator caused by the introduction of the liquid. For calculating the density, the system is considered to be represented by a hollow body of mass M suspended on a spring with an elasticity constant c, a volume V when filled and a sample of density d.

The natural frequency of this system is:

$$f = \frac{1}{2\pi}\sqrt{\frac{c}{M + dV}} \qquad 4.1$$

therefore, the period will be

$$T = 2\pi\sqrt{\frac{M + dV}{c}} \qquad 4.2$$

Taking the square of this expression and inserting

$$A = \frac{4\pi^2 V}{c} \quad , \quad B = \frac{4\pi^2 M}{c} \qquad 4.3$$

we therefore obtain

$$d = \frac{1}{A}\left(T^2 - B\right) \qquad 4.4$$

For the difference of densities of two samples:

$$d_1 - d_2 = \frac{1}{A}\left(T_1^2 - T_2^2\right) \qquad 4.5$$

Since the constants A and B contain the volume, spring constant and mass, they may be regarded as apparatus constants that may be determined from two calibration measurements of samples of known density.

4.3 CALIBRATION OF THE PAAR DENSITY METER

In practice a calibration constant, k, was determined for the DMA 602 cells over the temperature range 25-65°C at 5°C intervals. The samples used were HPLC grade carbon tetrachloride and air. The calibration constant, k, was calculated according to

$$k = \frac{d_{CCl_4} - d_{AIR}}{T^2_{CCl_4} - T^2_{AIR}} \qquad 4.6$$

The density of air and the density of the carbon tetrachloride at various temperatures were obtained from various sources[69,70]. Measurements of the period of oscillation of the U-tube were taken with the "Period Select" switch set to 2k. The calibration constant for both cells over the above temperature range can be seen in Table 4.4. The density of an unknown sample, d_x with a period value of T_x can now be determined from

$$d_x = k\left(T_x^2 - T_{AIR}^2\right) + d_{AIR} \qquad 4.7$$

4.4 EXPERIMENTAL DENSITY RESULTS

Samples were introduced into the cells of the PAAR density meter using a $2cm^3$ P.T.F.E syringe connected to the cell via a length of P.T.F.E. tubing. The samples were all previously filtered using a 0.22μ Millipore Fluoropore filter and were introduced slowly into the

cell to prevent microscopic air bubbles forming in the cell.

The densities of aniline, nitrobenzene, p-nitroaniline, and 2-methyl-4-nitroaniline were all measured as solutions dissolved in HPLC grade 1,4-dioxane. Density measurements were also made on pure 1,4-dioxane and toluene. Graphs of the experimental results can be seen in the following figures. Tables of the results can be seen in Appendix G. As the density of the various solutions of aniline is so close to that of 1,4-dioxane the density results have been displaced up the ordinate axis.

Table 4.1 Temperature dependence of the density for air and carbon tetrachloride.

Temp. °C	Density Air gcm^{-3}	Density CCl_4 kgm^{-3}
25	1.16896E-03	1584.26
30	1.14963E-03	1574.45
35	1.13092E-03	1564.66
40	1.11282E-03	1554.90
45	1.09528E-03	1545.16
50	1.07829E-03	1535.45
55	1.06182E-03	1525.76
60	1.04584E-03	1516.10
65	1.03033E-03	1506.46

Table 4.2 Period readings for air and CCl_4 for Cell 1.

Temp. °C	Cell 1 Period (T) of Air	Cell 1 Period (T) of CCl_4
25	0.55217(8)	0.87222(3)
30	0.55200(2)	0.87036(2)
35	0.55183(4)	0.86856(0)
40	0.55166(2)	0.86667(9)
45	0.55150(2)	0.86485(0)
50	0.55134(1)	0.86294(6)
55	0.55118(5)	0.86110(3)
60	0.55102(0)	0.85920(1)
65	0.55086(8)	0.85734(9)

Table 4.3 Period readings for Air and CCl_4 for Cell 2.

Temp. °C	Cell 2 Period (T) for Air	Cell 2 Period (T) for CCl_4
25	0.50632(2)	0.73191(7)
30	0.50616(1)	0.73051(3)
35	0.50601(1)	0.72915(1)
40	0.50585(5)	0.72772(7)
45	0.50570(9)	0.72631(2)
50	0.50555(8)	0.72489(4)
55	0.50541(9)	0.72349(2)
60	0.50527(8)	0.72205(6)
65	0.50515(2)	0.72068(3)

Table 4.4 PAAR Density meter cell constants (k).

Temp. °C	Cell 1 Constant (k) kgm^{-3}	Cell 2 Constant (k) kgm^{-3}
25	3475.(23)	5652.(54)
30	3476.(95)	5655.(80)
35	3477.(98)	5658.(09)
40	3480.(06)	5662.(17)
45	3481.(56)	5666.(26)
50	3484.(11)	5670.(41)
55	3485.(90)	5674.(39)
60	3488.(46)	5679.(44)
65	3490.(47)	5682.(95)

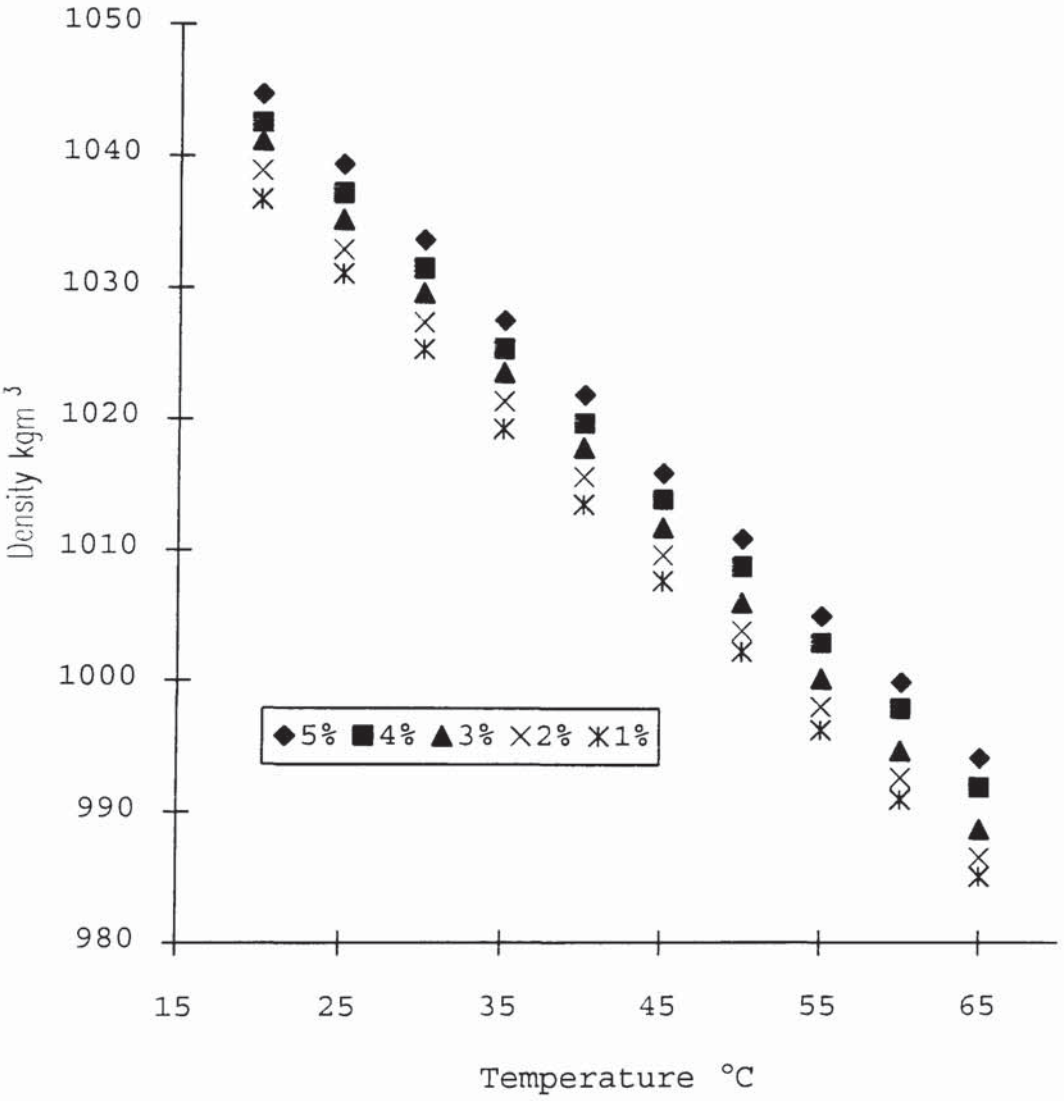

Figure 4.1 Density for solutions of 2-methyl-4-nitroaniline in 1,4-dioxane plotted as a function of temperature.

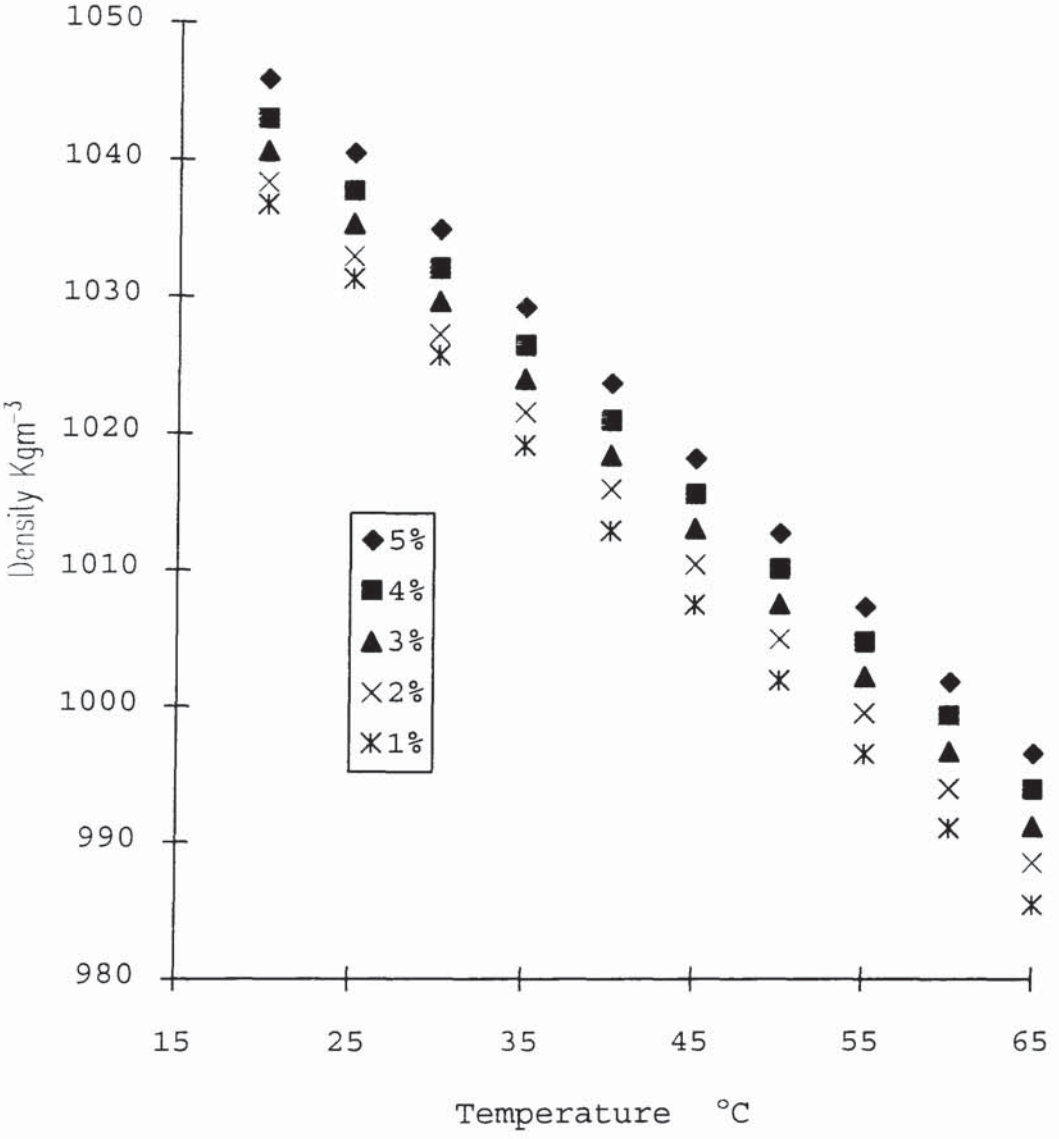

Figure 4.2 Density for solutions of p-nitroaniline in 1,4-dioxane plotted as a function of temperature.

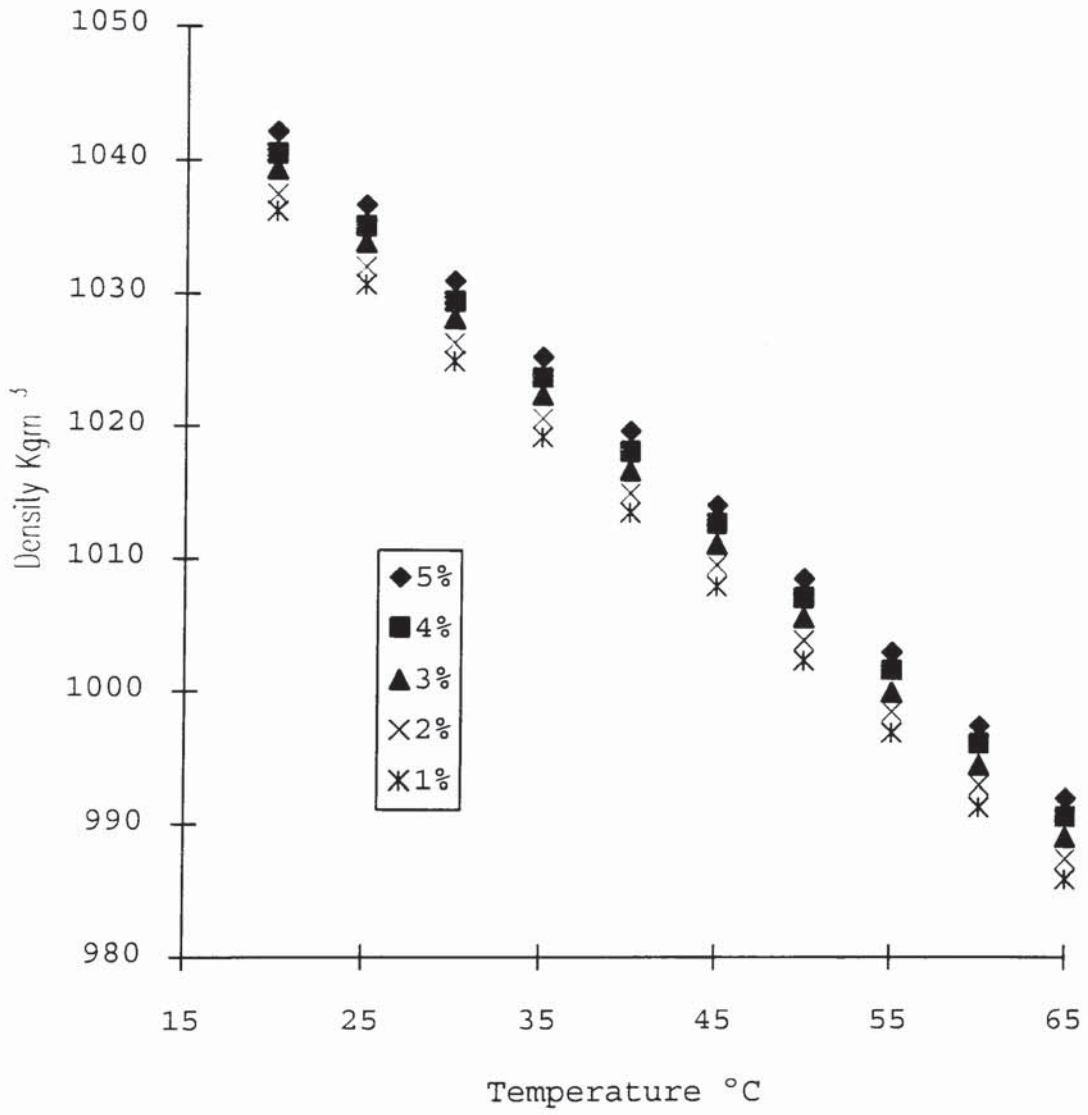

Figure 4.3 Density for solutions of nitrobenzene in 1,4-dioxane plotted as a function of temperature.

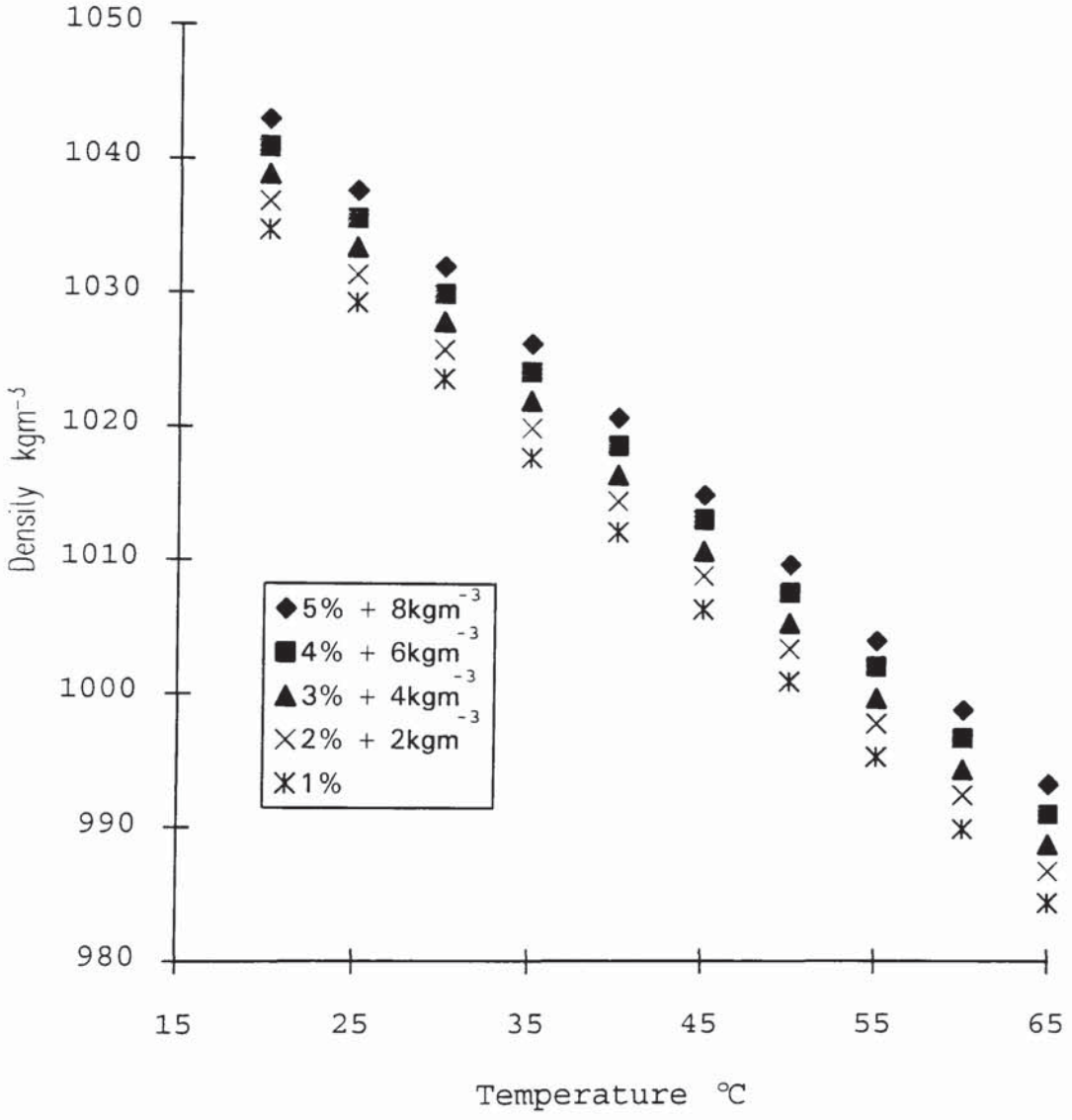

Figure 4.4 Density for solutions of aniline in 1,4-dioxane plotted as a function of temperature.

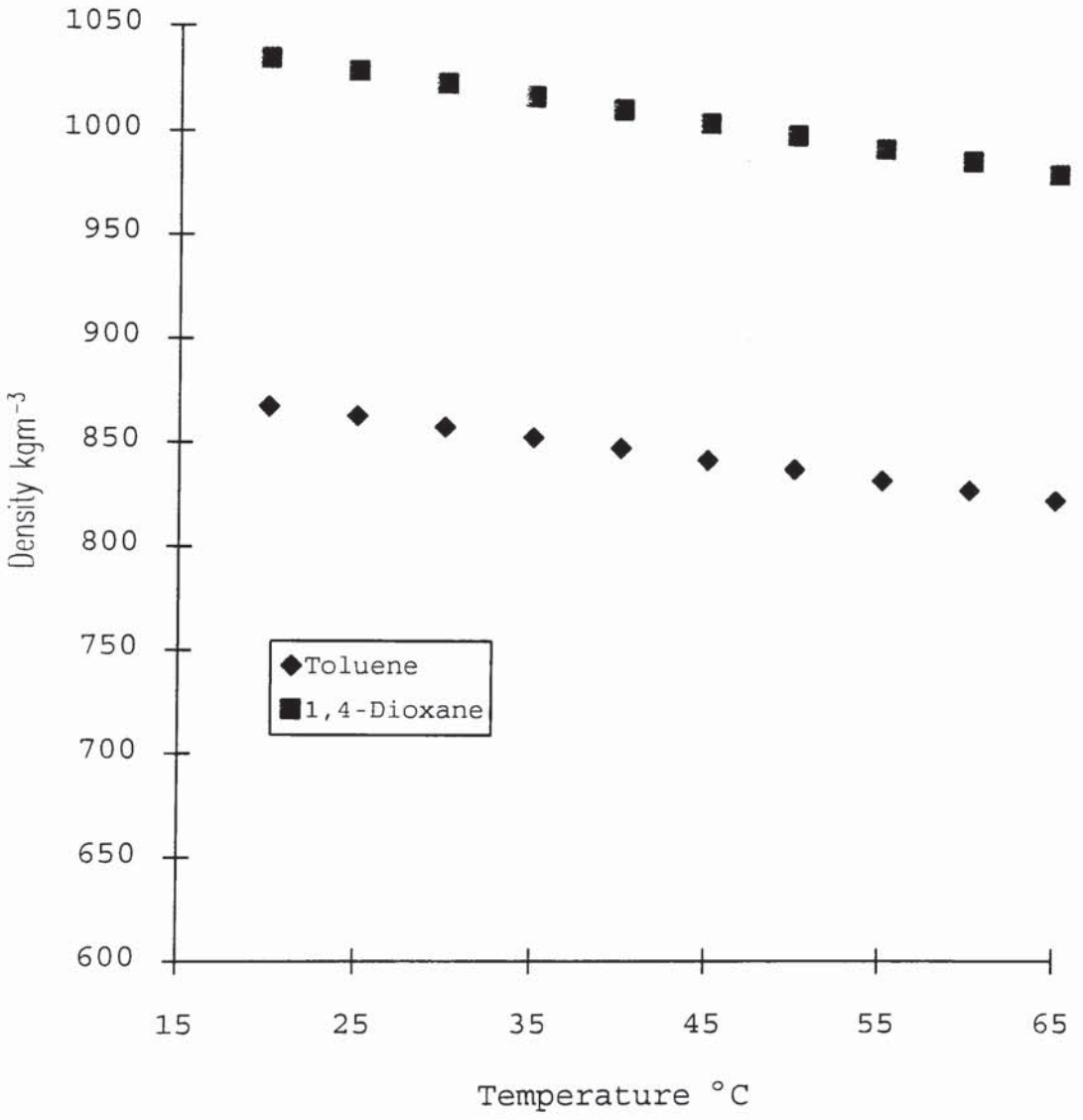

Figure 4.5 Density for toluene and 1,4-dioxane plotted as a function of temperature.

CHAPTER 5

DIELECTRIC CONSTANT AND DIPOLE MOMENT; THEORY AND MEASUREMENT.

5.1 INTRODUCTION

The effect of capacitance following the introduction of a particular substance into an electric field is reflected by its dielectric 'constant' (i.e. relative dielectric permittivity) ε. The original work of Faraday has been treated mathematically successively by Mosotti[71] and Clausius[72], and their conclusions are embodied in what is now known as the Clausius-Mosotti law. This indicates that the dielectric 'constant' of a substance varies with its density, d, according to the relationship

$$P_T = \frac{(\varepsilon - 1)M}{(\varepsilon + 2)d} \qquad 5.1$$

where M is the molecular weight and P_T is a constant known as the molecular polarisation of the molecule. According to the classical Debye[73,74] theory the molecular polarisation comprises two distinct terms. The first is the polarisation that the molecule would have without a permanent dipole. It arises through the displacement of the electrons and nuclei with respect to one another in the applied field, and is called the distortion

polarisation, P_D. The second term is the contribution to the molecular polarisation made by the orientation of the dipoles in the field, and is consequently known as the orientation polarisation, P_μ.

The distortion polarisation term, however is itself rather more complex than would at first be expected. When an electric field is applied to a non-polar molecule the major contribution to the induced dipole mainly results from the displacement of the electrons with respect to the centre of mass of the molecule as the mass of an electron is so much smaller that of the nuclei. The contribution of this effect to the distortion polarisation is known as the electron polarisation, P_E. However whether a molecule has a permanent dipole or not it generally possesses polar bonds. The latter are a consequence of the atoms carrying different effective charges. This effective charge will be displaced in an electric field therefore inducing an additional dipole moment superimposed upon that due to the electron displacements. The contribution this atomic effect makes to the distortion polarisation is therefore known as the atomic polarisation, P_A.

To a good approximation the total molecular polarisation P_T can then be defined as

$$P_T = P_E + P_A + P_\mu \qquad 5.2$$

where,

$$P_\mu = \frac{N\mu^2}{9\varepsilon_o kT} \qquad 5.3$$

and

$$P_D = P_E + P_A \qquad 5.4$$

where μ is the permanent dipole moment, ε_o is the permittivity of free space, N is the Avogadro constant, and k is the Boltzmann constant. Therefore if the temperature dependence of equation 5.1 can be ascertained then it theoretically possible to determine the dipole moment of a substance through the measurement of the dielectric constant and density.

The following sections describe the theoretical basis and the equipment used to determine the dielectric constant of a substance. The dielectric constant has been measured for solutions of various solutes in 1,4-dioxane and the dipole moment for the solute has been calculated according to the methods described in section 5.4. The advantages/disadvantages of various theoretical methods of evaluating the dipole moment from dielectric measurements are discussed.

5.2 DIELECTRIC APPARATUS

The dielectric cell used to measure the static dielectric constant through-out this thesis was of a German commercial origin, manufacturer unknown (Figure 5.1). It was constructed of two gold-plated concentric cylinders of brass, the outer cylinder (A) being hollow to allow the passage of a heating/cooling liquid. The

inner cylindrical electrode (B) was electrically guarded by way of an internal perforated lid (C) to ensure that slight variations in sample volume did not affect the value of the measured capacitance. The cell was filled through an external screw-top lid (D). Measurements of the static dielectric constant were taken over the temperature range 278-338K using a Jubaloo water heater/circulator controllable to ±0.01K. The temperature of the cell was measured using a K-type thermocouple and a digital thermometer accurate to ±0.1K. The sample volume of the cell was approximately 25cm^3.

The electrical capacitance of the cell was measured using a GenRad GR 1689 Precision RLC Digibridge with a basic accuracy of ±0.02%. Measurements of the sample capacitance for calculating the static dielectric constant were performed at 1kHz.

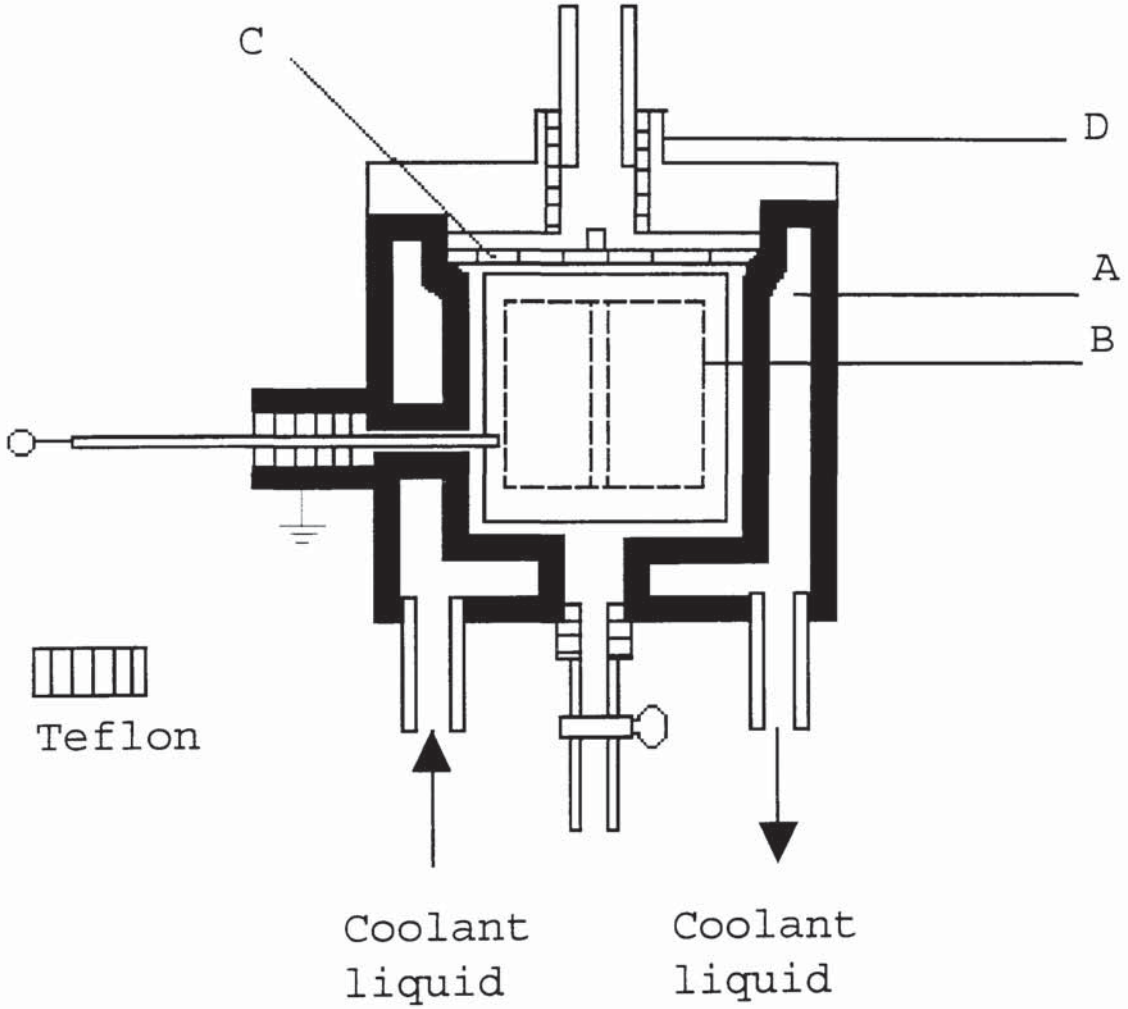

A - Outer cylinder

B - Inner cylindrical lid

C - Perforated lid

D - Screw-top lid

Figure 5.1 Dielectric cell

5.3 THEORY AND MEASUREMENT OF THE DIELECTRIC CONSTANT

A substitution method was used to calculate the static dielectric permittivities of liquids. This entails measuring the capacitance of the cell when empty, when filled with the standard dielectric (HPLC grade toluene from Aldrich), and when filled with the liquid under test. The measured capacitance's under these three conditions are defined as C_a, C_s and C_t respectively. The dielectric constants of the standard medium and the material under test are defined as ε_s and ε, respectively. Assuming that the "stray capacitance" involved with the leads and edge effects does not change upon introducing a liquid into the empty cell (see Appendix H), then

$$\varepsilon = 1 + \frac{(C_t - C_a)}{(C_s - C_a)}(\varepsilon_s - 1) \qquad 5.5$$

All capacitance measurements were performed using a GenRad 1689 precision RLC Digibridge. In practice the GenRad digibridge is zeroed when the cell is empty, thus setting C_a equal to zero. The dielectric constant of the test material is then

$$\varepsilon = 1 + \frac{C_t}{C_s}(\varepsilon_s - 1) \qquad 5.6$$

Table 5.1 shows the measured capacitance of HPLC grade toluene from 278-338K and its associated dielectric constant[75].

The static dielectric permittivities of the liquids used in this thesis were measured in this way, experimental errors were estimated to be less than ±1%. Appendix I contains tables of the static dielectric permittivities determined for the solutions used in this thesis.

Table 5.1 Capacitance and dielectric constant for HPLC grade toluene and 1,4-dioxane.

Temp. °C	Capacitance pF Toluene	Dielectric Constant Toluene
20	43.859	2.39115
25	43.528	2.37900
30	43.183	2.36685
35	42.823	2.35470
40	42.463	2.34255
45	42.118	2.33040
50	41.767	2.31825
55	41.439	2.30610
60	41.104	2.29395
65	40.761	2.28180

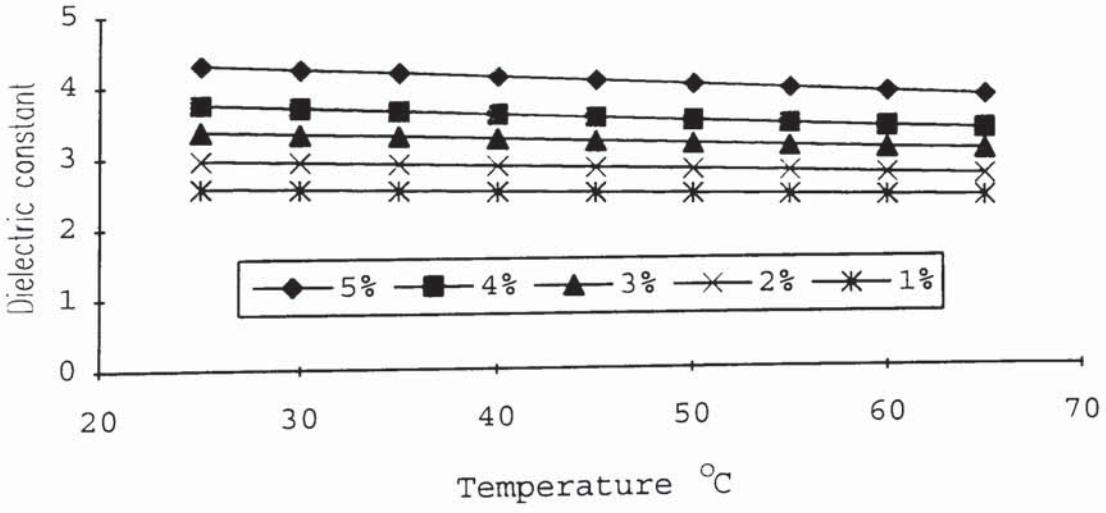

Figure 5.2 Dielectric constant for solutions of 2-methyl-4-nitroaniline in 1,4-dioxane plotted as a function of temperature.

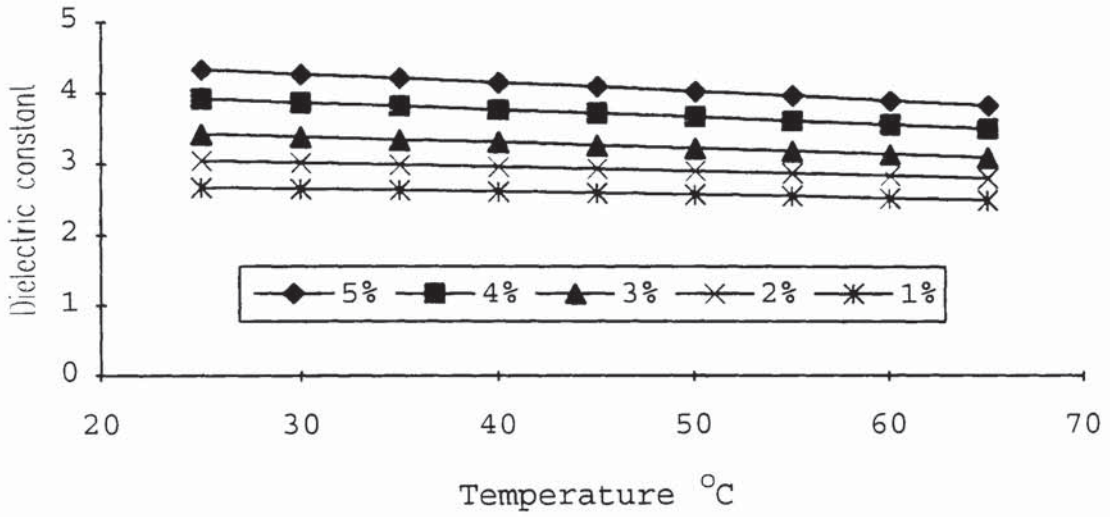

Figure 5.3 Dielectric constant for solutions of p-nitroaniline in 1,4-dioxane plotted as a function of temperature.

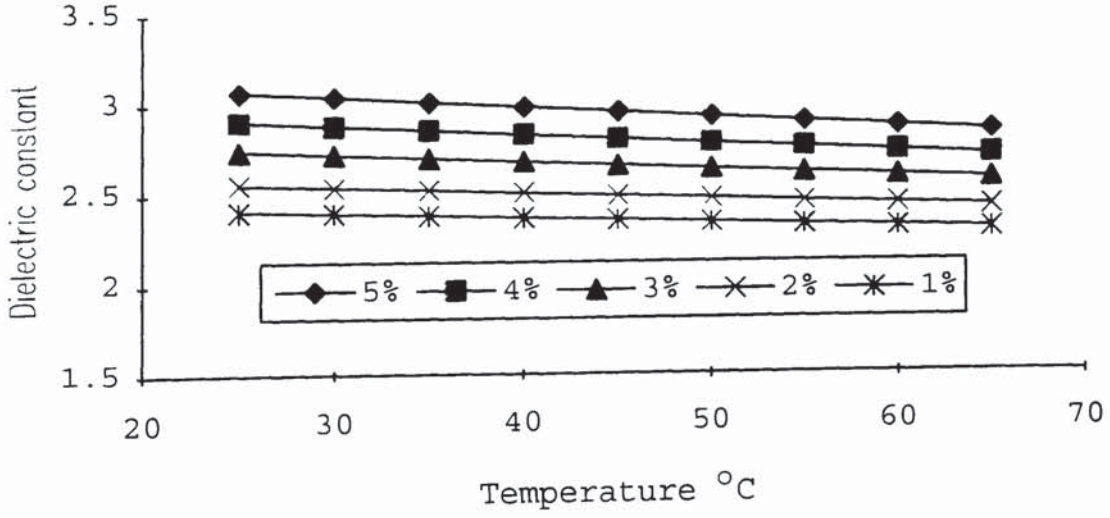

Figure 5.4 Dielectric constant for solutions of nitrobenzene in 1,4-dioxane plotted as a function of temperature.

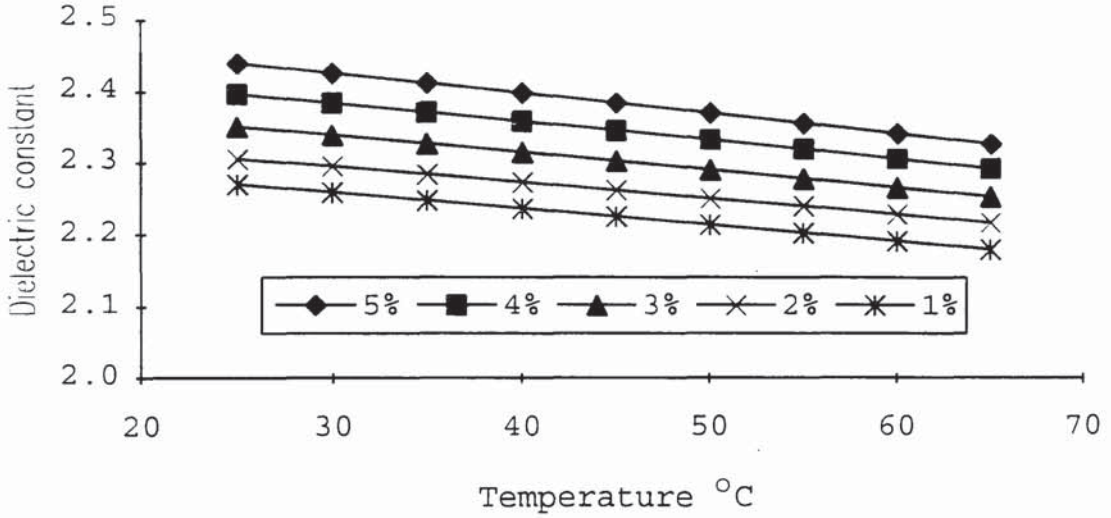

Figure 5.5 Dielectric constant for solutions of aniline in 1,4-dioxane plotted as a function of temperature.

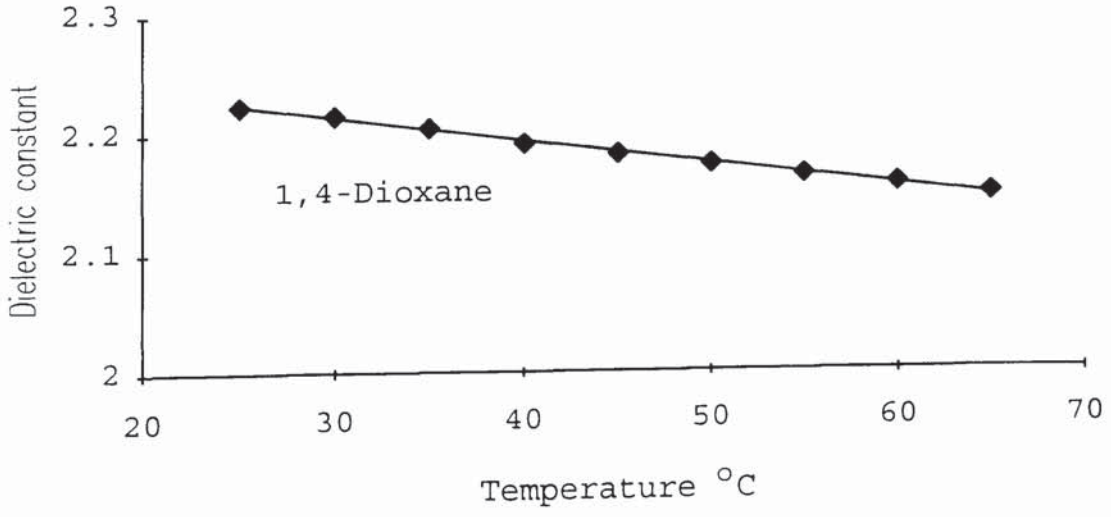

Figure 5.6 Dielectric constant for 1,4-dioxane plotted as a function of temperature.

5.4 DIPOLE MOMENTS: THEORY AND MEASUREMENT

5.4.1 Introduction

The Debye equation for the molecular polarisation of a molecule was derived upon the assumption that the polar and non-polar molecules in a solution do not interact with one another. This gross simplification makes equation 5.1 only truly applicable to gases and vapours at very low pressures. However, it is assumed that as the concentration of a polar solute in a non-polar solvent is decreased then the interaction between the dipoles is diminished and at zero concentration it disappears altogether. Therefore, if the molecular polarisation of finite concentrations of the polar solute in a non-polar solvent can be determined, then these values can then be extrapolated to obtain the limiting value of the molecular polarisation at zero concentration. This limiting value for the molecular polarisation should not then be debased through interaction between the dipoles.

In general for a system comprised of two components the molecular polarisation can be expressed as

$$P_T = P_1 f_1 + P_2 f_2 \qquad 5.7$$

where f_1 and f_2 are the mole fractions of the non-polar solvent and the polar solute respectively, P_1 and P_2 are the molecular polarisation of the non-polar solvent and

the polar solute respectively. P_T is then the molecular polarisation of the solution and is calculated in the same manner as P_1, i.e., using equation 5.1. If it is assumed that the polarisation of the non-polar solvent is unaffected by the presence of the solute molecules, i.e., P_1 remains constant then

$$P_2 = (P_T - P_1 f_1)/f_2 \qquad 5.8$$

The limiting value of P_2 ($_\infty P_2$ - infinite dilution polarisation) obtained as the solute concentration approaches zero can then be considered to be the molecular polarisation of the solute under conditions described by the Debye equation. To calculate the dipole moment of a molecule the orientation polarisation P_μ must be extracted from the measured total infinite dilution polarisation $_\infty P_2$. A standard method is to measure $_\infty P_2$ at various temperatures and then plot $_\infty P_2$ against 1/T. The gradient of a plot of $_\infty P_2$ against 1/T will then be proportional to the dipole moment of the solute. A failing in this method is that the possible error in the values of P_2 deduced experimentally are inversely proportional to the concentrations of the solutions. Consequently, the values for low concentrations, which are the most important in the extrapolation to zero concentration, tend to be the most inaccurate. Since the rate of change of P_2 with f_2 is generally quite considerable at low concentrations, implicitly assuming that P_2 is invariant with concentration leads to a value

of $_{\infty}P_2$ that is lower than that obtained by simply drawing a straight line through the points. Hoecker[76] suggested plotting the product of P_2f_2 against f_2, and using the slope of the resulting curve at zero concentration as the resulting value of $_{\infty}P_2$. Drawing a tangent to such a curve at zero concentration is not easy but with modern computational aids it is possible to fit a polynomial with some accuracy to the points and hence determine the gradient at zero concentration. However, this method has not proved very popular and methods that avoid calculating the polarisation values at each concentration, and hence save considerable effort, have proved more popular. In general, these theories involve determining the gradient in the limit of zero concentration of the density, refractive index, dielectric constant as functions of either the mole fraction or the weight fraction of the solute. These approaches partially isolate the orientation polarisation contribution by excluding the effects of the electronic polarisation that are derived from refractive index measurements. However, these approaches all suffer from the problem of having to determine the atomic polarisation in order to totally isolate the orientation contribution. It is not possible to directly determine the atomic polarisation but a value can be obtained indirectly by measuring the displacement polarisation and then subtracting the electronic polarisation. Some methods of evaluating P_D are microwave measurements of dielectric permittivity, dielectric polarisation

measurements on frozen solutions and the measurement of the temperature dependence of the molecular polarisation (see section 5.4.3). Unfortunately these measurements are often complex and difficult experimentally and tend to lead to large uncertainties in P_A. Consequently, several prominent theories for determining the dipole moment involve an estimate of P_A (typically 5-15% of P_E) or have neglected the contribution made by P_A to P_T.

5.4.2 The solvent effect

Prior to about 1932 it was generally believed that dipole moments derived from measurements of a polar solute in various non-polar solvents gave a value that was equivalent to the so called 'true' value for the isolated (gas phase) molecule. However, as measurements became more accurate it was soon discovered that these inferences were not correct.

Müller[77,78] in 1933 found that the apparent dipole moment for chlorobenzene varied with the nature of the solvent used. Müller also pointed out that the observed variations in the dipole moment were unlikely to be due to molecular association, since no association had been observed in chlorobenzene in the vapour state up to pressures of one atmosphere, and his measurements on dilute solutions had been extended down to concentrations equivalent to 0.1 atmospheres. Faced with this new information the so-called solvent effect began to gain credence.

It is now a well-established fact that a Solvent Effect does exist and if the apparent dipole moment in solution is greater than that for the vapour it is known as the *negative solvent effect* and if the dipole moment is less then it is referred to as the *positive solvent effect*. Many approaches have been made to resolve problems associated with the measurement of the dipole moments of solutes. These have included theoretical treatments based upon the electrostatic inductive effects of the dipoles on the medium in their vicinity and/or drastic modifications of the Clausius-Mosotti-Debye theory.

It is worth noting that carbon tetrachloride, as a result of its symmetrical character and small tendency for mutual interaction with other compounds, behaves as the nearest possible approach to an ideal solvent for the purpose of measuring dipole moments in solution. Unfortunately, it was found that some of the compounds investigated in this thesis were insoluble in carbon-tetrachloride. An acceptable alternative solvent was 1,4-dioxane which was used as the sole solvent throughout this study, to ensure consistency in subsequent calculations of solute dipole moments etc.

5.4.3 Temperature method for the evaluation of dipole moments.

From equations (5.2, 5.3 and 5.4) it can be seen that the dispersion polarisation P_D of a molecule is independent of temperature. If the dipole moment is assumed to be independent of temperature, then it follows that the orientation polarisation will be inversely proportional to the temperature. It is, therefore possible to write the total molecular polarisation in the form

$$P_T = A + B/T \qquad 5.9$$

where A and B are constants. Hence, a plot of infinite dilution molecular polarisation (see section 5.1) against 1/T should be a straight line with an intercept equivalent to the dispersion polarisation P_D. The slope of the plot will be proportional to the square of the dipole. It follows from equation 5.3 that

$$\mu^2 = \frac{9\varepsilon_o kB}{N} \qquad 5.10$$

The atomic polarisation can be obtained by subtracting the infinite dilution electronic polarisation from the dispersion polarisation according to

$$_\infty P_A = {}_\infty P_D - {}_\infty P_E \qquad 5.11$$

For solutions it is normally only possible to determine the density, dielectric constant and infinite wavelength refractive index over a limited temperature range. This means that a long extrapolation of $_{\infty}P_2$ against 1/T is required to calculate $_{\infty}P_D$ and therefore it is not easy to determine $_{\infty}P_A$ accurately. Graphs of $_{\infty}P_2$ for the various compounds used in this thesis are plotted in Figures 5.7 to 5.10 as a function of temperature. The gradients of these graphs are used to calculate the dipole moment of the solute according to equation 5.10. The dipole moment results are shown in Table 5.2.

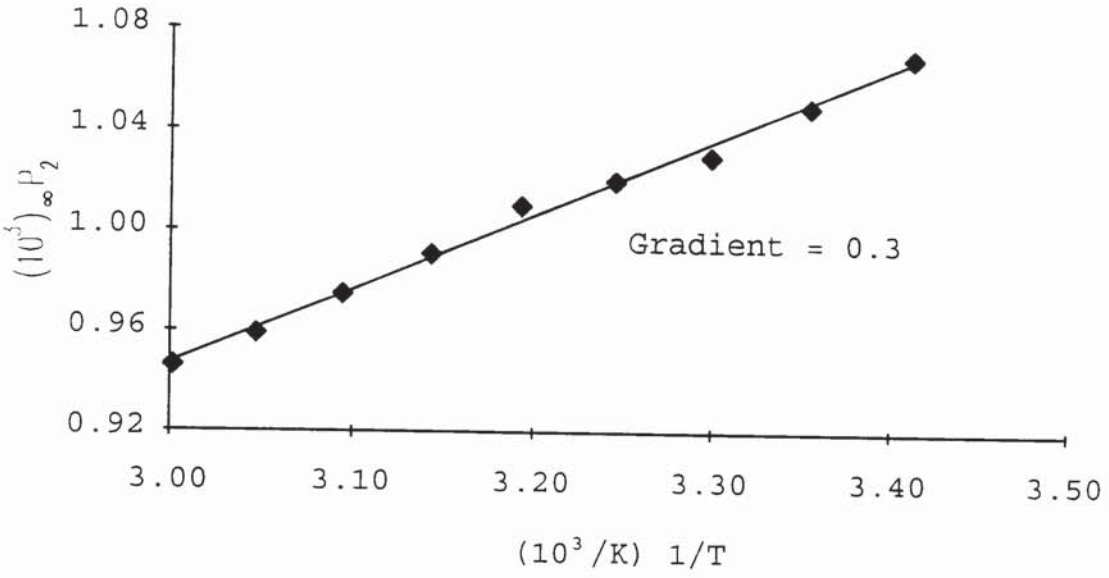

Figure 5.7 Infinite dilution total polarisation, $_\infty P_2$, for 2-methyl-4-nitroaniline in 1,4-dioxane plotted as a function of temperature.

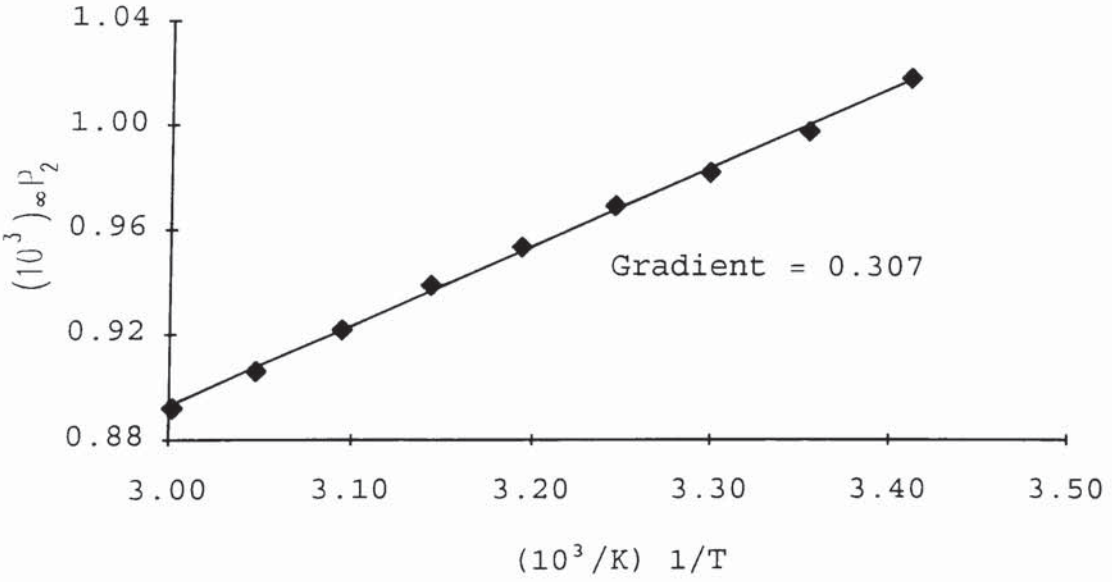

Figure 5.8 Infinite dilution total polarisation, $_\infty P_2$, for p-nitroaniline in 1,4-dioxane plotted as a function of temperature.

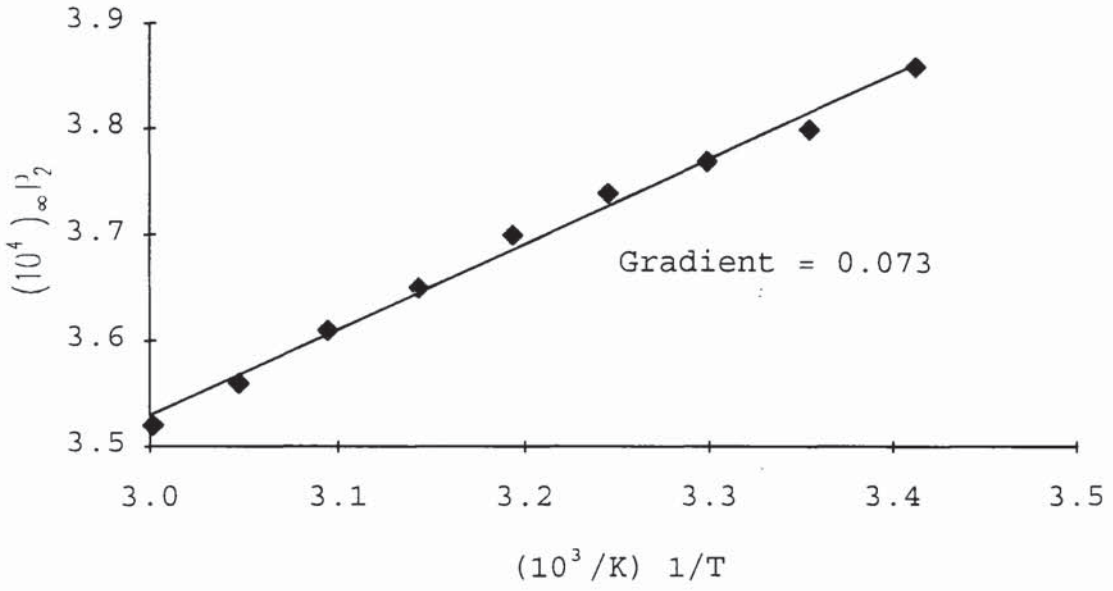

Figure 5.9 Infinite dilution total polarisation, $_\infty P_2$, for nitrobenzene in 1,4-dioxane plotted as a function of temperature.

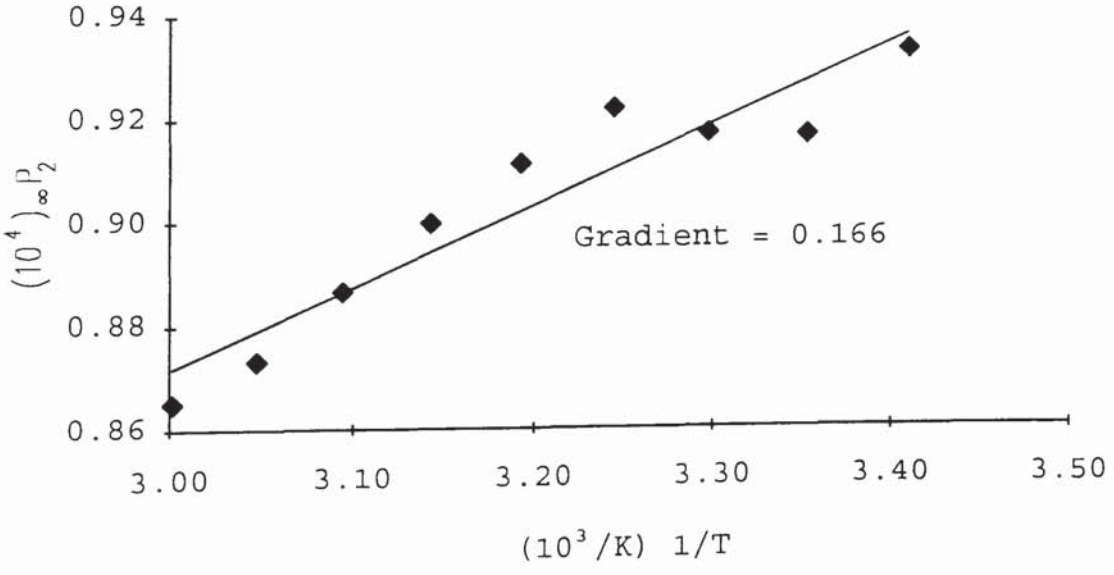

Figure 5.10 Infinite dilution total polarisation, $_\infty P_2$, for aniline in 1,4-dioxane plotted as a function of temperature.

Table 5.2 Infinite dilution total polarisability, $_{\infty}P_2$.

Temp. °C	$(10^3)_{\infty}P_2$ 2-Methyl-4-nitroaniline	$(10^3)_{\infty}P_2$ p-Nitroaniline	$(10^3)_{\infty}P_2$ Nitrobenzene	$(10^3)_{\infty}P_2$ Aniline
20	1.0(7)	1.0(2)	3.8(6)	0.93(4)
25	1.0(5)	1.0(0)	3.8(0)	0.91(7)
30	1.0(3)	0.9(8)	3.7(7)	0.91(8)
35	1.0(2)	0.9(7)	3.7(4)	0.92(2)
40	1.0(1)	0.9(5)	3.7(0)	0.91(2)
45	0.9(9)	0.9(4)	3.6(5)	0.90(0)
50	0.9(7)	0.9(2)	3.6(1)	0.88(7)
55	0.9(6)	0.9(1)	3.5(6)	0.87(3)
60	0.9(5)	0.8(9)	3.5(2)	0.86(5)

Temp. = Temperature

5.4.4 The Guggenheim method for the evaluation of dipole moments

The Guggenheim[79] method of determining the dipole moment of a solute molecule in a non-polar solvent has two distinct advantages over the temperature method. As the Guggenheim method avoids the need for measuring the densities of the solutions accurately and as the dipole moment is determined at a specific temperature the potential problem associated with a temperature dependent dipole moment is avoided. Guggenheim's treatment does not involve any assumptions not already embodied in the general Debye theory, but the assumption regarding the value of P_A poses a major problem in all theories except the temperature method (see section 5.13). Guggenheim suggested that atomic polarisation's could be considered proportional to molecular volumes. If this approximation is accepted then

$$\mu^2 = \frac{9\varepsilon_o kT}{N} \operatorname{Lim}_{c \to 0} \frac{\partial D}{\partial C} \qquad 5.12$$

where,

$$D = \frac{3\left(\varepsilon_{12} - n_{12}^2\right)}{\left(\varepsilon_{12} + 2\right)\left(n_{12}^2 + 2\right)} \qquad 5.13$$

and c is the concentration of the solution in moles/m^3. A simplification to equation 5.12 and equation 5.13 is to

plot $\varepsilon_{12} - n_{12}^2$ against c, where a curve is obtained with intercept $\varepsilon_1 - n_1^2$. The dipole moment is then

$$\mu^2 = \frac{27\varepsilon_o kT}{N(\varepsilon_1 + 2)(n_1^2 + 2)} \text{ Lim } {}_{(c\to 0)} \frac{\partial(\varepsilon_{12} - n_{12}^2)}{\partial C} \qquad 5.14$$

Often, solutions are made up by weight, and hence the simplest form in which to express the concentration of the solute is by its weight fraction, w_2. The weight fraction is related to c by the expression

$$c = \frac{d_{12} w_2}{M_2} \qquad 5.15$$

Also, from equation 5.13 we can write $\partial D/\partial w_2$ in the form

$$\frac{\partial D}{\partial w_2} = \frac{3}{(\varepsilon_{12} + 2)^2} \cdot \frac{\partial \varepsilon}{\partial w_2} - \frac{3}{(n_{12}^2 + 2)^2} \cdot \frac{\partial n^2}{\partial w_2} \qquad 5.16$$

Therefore, if the limiting values of $\partial\varepsilon_{12}/\partial w_2$ (defined as a) and $\partial n_{12}^2/\partial w_2$ (defined as b), at zero concentration, are determined then

$$\mu^2 = \frac{27k\varepsilon_o TM_2}{d_1 N} \left\{ \frac{a}{(\varepsilon_1 + 2)^2} - \frac{b}{(n_1^2 + 2)^2} \right\} \qquad 5.17$$

Weight fractions can also be applied to the simplified Guggenheim equation such that equation 5.14 can be rewritten as

$$\mu^2 = \frac{27k\varepsilon_o TM_2}{d_1 N(\varepsilon_1 + 2)(n_1^2 + 2)} \lim_{(w_2 \to 0)} \frac{\partial(\varepsilon - n^2)}{\partial w_2} \qquad 5.18$$

The difference obtained in the dipole moment from using the simplified Guggenheim equation rather than equations 5.12 or 5.17 will be small as long as $\varepsilon_1 - n_1^2$ is small. Amongst the solvents normally used for dielectric constant determinations the greatest difference between ε and n^2 (about 0.18) occurs with 1,4-dioxane. This introduces a difference in the calculated dipole moment that is approximately 2.74% greater than the value obtained using equation 5.12 or 5.17. Hence as the solutions where made up by weight equation 5.17 was used to calculate the dipole moments of the solutes.

Table 5.3 Dipole moment of 2-methyl-4-nitroaniline in 1,4-dioxane using the Guggenheim method.

Temp. °C	a $\partial\varepsilon_{12}/\partial w_2$	b $\partial n_{12}^2/\partial w_2$	μ debye
25	43	0.44	7.(20)
30	42	0.52	7.(18)
35	41	0.59	7.(19)
40	40	0.67	7.(19)
45	39	0.74	7.(19)
50	38	0.81	7.(19)
55	37	0.89	7.(18)
60	36	0.96	7.(17)

Temp. = Temperature

Table 5.4 Dipole moment of p-nitroaniline in 1,4-dioxane using the Guggenheim method.

Temp. °C	a $\partial\varepsilon_{12}/\partial w_2$	b $\partial n_{12}^2/\partial w_2$	μ debye
25	44	0.50	6.(93)
30	43	0.55	6.(91)
35	42	0.60	6.(90)
40	41	0.65	6.(90)
45	39	0.70	6.(89)
50	38	0.75	6.(88)
55	37	0.80	6.(86)
60	36	0.85	6.(84)

Temp. = Temperature

Table 5.5 Dipole moment of nitrobenzene in 1,4-dioxane using the Guggenheim method.

Temp. °C	a $\partial\varepsilon_{12}/\partial w_2$	b $\partial n_{12}^2/\partial w_2$	μ : debye
25	18	0.10	4.(15)
30	17	0.15	4.(14)
35	17	0.21	4.(14)
40	16	0.26	4.(15)
45	16	0.31	4.(15)
50	16	0.36	4.(14)
55	15	0.41	4.(14)
60	15	0.46	4.(13)

Temp. = Temperature

Table 5.6 Dipole moment of aniline in 1,4-dioxane using the Guggenheim method.

Temp. °C	a $\partial\varepsilon_{12}/\partial w_2$	b $\partial n_{12}^2/\partial w_2$	μ debye
25	4.5	0.49	1.(70)
30	4.3	0.47	1.(69)
35	4.3	0.46	1.(71)
40	4.2	0.44	1.(73)
45	4.1	0.42	1.(73)
50	4.0	0.41	1.(74)
55	3.9	0.39	1.(74)
60	3.8	0.38	1.(74)

Temp. = Temperature

5.5 DIPOLE MOMENT MEASUREMENTS IN CONDENSED SYSTEMS

5.5.1 Onsager's theory

Onsager's[80] theory is in principal based upon the Clausius-Mosotti-Debye theory but it does have the important distinction of including what Onsager himself called the "Reaction Field". The direction of the reaction field which is assumed to be parallel to the axial direction of the dipole moment, is caused by electrical displacements in the non-polar solvent molecules following the addition of a polar solute molecule. Evidently, therefore, the reaction field must be proportional to the total dipole moment of the solute molecule and dependent on the instantaneous orientation of the dipole moment.

Onsager adopted the same molecular model as Debye, and developed the following equation for the dipole moment of a pure polar liquid.

$$\mu^2 = \frac{9\varepsilon_o kT}{N} \cdot \frac{\left(\varepsilon - n^2\right)\left(2\varepsilon + n^2\right)}{\varepsilon\left(n^2 + 2\right)^2} \cdot \frac{M}{d} \qquad 5.19$$

5.6 DISCUSSION OF DIPOLE MOMENT RESULTS

The calculated value of the dipole moment for aniline (1.6 and 1.7 debye) dissolved in 1,4-dioxane compares very favourably with the previously published values of 1.78 debye[81], 1.75 debye[82], and 1.75-1.91 debye[83]. These

published values for aniline can be directly compared to the Guggenheim value presented here as the solvent and method of calculating the dipole moment were identical. Published values for the dipole moment of nitrobenzene vary from 3.95-4.22 debye[83,84,85,86,49,87] these include values calculated from a variety of solvents and as a pure liquid and gas. It is worth noting that the value of the dipole moment calculated using Guggenheims method are 3.97 debye and 3.96 debye[49] using CCl_4 and C_6H_6 respectively as solvents. As 1,4-dioxane tends to have a positive solvent effect the value presented here of 4.1 debye using the Guggenheim method is not unexpected. Toluene has a published value of 0.34 debye[85] that compares well with our value of 0.36 debye using the Onsager equation, unfortunately the method by which the published value was determined was not reported. The dipole moment of p-nitroaniline has been reported as 7.2 debye[88] measured as a neat melt, 6.2 debye[87] as a solute dissolved in acetone, and 6.8 debye[89] as a solute in 1,4-dioxane. Again as 1,4-dioxane tends to have a positive solvent effect the value presented here of 6.9 and 7.1 debye is not unexpected especially when compared to the literature value of 6.8 debye. It would be expected that the addition of the CH_3 to p-nitroaniline would result in a slightly larger dipole moment for 2-methyl-4-nitroaniline than that for p-nitroaniline. The value of the dipole moment of 2-methyl-4-nitroaniline determined here is 6.9 and 7.2 debye which is on average slightly

larger than the average value determined for p-nitroaniline.

Therefore, for all the compounds investigated the present dipole moments agree very closely with previously published values when the method of calculation and the solvent used are taken into account. In general, the Guggenheim method of calculating the dipole moment of a solute is considered superior because it involves a smaller number of calculations than the temperature method.

Table 5.7 Dipole moment results for various compounds using different methods of calculation.

Compound	Solvent	Method of Calculation	Dipole moment debye	Error ± debye
2-Methyl-4-nitroaniline	1,4-dioxane	Temperature	6.9	0.1
	1,4-dioxane	Guggenheim	7.2	0.1
		Average	7.1	0.1
p-Nitroaniline	1,4-dioxane	Temperature	7.1	0.1
	1,4-dioxane	Guggenheim	6.9	0.1
		Average	7.0	0.1
Nitrobenzene	1,4-dioxane	Temperature	3.7	0.2
	1,4-dioxane	Guggenheim	4.1	0.1
		Average	3.9	0.2
Aniline	1,4-dioxane	Temperature	1.6	0.1
	1,4-dioxane	Guggenheim	1.7	0.1
		Average	1.7	0.1
Toluene	None	Temperature	0.22	0.1
	None	Onsager	0.36	0.1

CHAPTER 6

REFRACTIVE INDEX AND ELECTRONIC POLARISATION

6.1 REFRACTIVE INDEX EQUIPMENT

The refractive indices of solvents and solutions were measured using a Zeiss Abbe refractometer (Model A Series 7) which can take readings of the refractive index to an accuracy of ±0.0001. Although the Abbe refractometer is not generally as accurate as some other methods of measuring refractive indices it does have the advantage that thermal equilibrium is established extremely rapidly. This means that a series of measurements on one solution can be made very quickly and a good mean value obtained. Refractive indices were measured at 593nm and 633nm and over the temperature range 298-338K.

6.2 CALIBRATION OF THE ABBE REFRACTOMETER

Refractive indices measured using an Abbe refractometer involve the initial measurement of the angular displacement of a beam of light following the insertion of a sample. The angle of deviation is measured in minutes and seconds. As the refractive index is proportional to the angle of deviation the refractive

index can therefore be readily obtained from the calibration chart provided with the instrument. For ease of use with a spreadsheet the calibration chart was converted into a third order polynomial equation.

6.3 CALCULATION OF THE INFINITE-WAVELENGTH REFRACTIVE INDEX (CAUCHY THEOREM)

For all the compounds examined in this thesis the refractive index decreases with increasing wavelength (see Appendix I) which is the phenomenon of normal dispersion. Therefore, it may be assumed that the main part of the dispersion of these compounds corresponds to an absorption in the ultraviolet region. This implies that in order to obtain accurate values for the electronic polarisability, α, of a molecule, it is necessary to use the values of the refractive index extrapolated to zero frequency or infinite wavelength, without taking into account any contributions by the atomic or the orientational polarisation. One way to obtain an extrapolated value to n_∞ is to use the Cauchy dispersion formula[90,91] which develops the refractive index in a series such that

$$n = n_\infty + \frac{a}{\lambda^2} + \frac{b}{\lambda^4} + \ldots\ldots\ldots \qquad 6.1$$

where a and b are constants. The refractive index at infinite wavelength, n_∞, may be calculated with

acceptable accuracy by using only the first two terms in equation 6.1. Therefore if n_1 and n_2 are the refractive indices of a sample at wavelengths of λ_1 and λ_2 respectively then

$$n_\infty = \frac{\lambda_1^2 n_1 - \lambda_2^2 n_2}{\lambda_1^2 - \lambda_2^2} \qquad 6.2$$

6.4 MOLECULAR REFRACTION - ELECTRONIC POLARISATION

As already shown in Chapter 5 the total molecular polarisation, P_T, of a substance is defined by

$$P_T = \frac{(\varepsilon - 1)M}{(\varepsilon + 2)\rho} \qquad 6.3$$

It was shown by Maxwell[92] that the dielectric constant of a medium is related to its refractive index, measured for the same frequency of radiation, by the function

$$n^2 = \varepsilon\psi \qquad 6.4$$

where ψ is the magnetic permeability of the medium considered. Except for ferromagnetic materials ψ is almost equal to unity, it therefore follows that

$$\varepsilon_\lambda = n_\lambda^2 \qquad 6.5$$

Thus by re-arranging equation 6.4 and equation 6.5 it may be shown that[93]

$$P_E = \frac{(n^2 - 1)M}{(n^2 + 2)\rho} \qquad 6.6$$

From the wave and electromagnetic theory of light Lorenz[94,95] and Lorentz[96] also independently showed that the function

$$R = \frac{(n^2 - 1)M}{(n^2 + 2)d} \qquad 6.7$$

where M is the mass and d is the density, is a constant independent of temperature. The quantity R, is known as the molecular refraction.

6.4.1 MEASUREMENT OF THE ELECTRONIC POLARISABILITY

As the refractive index extrapolated to infinite wavelength (see section 6.3) is entirely due to the electronic contribution, equation 6.5 can be re-written as

$$P_E = \frac{(n_\infty^2 - 1)M}{(n_\infty^2 + 2)\rho} = \frac{N(\alpha_1 + \alpha_2 + \alpha_3)}{9\varepsilon_o} \qquad 6.8$$

From chapter 2

$$\alpha = \frac{1}{3}\left(\alpha_1 + \alpha_2 + \alpha_3\right) \qquad 6.9$$

Therefore substituting equation 6.8 into equation 6.7 and rearranging gives:-

$$\alpha = \frac{3\varepsilon_o P_E}{N} \qquad 6.10$$

Strictly speaking, equation 6.6 is only valid for gases or vapours at very low pressures, therefore for polar solutes the infinite dilution electronic polarisation P_E is generally determined by employing a method similar to that used for determining the infinite dilution molecular polarisation (see Chapter 5). In practice the electronic polarisation of a solute is evaluated for a fixed concentration of solute over a temperature range. As the electronic polarisation is effectively temperature independent the average value is taken for the chosen temperature range. It is assumed that

$$P_E = f_1 P_{E1} + f_2 P_{E2} \qquad 6.11$$

where P_E is the electronic polarisation for the solution, f_1 and f_2 are the mole fractions of the solvent and solute respectively, and P_{E1} and P_{E2} are the electronic polarisations of the solvent and solute respectively. Using equation 6.10 it is then possible to calculate P_{E2}

by measuring the refractive index of the solutions. The polarisability, α_2, of the solute may be determined using equation 6.9. In general, α_2 will depend on the concentration of solute and must be extrapolated to zero concentration to obtain the infinite dilution value, ${}_\infty\alpha_2$. This may be achieved by fitting a graph of α_2 against f_2 to a straight line and taking the intercept on the y-axis to be equal to ${}_\infty\alpha_2$. The refractive index is accurate to the third decimal place. The error in the infinite wavelength refractive index is expressed as the most probable error and is defined by

$$g = \left(g_1^2 + g_2^2\right)^{1/2} \qquad 6.12$$

where f is the percentage error in n_∞ and g_1 and g_2 are the percentage errors in n_1 and n_2 respectively. The most probable accuracy in n_∞ due to errors in n_1 and n_2 is to the second decimal place.

As an example the steps required to determine the electronic polarisability, α_2, (using the above equations) for a 5% solution of 2-methyl-4-nitroaniline in 1,4-dioxane and for pure 1,4-dioxane has been outlined in Table 6.1 to Table 6.5. Table 6.1 contains the density and refractive index data for 1,4-dioxane. The infinite wavelength refractive index in Table 6.1 is calculated from the refractive index data in Table 6.1 at 589.3nm and 632.8nm according to the Cauchy theorem. The infinite refractive index and the density data in Table 6.1 is then used to calculate the molecular refraction data in

Table 6.2 according to equation 6.8. Table 6.2 also contains the average electronic polarisability of 1,4-dioxane calculated from the molecular refraction data using equation 6.10. In a similar manner to that described above the molecular refraction of a 5% solution of 2-methyl-4-nitroaniline is calculated in Table 6.5. The molecular refraction of the solution in Table 6.5 is then converted into the electronic polarisation of the solute using equations 6.10 and 6.11. The electronic polarisability of the solute is calculated in exactly the same way for the remaining concentrations. The electronic polarisability for the solutions are then extrapolated to the infinite dilution electronic polarisation. The graphical extrapolation of P_E to the infinite dilution value for 2-methyl-4-nitroaniline is shown in Figure 6.1.

Table 6.6 contains all the infinite dilution electronic polarisation values, ${}_{\infty}\alpha_2$, determined for the compounds and solutes used in this thesis. The error in ${}_{\infty}\alpha_2$ is presented as the error in the intercept of the ordinate axis and has a 68% confidence limit.

Table 6.1 Refractive index and density data for HPLC grade 1,4-dioxane.

Temp. °C	Refractive Index at 589.3nm	Refractive Index at 632.8nm	Refractive Index at Infinite wavelength	Density kg m^{-3}
25	1.419(5)	1.417(4)	1.40(32)	1029.(12)
30	1.417(1)	1.415(0)	1.40(16)	1023.(30)
35	1.415(0)	1.412(9)	1.40(00)	1017.(26)
40	1.412(4)	1.410(4)	1.39(84)	1011.(54)
45	1.409(8)	1.408(3)	1.39(68)	1005.(61)
50	1.407(7)	1.406(0)	1.39(51)	1000.(00)
55	1.405(3)	1.403(7)	1.39(35)	994.(15)
60	1.403(1)	1.401(6)	1.39(19)	988.(56)

Table 6.2 Molecular refraction and electronic polarisation data for HPLC grade 1,4-dioxane.

Temp. °C	Molecular Refraction m^3	Average Electronic Polarisability (α) Cm^2V^{-1}
25	2.09E-05	9.3E-40
30	2.09E-05	
35	2.10E-05	
40	2.10E-05	
45	2.11E-05	
50	2.11E-05	
55	2.12E-05	
60	2.12E-05	

Table 6.3 Molar fractions and mean molecular weight for solutions of 2-methyl-4-nitroaniline in 1,4-dioxane.

Conc. Solution	Molar Fraction f_1	Molar Fraction f_2	Molecular Weight kg m^{-3}
5%	0.97171	0.02829	0.08993
4%	0.97741	0.02259	0.08957
3%	0.98311	0.01689	0.08920
2%	0.98876	0.01124	0.08884
1%	0.99439	0.00561	0.08848

Table 6.4 Refractive index and density data for a 5% solution of 2-methyl-4-nitroaniline in HPLC grade 1,4-dioxane.

Temp °C	Refractive Index at 589.3nm	Refractive Index at 632.8nm	Refractive Index at Infinite wavelength	Density kg m^{-3}
25	1.431(2)	1.428(2)	1.410(6)	1039.(47)
30	1.428(7)	1.426(6)	1.410(3)	1033.(77)
35	1.426(9)	1.424(6)	1.409(9)	1027.(67)
40	1.424(1)	1.422(2)	1.409(5)	1022.(01)
45	1.421(9)	1.420(2)	1.409(1)	1016.(90)
50	1.419(8)	1.417(9)	1.408(7)	1011.(03)
55	1.416(2)	1.415(7)	1.408(3)	1005.(16)
60	1.414(1)	1.413(1)	1.408(0)	1000.(08)

Table 6.5 Molecular refraction and electronic polarisation data for a 5% solution of 2-methyl-4-nitroaniline in HPLC grade 1,4-dioxane.

Temp. °C	Molecular Refraction Solution m^3	Molecular Refraction Solute m^3	Average Electronic Polarisability (α) Cm^2V^{-1}
25	2.15E-05	3.52E-05	2.1E-39
30	2.16E-05	3.87E-05	
35	2.17E-05	4.26E-05	
40	2.18E-05	4.63E-05	
45	2.19E-05	5.01E-05	
50	2.20E-05	5.33E-05	
55	2.21E-05	5.72E-05	
60	2.22E-05	6.5E-05	

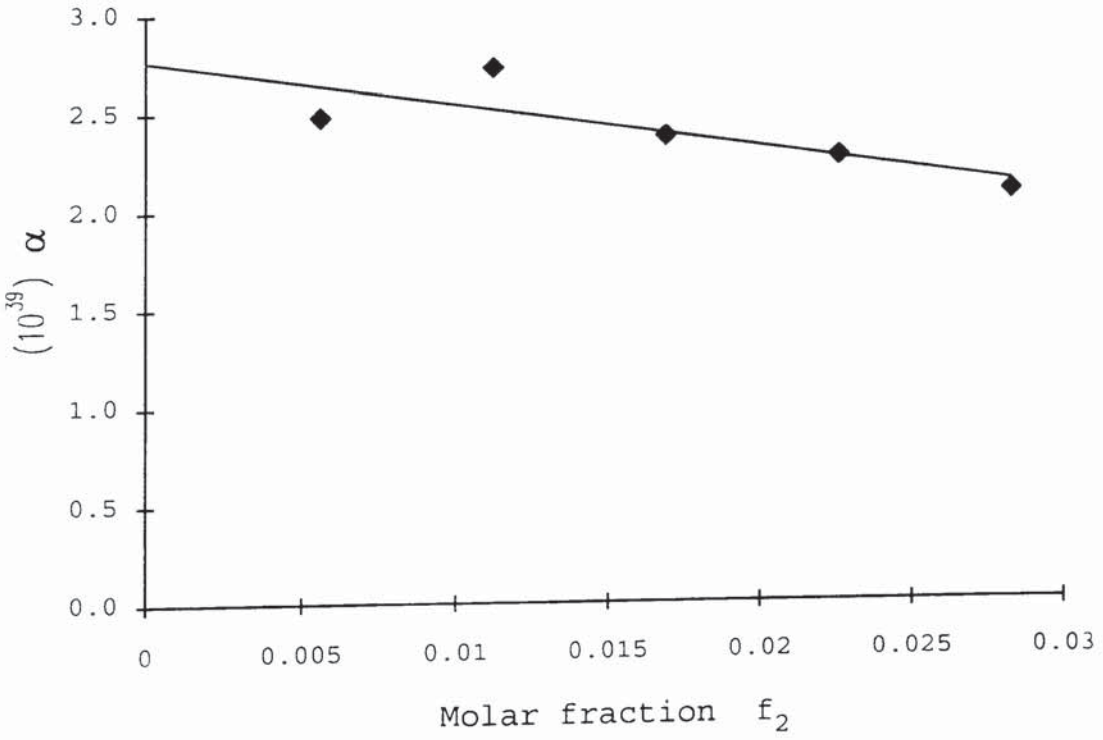

Figure 6.1 Electronic polarisability, α, for solutions of 2-methyl-4-nitroaniline in 1,4-dioxane plotted as a function of molar fraction.

Table 6.6 Electronic Polarisation data for various compounds.

Compound (or solute)	Solvent	Electronic Polarisability ($_{\infty}\alpha_2$) Cm^2V^{-1}	Error $\pm$ Cm^2V^{-1}
2-Methyl-4-nitroaniline	1,4-dioxane	2.8E-39	2E-40
p-Nitroaniline	1,4-dioxane	2.0E-39	1E-40
Nitrobenzene	1,4-dioxane	1.5E-39	2e-40
Aniline	1,4-dioxane	1.17E-39	5E-41
Toluene	None	1.19E-39	1E-41
1,4-Dioxane	None	9.28E-40	4E-42

CHAPTER 7

DEPOLARISATION THEORY AND MEASUREMENT

7.1 INTRODUCTION

The anisotropy of the electric dipole polarisability is a molecular property that, in addition to its' vital importance in all applications of the Kerr effect to problems of molecular structure, is needed in the evaluation of the molecular hyperpolarisabilities from the Kerr effect. The anisotropy parameter, δ^2, of a molecule can be determined from the Rayleigh depolarisation ratio of scattered light[97,98]. This Chapter deals with the theory, experimental method and results obtained for various molecules.

7.2 RAYLEIGH SCATTERING AND MOLECULAR ANISOTROPY

Rayleigh scattering makes use of the fact that for non-isotropic molecules the dipole induced by an incident light beam is in general not parallel to the electric field vector of incident light, which means that the light scattered in a direction perpendicular to that of the incident beam will contain a component with an electric field vector parallel to the direction of

propagation of the incident beam. The intensity of this component depends on the anisotropy of the molecules' polarisability. The anisotropy parameter for a molecule when the incident light beam is vertically polarised is determined from[99]:-

$$\delta^2 = \frac{5\Delta}{(3 - 4\Delta)} \qquad 7.1$$

where Δ is the "depolarisation factor" for light scattered transversely by the material when a light beam passes through it. The "depolarisation factor", Δ, is defined as[100]:-

$$\Delta = \frac{I_h}{I_v} \qquad 7.2$$

where I_h and I_v are the intensity of polarised light in the horizontal plane and vertical plane respectively for transversely scattered light.

Equation 7.1 is only valid for light scattered by low density gases. For liquids the effect of fluctuations in the number of molecules in an element of volume V has to be taken into consideration; this is given by $\overline{(\Delta v)}^2 = RT\beta v^2/NV$, where $\overline{(\Delta v)}^2$ is the mean square deviation of the number of molecules per unit volume from the mean value v, β is the isothermal compressibility, V is the volume, and N is Avogadro's number. Consequently, for liquids equation 7.3 (below) should be used instead of equation 7.1 (see reference 101).

$$\delta^2 = \frac{5RT\beta v\Delta}{(3 - 4\Delta)N} \qquad 7.3$$

7.3 MOLECULAR ANISOTROPY AT INFINITE DILUTION

In calculating the first hyperpolarisability of a molecule from the infinite dilution molar Kerr constant it was uncertain as to whether or not it was appropriate to use depolarisation data measured on dilute gases. This problem was addressed by Le Fèvre and Rao[102] who determined that depolarisation factors of solutions as the correct source in the circumstances stated. Le Fèvre and Rao developed a procedure for determining the molecular anisotropy of a molecule at infinite dilution, ${}_\infty\delta^2$, such that equation 7.3 is rewritten for a solution containing a molar fraction f_2 of solute of molecular weight M_2 in a solvent of molecular weight M_1:-

$$\delta_{12}^2 = \frac{5\Delta_{12}RT\beta_{12}d_{12}}{(3 - 4\Delta_{12})M_{12}} \qquad 7.4$$

where R = 8.314×10^7 erg K^{-1} mol^{-1}, T is the absolute temperature, and d is the density. In analogy with the determination of ${}_\infty K_2$ (see section 2.6) the following equations are assumed to apply at high dilution

$$\Delta_{12} = \Delta_1 + Af_2 \qquad 7.5$$

$$d_{12} = d_1 + Df_2 \qquad 7.6$$

$$\beta_{12} = \beta_1 + Bf_2 \qquad 7.7$$

$$M_{12} = M_1f_1 + M_2f_2 \qquad 7.8$$

If equation 7.4 is expanded, by substitution from equation 7.5 to equation 7.8, differentiated with respect to f_2 and $f_2=0$ then

$$ {}_{\infty}\delta_2^2 = \delta_1^2\left[1 + \frac{A}{\Delta_1} + \frac{B}{\beta_1} + \frac{D}{d_1} + \frac{(M_1 - M_2)}{M_1} + \frac{4A}{(3 - 4\Delta_1)}\right] \qquad 7.9 $$

Following Le Fèvre and Rao[102], B/β_1 is considered to be sufficiently small with respect to A/Δ_1 that it may be safely ignored in equation 7.9.

7.4 EXPERIMENTAL METHOD

Measurements of the depolarisation ratio were taken using a Otsuka DLS-700 Dynamic Light Scattering Spectrophotometer. The incident light source was a helium neon laser emitting vertically polarised light at 632.6nm. Samples were maintained at a constant temperature of 20°C using a water circulator connected to the light-scattering instrument.

Every sample was filtered using a Millipore Fluoropore 0.22μm filter before being inserted into the DLS spectrophotometer. All the compounds measured, except toluene and 1,4-dioxane, were made up as solutions in 1,4-dioxane and were of varying concentrations. Toluene and 1,4-dioxane were measured in the undiluted form. Measurements were repeated four times each of which was a set of ten measurements and then averaged to obtain a better degree of accuracy. The infinite dilution

anisotropy parameter was then calculated using the methods described in section 7.3.

7.4.1 Discussion of results

The anisotropy of the compounds increased with the increasing lack of symmetry in the molecules. Most depolarisation work has been done on gases and pure liquids and very little if any at all on infinite dilution methods. There are, therefore, only a few literature values with which to make any comparison with the results presented in this chapter.

The infinite dilution anisotropy for nitrobenzene has been previously determined by Le Fèvre in carbon-tetrachloride using white light. Le Fèvre obtained a value of 0.0325 that is lower than the value 0.0365 obtained in this thesis. However it should be noted that the gas value for nitrobenzene using white light has been measured as 0.0545. Therefore, considering that the anisotropy parameter calculated in this thesis was measured using a different light source and solvent, to Le Fèvre, the value of 0.0365 would appear to be quite reasonable (see Table 7.3). It can be seen from Tables 7.4 and 7.5 that the anisotropy parameters for toluene and 1,4-dioxane agree well with literature values. Appendix K contains tables of the depolarisation ratio determined for the solutions used in this thesis.

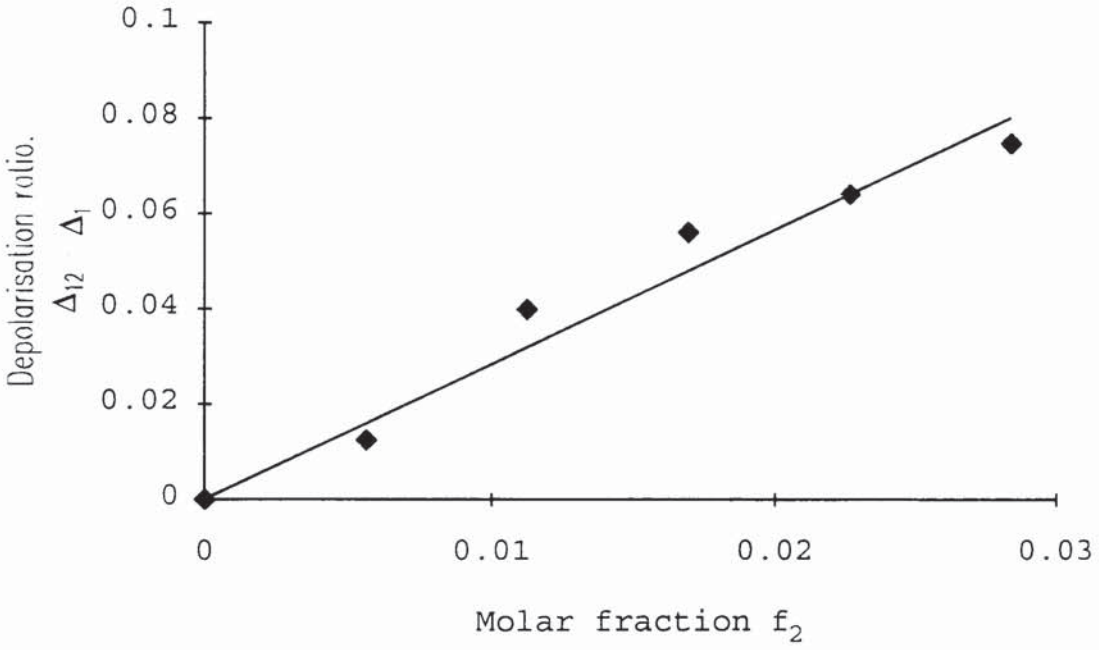

Figure 7.1 Depolarisation ratio for 2-methyl-4-nitroaniline in 1,4-dioxane plotted as a function of molar fraction.

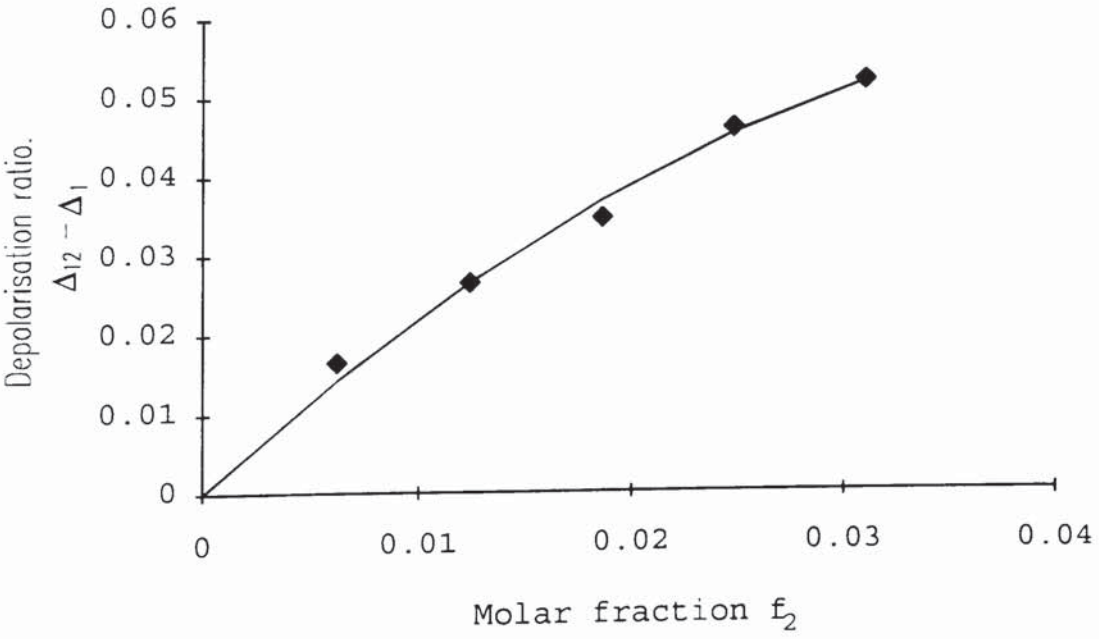

Figure 7.2 Depolarisation ratio for p-nitroaniline in 1,4-dioxane plotted as a function of molar fraction.

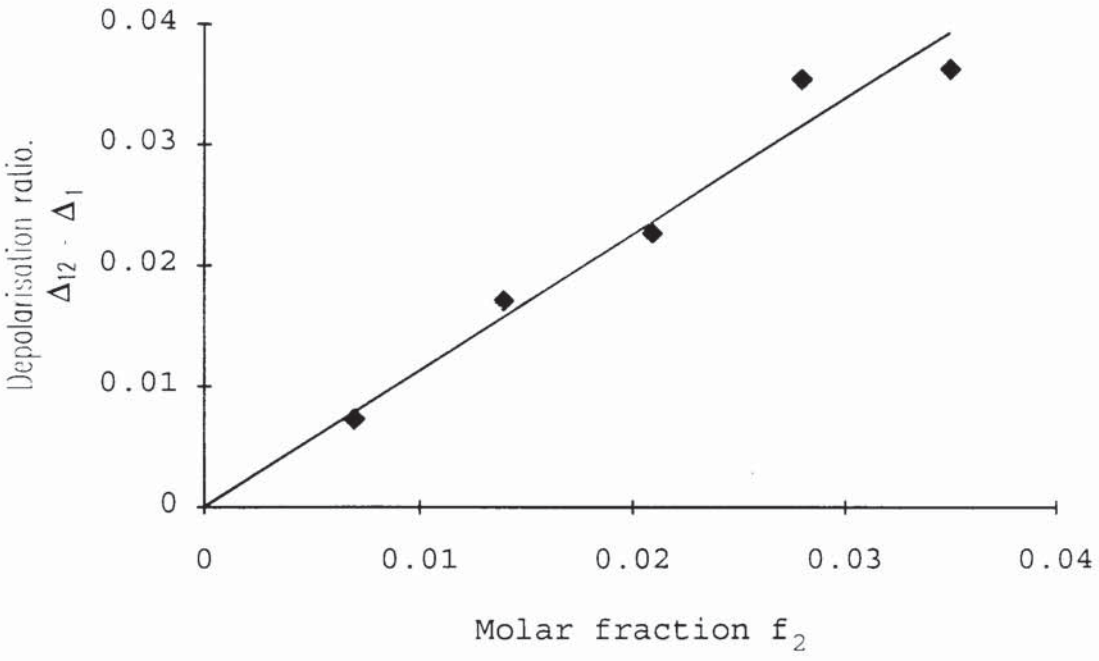

Figure 7.3 Depolarisation ratio for nitrobenzene in 1,4-dioxane plotted as a function of molar fraction.

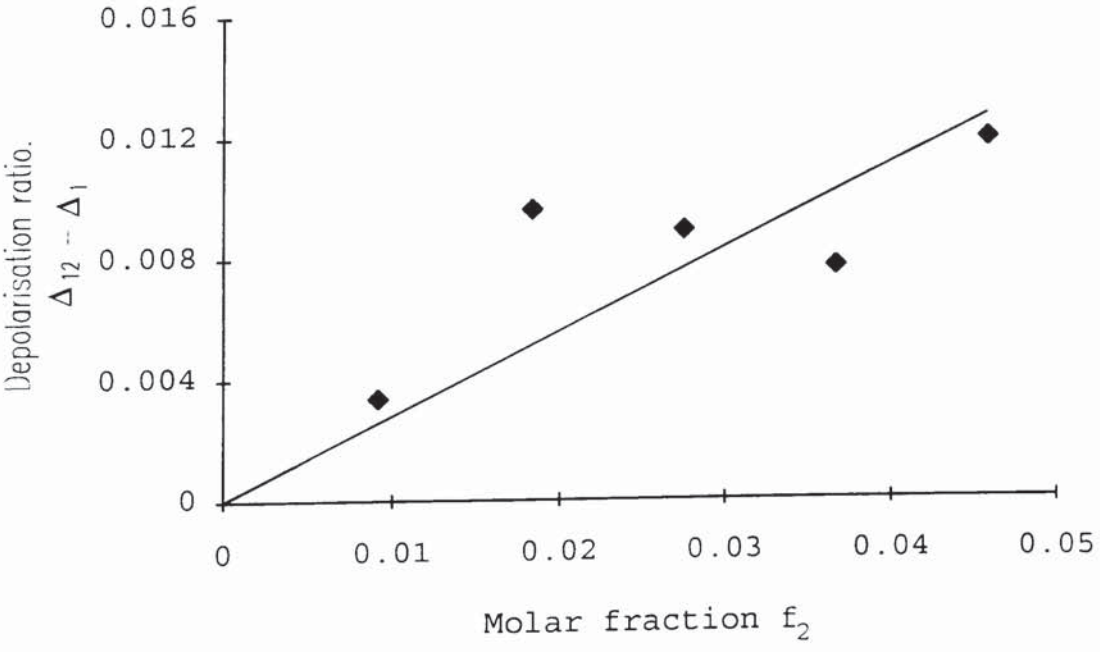

Figure 7.4 Depolarisation ratio for aniline in 1,4-dioxane plotted as a function of molar fraction.

Table 7.1 Depolarisation and anisotropy parameters for pure liquids.

Compound	Δ	β m^2N^{-1}	d kgm^{-3}	M_1 kg	δ^2 ±0.0005
1,4-Dioxane	0.064(5)	6.95e-10	1034.(56)	0.08812	0.023(4)
Toluene	0.323(4)	8.60e-10	867.(63)	0.09215	0.018(7)

Table 7.2 Anisotropy parameter for various compounds in 1,4-dioxane.

Compound	A	D	M_2	$_\infty\delta_2^2$	Error ±
Aniline	0.279	6.073	0.09313	0.01(67)	1E-3
Nitrobenzene	1.132	217.84	0.12311	0.03(65)	2E-3
p-Nitro-aniline	2.457	401.156	0.13813	0.10(32)	4E-3
2-Methyl-4-nitroaniline	2.847	334.288	0.15213	0.11(56)	7E-3

Table 7.3 Comparison of the anisotropy parameter for nitrobenzene with literature values.

Nitrobenzene	$_\infty\delta_2^2$	δ^2_{gas}	λ
This Work	**0.036(5)**	**-**	**632.8nm**
Ref. 102	0.0325	-	white light
Ref. 103	-	0.0545	white light

Table 7.4 Comparison of the anisotropy parameter for 1,4-dioxane with literature values.

1,4-Dioxane	Δ	δ^2_{liquid}	λ
This Work	**0.064(5)**	**0.0234**	**632.8nm**
Ref. 104	0.0699	0.0255	546nm

Table 7.5 Comparison of the anisotropy parameter for toluene with literature values.

Toluene	Δ	δ^2_{liquid}	$_{\infty}\delta^2_2$	δ^2_{gas}	λ
This Work	**0.323(4)**	**0.02(23)**	-	-	**632.8nm**
Ref.105*	0.359	0.0270	-	-	632.8nm
Ref.104	0.3678	0.0283	-	-	546nm
Ref.102	-	-	0.0177	-	white light
Ref.103	-	0.0204	-	0.0377	white light

* measured at 15°C

CHAPTER 8

INFINITE DILUTION MOLAR KERR CONSTANTS AND HYPERPOLARISABILITIES

8.1 INTRODUCTION

This chapter combines the refractive index, density, dielectric constant, and Kerr constant values derived in earlier chapters to determine the infinite dilution molar Kerr constants of the compounds used. The temperature dependence of the infinite dilution molar Kerr constant is then combined with the dipole moment, electronic polarisation, and anisotropy parameter data to determine the hyperpolarisability and the polarisability ellipsoid of the solute. The hyperpolarisability and the polarisability ellipsoid of the solvents are calculated using the molar Kerr constant.

8.2 ERROR ANALYSIS

All the errors quoted have a 68% confidence limit. The error in a quantity containing several measured quantities is determined as follows. If a quantity Q is a function of several measured quantities x, y, z,... then

the error in Q due to errors $\partial x, \partial y, \partial z, \ldots$ in x, y, z, ... respectively is given by

$$\partial Q \cong \frac{\partial Q}{\partial x}\partial x + \frac{\partial Q}{\partial y}\partial y + \frac{\partial Q}{\partial z}\partial z + \ldots\ldots \qquad 8.1$$

The first term $\frac{\partial Q}{\partial x}\partial x$ is the error in Q due to an error ∂x in x only (that is, corresponding to $\partial y, \partial z, \ldots$ all being zero), and similarly the second term $\frac{\partial Q}{\partial y}\partial y$ is the error in Q due to an error ∂y in y only. This result is often referred to as the *principal of superposition of errors*[106]. Errors in straight line and/or polynomial fits are calculated according to the normal method associated with the *method of least squares*[106].

8.3 HYPERPOLARISABILITIES OF SOLUTIONS

The infinite dilution molar Kerr constant for the solutes was determined using the method derived by Le Fèvre (see section 2.6). All the calculations were performed on an EXCEL 4.0™ spreadsheet designed by the author for this purpose. The variation of B_{12}, ε_{12}, and d_{12} for solutions of 2-methyl-4-nitroaniline were found to have a linear relationship with w_2. However B_{12}, ε_{12}, and d_{12} for solutions of p-nitroaniline, nitrobenzene, and aniline were found to have a non-linear relationship with w_2 and were therefore fitted to an equation of the type shown in equation 2.39. Where-ever possible data fitted

to a straight line or a curve was accomplished using a *weighted* fit. All of the solutes used except aniline had, by a consequence of their symmetry, the direction of the dipole moment aligned along the direction of maximum polarisability. This direction was denoted as the 3rd axis (see Figure 8.1).

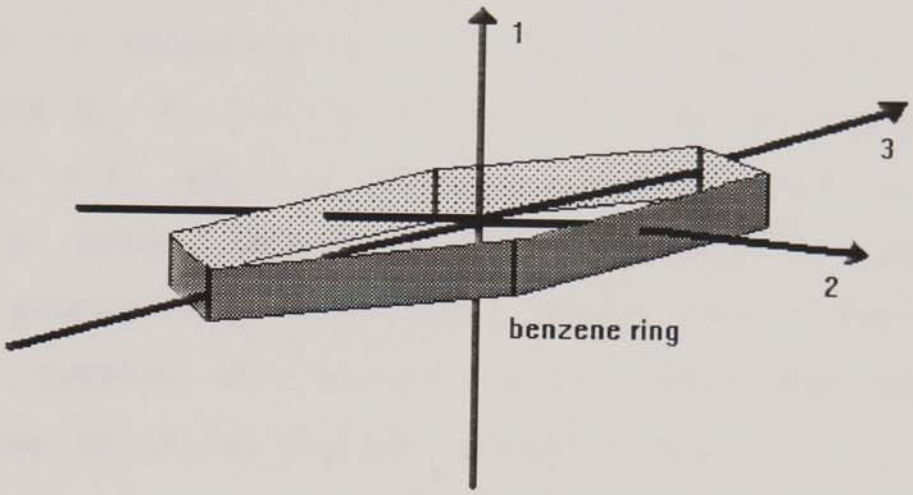

Figure 8.1 Polarisability axes associated with the benzene ring.

Using this nomenclature simplifies the molar Kerr constant as μ_2 and μ_1 are therefore zero (except for aniline). This makes it easier to solve for α_1, α_2, and α_3. The dipole moment for aniline does not lie in the plane of the benzene ring therefore only the μ_2 component is zero. This greatly increases the mathematical complexity in calculating α_1, α_2, and α_3. The hyperpolarisability calculated will therefore be the value lying at an angle to the benzene plane since β is a vector quantity. The β value for aniline can be compared

with that for the other solutes which lie along axis 3 by multiplying by cosθ, where θ is the angle made by the dipole moment and the benzene plane. Published values for the angle of the dipole moment with respect to the plane of the phenyl ring vary considerably and cover the range 34° to 47.7° (see references 107,108,109,and 110). Aroney[109] *et al* calculated the angle as 34° for aniline as a solute in 1,4-dioxane and this angle has been adopted here to calculate α_1, α_2, and α_3. The polarisability values α_1, α_2, and α_3 are calculated by solving equations 2.26, 6.9, and 7.9. Results are presented in SI and e.s.u. units, Appendix L contains conversion factors for the properties used in this thesis. Tables and diagrams that compare the results reported here with literature values can be seen on the following pages.

8.4 HYPERPOLARISABILITIES OF SOLVENTS

To determine the infinite dilution molar Kerr constant of the solutes in 1,4-dioxane it was necessary to determine the molar Kerr constant of pure 1,4-dioxane. Measurements performed on 1,4-dioxane were identical to the method used for the solutions. The molar Kerr constant results for 1,4-dioxane are presented in Appendix F. As 1,4-dioxane does not have a dipole moment the $[K_3]$ term of the molar Kerr constant is zero. This enables the temperature dependence of the molar Kerr

constant for 1,4-dioxane to be fitted to an equation of the form

$$y = a + b/T \qquad 8.1$$

Using the data shown in Appendix F we obtain

$$a = 1.3 \pm 0.1 \times 10^{-27}\ m^5V^{-2}mol^{-1} \qquad 8.2$$

and

$$b = -6.8 \pm 2.3 \times 10^{-26}\ m^5V^{-2}mol^{-1}K \qquad 8.3$$

The value of the second hyperpolarisability, calculated from the intercept, is $\gamma = 7.6 \pm 0.4 \times 10^{-60}\ C^4m^4J^{-3}$. Mendicuti and Saiz[111] quote values for 1,4-dioxane as

$$a = 3.9 \pm 0.9 \times 10^{-26}\ m^5V^{-2}mol^{-1} \qquad 8.4$$

$$b = -8.2 \pm 2.6 \times 10^{-24}\ m^5V^{-2}mol^{-1}K \qquad 8.5$$

and,

$$\gamma = 5.1 \pm 1.2 \times 10^{-60}\ C^4m^4J^{-3} \qquad 8.6$$

where Mendicuti and Saiz defined ${}_{\infty}K_2$ as nine times larger than that defined in this thesis (note γ is directly comparable). Mendicuti and Saiz[111] computed the refractive index of 1,4-dioxane as $n^2 \approx \varepsilon$, which may be the origin of

the difference between the value of γ calculated by Mendicuti and Saiz compared with that reported here.

Originally, toluene was dissolved in cyclohexane in attempt to determine the first hyperpolarisability of toluene. However, the errors in the infinite dilution molar Kerr constant, ${}_{\infty}K_2$, were so large that this method was impractical. It has been reported by Le Fèvre and Le Fèvre[85] that the molar Kerr constant of pure liquid toluene is close to the apparent ${}_{\infty}K_2$ values found in carbon tetrachloride - i.e. no marked solvent action is apparent. It was therefore decided for simplicity to determine the first hyperpolarisability, β, of toluene from the temperature dependence of the molar Kerr constant of the pure liquid rather than from its infinite dilution molar Kerr constant value in 1,4-dioxane. For greater accuracy the experimental determination of toluene over temperature was performed twice. The results for toluene can be seen in Table 8.13, 8.14 and 8.15.

Literature values are available for the polarisability axis for nitrobenzene, toluene, and aniline as dilute solutions in various solvents; these are summarised in Table 8.16. The polarisabilities reported here are plotted against the literature values (see Figure 8.7) and it can be seen that the values reported here for the polarisability axes of nitrobenzene are proportional to the literature values.

Table 8.1 Infinite dilution molar Kerr constant, $_{\infty}K_2$, for 2-methyl-4-nitroaniline in 1,4-dioxane.

Temp °C	$\alpha\varepsilon_1$	β	γ	δ	10^{27} $_{\infty}K_2$	10^{27} error ±
15	43.31	0.2000	0.1585	5383.3	9647	102
20	42.35	0.2035	0.1616	5122.7	9209	41
25	41.39	0.2071	0.1646	4921.1	8876	44
30	40.44	0.2108	0.1677	4713.7	8533	55
35	39.48	0.2145	0.1708	4533.0	8238	45
40	38.52	0.2182	0.1739	4347.2	7933	47
45	37.57	0.2220	0.1770	4146.1	7598	70
50	36.61	0.2258	0.1802	3970.1	7309	81
55	35.65	0.2297	0.1833	3818.2	7063	95
60	34.70	0.2336	0.1865	3667.1	6817	95
65	33.74	0.2376	0.1896	3493.8	6528	136
70	32.78	0.2416	0.1928	3347.7	6289	135

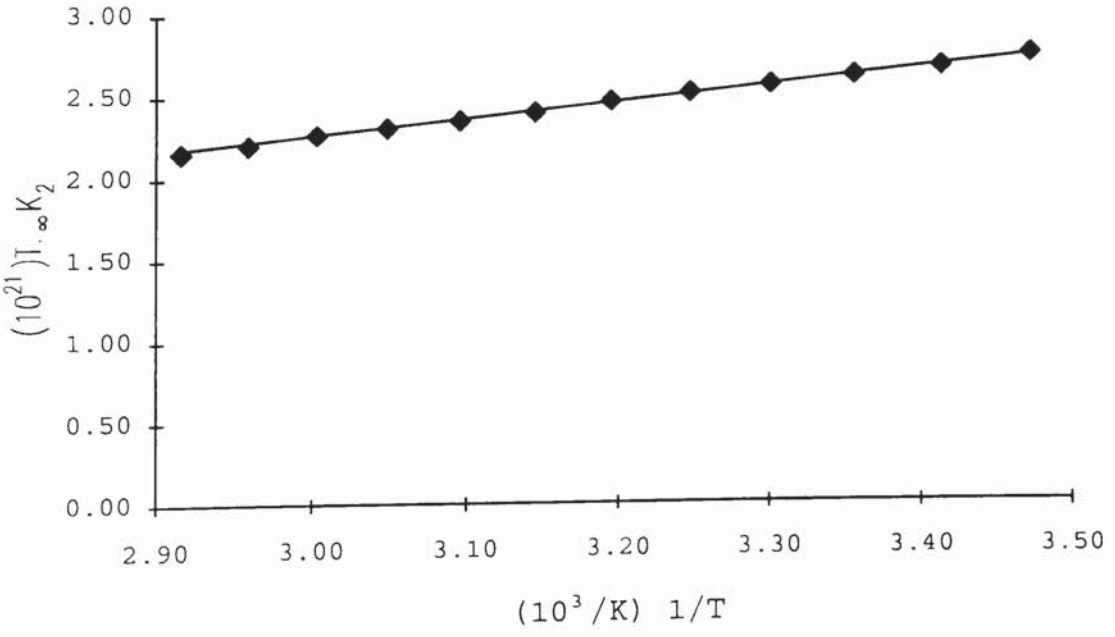

Figure 8.2 Infinite dilution molar Kerr constant, $_{\infty}K_2$, multiplied by temperature for 2-methyl-4-nitroaniline in 1,4 dioxane plotted as a function of temperature.

Table 8.2 Analysis of the temperature dependence of the infinite dilution molar Kerr constant ${}_{\infty}K_2$, for 2-methyl-4-nitroaniline in 1,4-dioxane (SI units).

Property S.I.	Value	error ±	Units
10^{20} x slope	106	2	$m^5V^{-2}K^2mol^{-1}$
10^{22} x Intercept	-9.2	0.6	$m^5V^{-2}Kmol^{-1}$
$10^{30}\mu$	23.7	0.1	Cm
$10^{40}\alpha$	23	1	Cm^2V^{-1}
$10^2{}_{\infty}\delta_2^2$	11.6	0.7	-
$10^{50}\beta$	-103	6	Cm^3V^{-2}
$10^{40}\alpha_1$	21	1	Cm^2V^{-1}
$10^{40}\alpha_2$	11	1	Cm^2V^{-1}
$10^{40}\alpha_3$	37	2	Cm^2V^{-1}

Table 8.3 Analysis of the temperature dependence of the infinite dilution molar Kerr constant ${}_{\infty}K_2$, for 2-methyl-4-nitroaniline in 1,4-dioxane (e.s.u. units).

Property e.s.u	Value	error ±
debye μ	7.1	0.02
$10^{24}\alpha$	20	1
$10^{30}\beta$	-277	15
$10^{24}\alpha_1$	19	1
$10^{24}\alpha_2$	9.1	0.5
$10^{24}\alpha_3$	33	2

Table 8.4 Infinite dilution molar Kerr constant, ${}_{\infty}K_2$, for p-nitroaniline in 1,4-dioxane.

Temp °C	$\alpha\varepsilon_1$	β	γ	δ	10^{27} ${}_{\infty}K_2$	10^{27} error ±
15	45.74	0.2036	0.1449	4986.1	7003	430
20	44.68	0.2074	0.1478	4756.6	6413	558
25	43.62	0.2113	0.1506	4496.9	6117	469
30	42.57	0.2152	0.1535	4249.4	5891	348
35	41.51	0.2192	0.1564	4052.9	5911	390
40	40.45	0.2232	0.1593	3857.6	5984	347
45	39.39	0.2273	0.1622	3699.3	5575	346
50	38.33	0.2314	0.1652	3490.7	4953	369
55	37.27	0.2355	0.1681	3337.8	4895	208
60	36.21	0.2397	0.1710	3186.5	4713	309
65	35.15	0.2440	0.1740	3033.0	4445	479
70	34.09	0.2483	0.1770	2851.0	4610	333

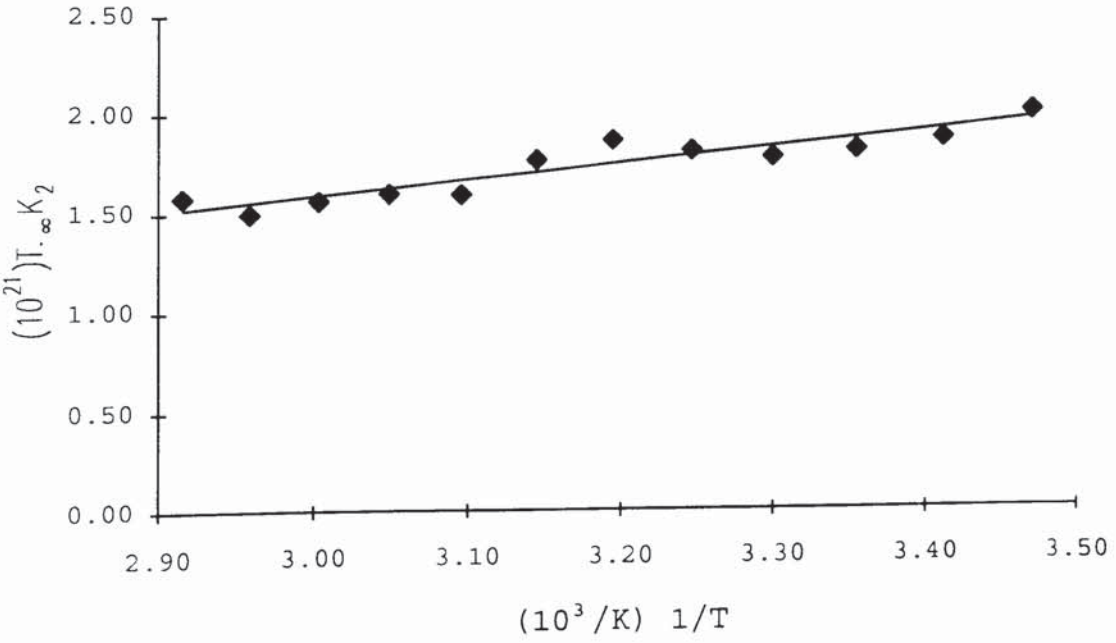

Figure 8.3 Infinite dilution molar Kerr constant, ${}_{\infty}K_2$, multiplied by temperature for p-nitroaniline in 1,4 dioxane plotted as a function of temperature.

Table 8.5 Analysis of the temperature dependence of the infinite dilution molar Kerr constant, ${}_{\infty}K_2$, for p-nitroaniline in 1,4-dioxane (SI units).

Property S.I.	Value	error ±	Units
10^{20} x slope	82	2	$m^5V^{-2}K^2mol^{-1}$
10^{22} x Intercept	-8.8	0.5	$m^5V^{-2}Kmol^{-1}$
$10^{30}\mu$	23.4	0.07	Cm
$10^{40}\alpha$	19	1	Cm^2V^{-1}
$10^2{}_{\infty}\delta_2^2$	10.3	0.5	-
$10^{50}\beta$	-98	5	Cm^3V^{-2}
$10^{40}\alpha_1$	17	1	Cm^2V^{-1}
$10^{40}\alpha_2$	9.5	0.6	Cm^2V^{-1}
$10^{40}\alpha_3$	31	2	Cm^2V^{-1}

Table 8.6 Analysis of the temperature dependence of the infinite dilution molar Kerr constant, ${}_{\infty}K_2$, for p-nitroaniline in 1,4-dioxane (e.s.u. units).

Property e.s.u.	Value	error ±
debye μ	7.01	0.02
$10^{24}\alpha$	17	1
$10^{30}\beta$	-263	14
$10^{24}\alpha_1$	16	1
$10^{24}\alpha_2$	8.5	0.6
$10^{24}\alpha_3$	27	2

Table 8.7 Infinite dilution molar Kerr constant, $_{\infty}K_2$, for nitrobenzene in 1,4-dioxane.

Temp °C	$\alpha\varepsilon_1$	β	γ	δ	10^{27} $_{\infty}K_2$	10^{27} error $\pm$
15	18.43	0.1420	0.0745	735.2	1025	94
20	18.06	0.1435	0.0761	698.5	924	107
25	17.70	0.1450	0.0777	658.3	1062	105
30	17.33	0.1466	0.0793	628.0	951	44
35	16.97	0.1481	0.0809	619.7	873	70
40	16.60	0.1497	0.0826	584.0	910	38
45	16.24	0.1513	0.0842	562.1	886	35
50	15.87	0.1529	0.0858	549.4	839	40
55	15.51	0.1546	0.0875	533.0	798	37
60	15.15	0.1562	0.0891	517.1	772	42
65	14.78	0.1579	0.0908	499.6	763	36
70	14.42	0.1596	0.0924	480.1	722	17

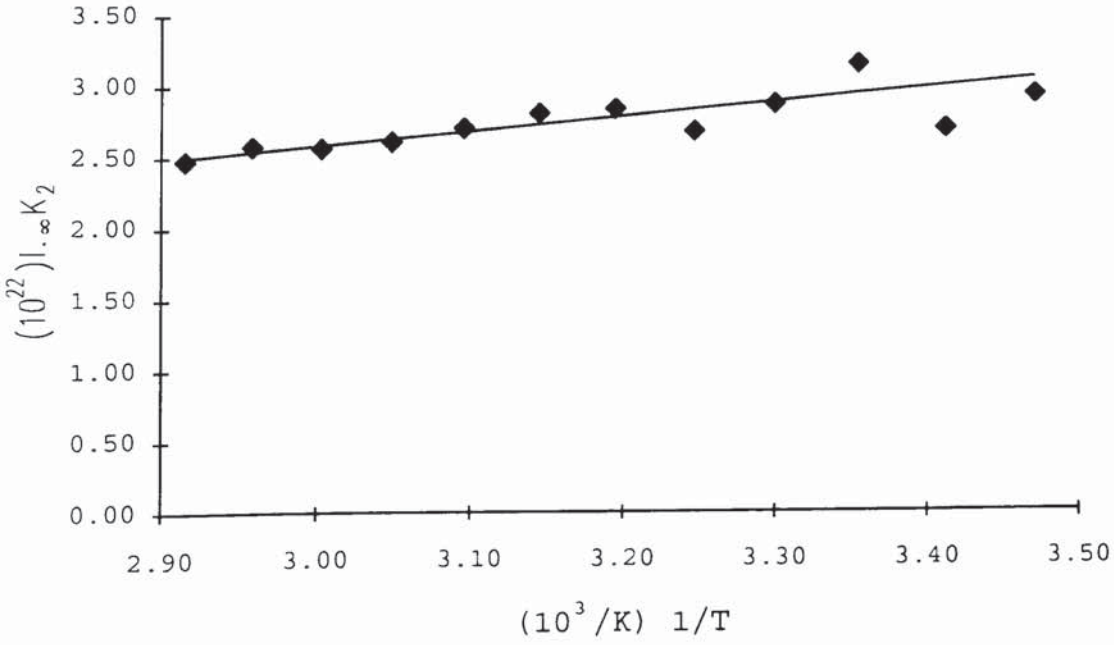

Figure 8.4 Infinite dilution molar Kerr constant, $_{\infty}K_2$, multiplied by temperature for nitrobenzene in 1,4 dioxane plotted as a function of temperature.

Table 8.8 Analysis of the temperature dependence of the infinite dilution molar Kerr constant, ${}_{\infty}K_2$, for nitrobenzene in 1,4-dioxane (SI units).

Property S.I.	Value	error ±	Units
10^{20} x slope	10	1	$m^5V^{-2}K^2mol^{-1}$
10^{22} x Intercept	-0.52	0.4	$m^5V^{-2}Kmol^{-1}$
$10^{30}\mu$	13	0.1	Cm
$10^{40}\alpha$	14	1	Cm^2V^{-1}
$10^2{}_{\infty}\delta_2^2$	4.96	0.1	-
$10^{50}\beta$	-11	7	Cm^3V^{-2}
$10^{40}\alpha_1$	13.9	1	Cm^2V^{-1}
$10^{40}\alpha_2$	9.4	0.7	Cm^2V^{-1}
$10^{40}\alpha_3$	18.6	2	Cm^2V^{-1}

Table 8.9 Analysis of the temperature dependence of the infinite dilution molar Kerr constant, ${}_{\infty}K_2$, for nitrobenzene in 1,4-dioxane (e.s.u. units).

Property e.s.u.	Value	error ±
debye μ	3.9	0.02
$10^{24}\alpha$	13	1
$10^{30}\beta$	-31	19
$10^{24}\alpha_1$	13	1
$10^{24}\alpha_2$	8.4	0.6
$10^{24}\alpha_3$	17	1

Table 8.10 Infinite dilution molar Kerr constant, ${}_{\infty}K_2$, for aniline in 1,4-dioxane.

Temp °C	$\alpha\varepsilon_1$	β	γ	δ	10^{27} ${}_{\infty}K_2$	10^{27} error $\pm$
15	4.52	0.0142	0.0863	72.18	82.0	10.0
20	4.43	0.0152	0.0850	62.30	62.7	15.5
25	4.34	0.0163	0.0836	61.38	62.6	2.5
30	4.24	0.0174	0.0822	58.37	56.4	6.4
35	4.15	0.0184	0.0809	57.47	55.7	3.0
40	4.06	0.0195	0.0795	56.12	59.2	3.4
45	3.97	0.0206	0.0781	53.31	58.2	4.1
50	3.88	0.0218	0.0767	52.22	58.7	6.7
55	3.78	0.0229	0.0753	49.14	47.8	6.2
60	3.69	0.0240	0.0740	48.73	51.4	5.7
65	3.60	0.0252	0.0726	45.06	44.6	7.2
70	3.51	0.0263	0.0711	43.14	38.9	4.9

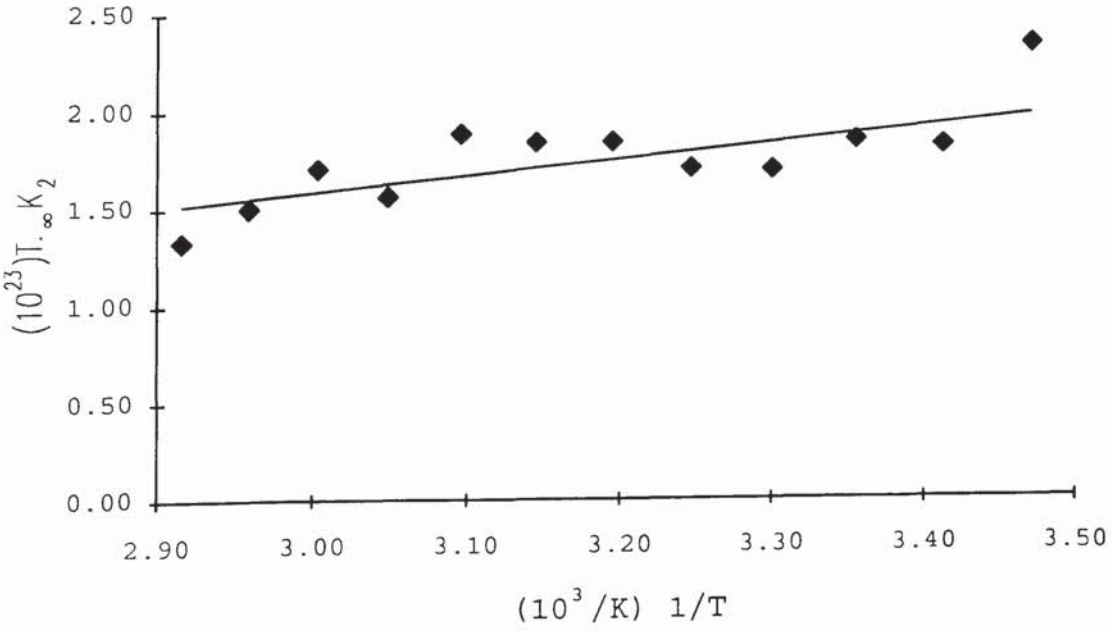

Figure 8.5 Infinite dilution molar Kerr constant, ${}_{\infty}K_2$, multiplied by temperature for aniline in 1,4-dioxane plotted as a function of temperature.

Table 8.11 Analysis of the temperature dependence of the infinite dilution molar Kerr constant, ${}_{\infty}K_2$, for aniline in 1,4-dioxane (SI units).

Property S.I.	Value	error ±	Units
10^{22} x slope	65	26	$m^5V^{-2}K^2mol^{-1}$
10^{24} x Intercept	-10	8	$m^5V^{-2}Kmol^{-1}$
$10^{30}\mu$	5.7	0.4	Cm
Dipole angle	34	-	degrees
$10^{30}\mu_1$	3.2	0.2	Cm
$10^{30}\mu_2$	4.7	0.3	Cm
$10^{40}\alpha$	12	1	Cm^2V^{-1}
$10^2{}_{\infty}\delta_2^2$	1.7	0.5	-
$10^{50}\beta$	-6	4	Cm^3V^{-2}
$10^{40}\alpha_1$	11	1	Cm^2V^{-1}
$10^{40}\alpha_2$	11	1	Cm^2V^{-1}
$10^{40}\alpha_3$	15	2	Cm^2V^{-1}

Table 8.12 Analysis of the temperature dependence of the infinite dilution molar Kerr constant, ${}_{\infty}K_2$, for aniline in 1,4-dioxane (e.s.u. units).

Property e.s.u	Value	error ±
debye μ	1.7	0.11
debye μ_1	0.95	0.06
debye μ_2	1.41	0.09
$10^{24}\alpha$	11	1
$10^{30}\beta$	-15	10
$10^{24}\alpha_1$	10	1
$10^{24}\alpha_2$	10	1
$10^{24}\alpha_3$	14	1

Table 8.13 Molar Kerr constant, ${}_mK_2$, for pure liquid HPLC grade toluene.

Temp °C	10^{27} ${}_\infty K_2$	10^{27} error ±	10^{27} ${}_\infty K_2$	10^{27} error ±
15	14.5	0.3	-	0.3
20	14.8	0.3	-	0.3
25	15.3	0.3	14.7	0.3
30	14.8	0.3	14.7	0.3
35	14.8	0.3	14.6	0.3
40	14.2	0.3	14.6	0.3
45	14.3	0.3	14.2	0.3
50	14.3	0.3	14.2	0.3
55	14.0	0.3	13.6	0.3
60	14.1	0.3	13.6	0.3
65	13.6	0.3	13.9	0.3
70	13.4	0.3	-	0.3

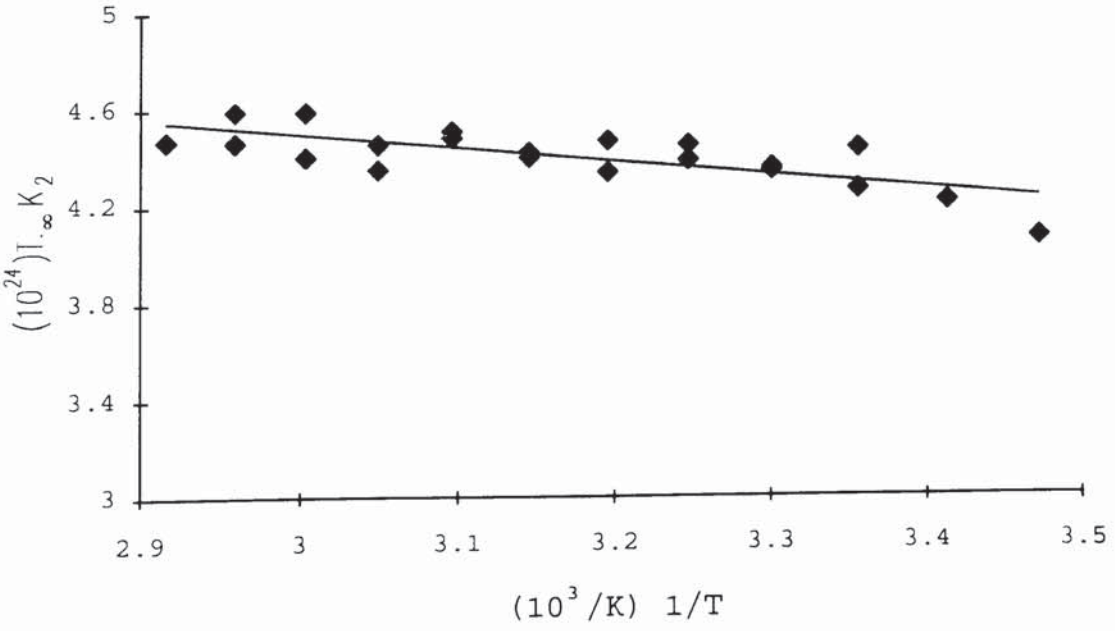

Figure 8.6 Molar Kerr constant, ${}_mK_2$, multiplied by temperature for pure liquid toluene plotted as a function of temperature.

Table 8.14 Analysis of the temperature dependence of the molar Kerr constant, ${}_mK_2$, for pure liquid toluene(SI units).

Property S.I.	Value	error ±	Units
10^{22} x slope	-5.5	1.1	$m^5V^{-2}K^2mol^{-1}$
10^{24} x Intercept	6.1	0.4	$m^5V^{-2}Kmol^{-1}$
$10^{30}\mu$	1.2	0.07	Cm
Dipole angle	0	-	degrees
$10^{40}\alpha$	13	2	Cm^2V^{-1}
$10^2{}_\infty\delta_2^2$	2.2	0.02	-
$10^{50}\beta$	3.6	2	Cm^3V^{-2}
$10^{40}\alpha_1$	12	2	Cm^2V^{-1}
$10^{40}\alpha_2$	11	1	Cm^2V^{-1}
$10^{40}\alpha_3$	17	2	Cm^2V^{-1}

Table 8.15 Analysis of the temperature dependence of the molar Kerr constant, ${}_\infty K_2$, for pure liquid toluene (e.s.u. units).

Property e.s.u.	Value	error ±
debye μ	0.36	0.02
$10^{24}\alpha$	12	0.2
$10^{30}\beta$	10	6
$10^{24}\alpha_1$	11	1
$10^{24}\alpha_2$	9	1
$10^{24}\alpha_3$	15	1

Table 8.16 Polarisabilities (in cm^3) for nitrobenzene, toluene and aniline.

Compound	$10^{24}\alpha_1$	$10^{24}\alpha_2$	$10^{24}\alpha_3$	Reference
Nitrobenzene	**12.5**	**8.4**	**16.7**	**This work**
	13.3	7.8	17.8	*13,112
	13.6	6.9	16.0	49
	13.8	6.6	16.0	13
	12.0	8.6	16.1	102
Toluene	**11**	**9**	**15**	**This work**
	12.5	9	13.7	102
	14.0	8.7	12.7	**102
Aniline	**10**	**10**	**14**	**This work**
	11.7	8.2	14.7	109

*Gas Value

**Does not use ${}_{\infty}\delta^2$

Table 8.17 Infinite dilution molar Kerr constants, ${}_{\infty}K_2$.

Compound	Temp.	${}_{\infty}K_2$	reference
Nitrobenzene	**20**	**924**	**This work**
	20	1073	[a]49
	22	1050	[b]49
	20	1332	[c]49
	22	1315	[c]49
Aniline	**25**	**56.3**	**This work**
	25	75.6	[d]109
Toluene	**25**	**13.5**	**This work**
	25	12.8	[a]85

[a] Solvent = CCl_4 , [b] Solvent = C_6H_6

[c] gas value, [d]Solvent = 1,4-dioxane

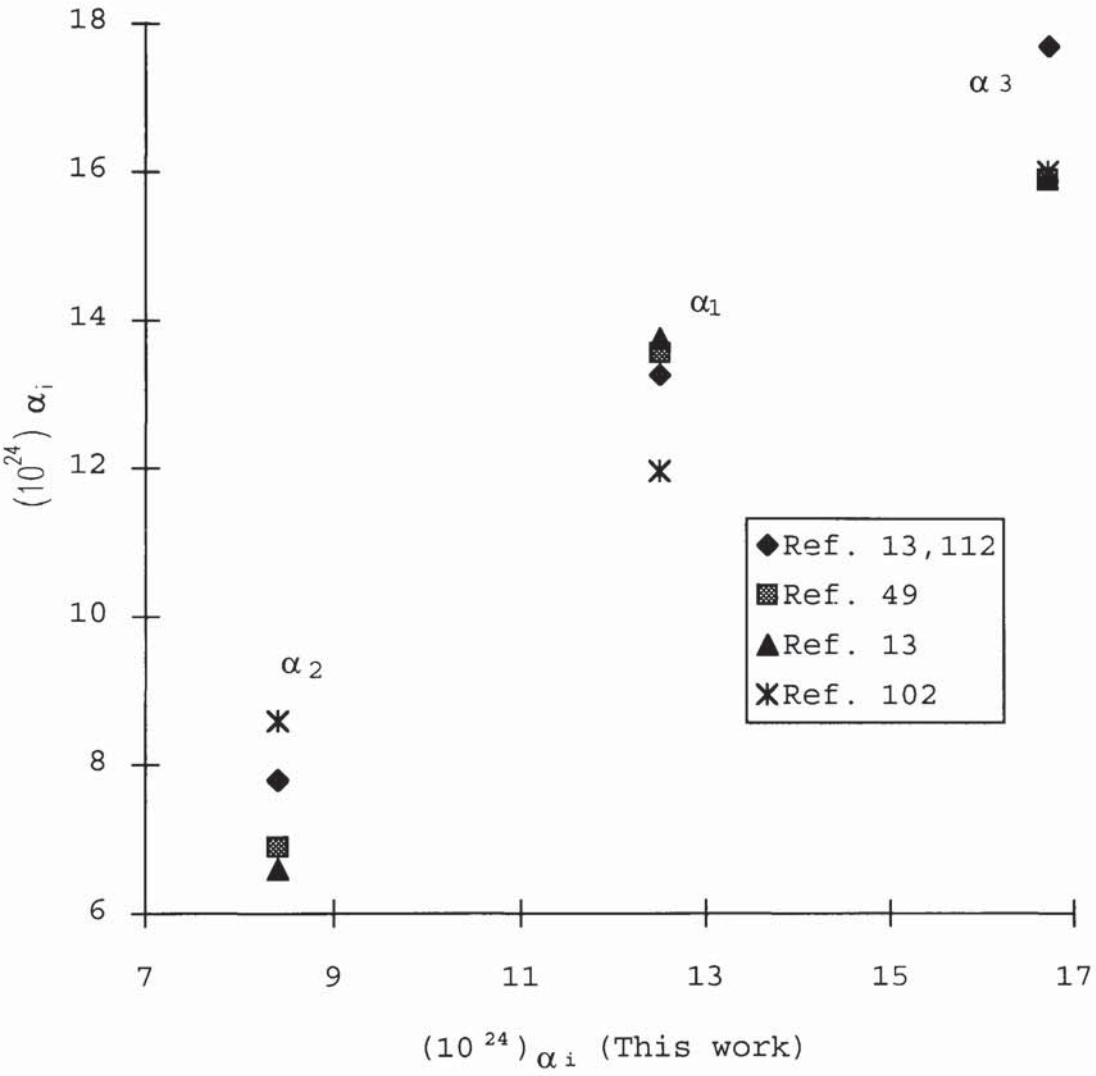

Figure 8.7 Polarisabilities for nitrobenzene α_i plotted against literature values. (i=1,2,3)

Table 8.18 First-hyperpolarisability data.

Compound	λ/nm	Solvent/Method	$10^{30}\|\beta\|$ e.s.u.	Ref.
2-Methyl-4-nitroaniline	**633**	**1,4-dioxane**	**277±15**	**This work**
	1060	SHG powder	42	35
	1060	calculated	25	113
	1060	SHG powder	42	113
p-Nitroaniline	**633**	**1,4-dioxane**	**263±14**	**This work**
	1060	calculated	23	113
	1060	SHG powder	34.5	113
	1060	methanol	20-24.5	114
	1890	Dimethyl sulfoxide	47.7-46	115
	365	acetone	9.2	116
	1320	melt	21.1	114
	833	1,4-dioxane	40	117
	833	gas	19.6	117
	1064	1,4-dioxane	16.7	117
	1064	gas	12.3	117
	1890	gas	8.9	117
Nitrobenzene	**633**	**1,4-dioxane**	**31±19**	**This work**
	365	pure liquid	1.9	116
	-	in solution	7.5	118
	1064		2	119, 110
	589	dilute gas	25	91
Aniline	**633**	**1,4-dioxane**	**15±10**	**This work**
	1064	pure liquid	0.8	119
	1064	pure liquid	0.9	110
Toluene	**633**	**pure liquid**	**10±6**	**This work**
	1064	pure liquid	0.2	110

CHAPTER 9

DISCUSSION/FURTHER WORK

The primary objectives of this project were to determine the feasibility of determining the non-linear properties of a compound by utilising the temperature dependence of the electro-optic Kerr effect in solutions. Ultimately, if the process proves to be acceptable, then if the molecular basis for the non-linear behaviour can be defined, materials with substantially greater non-linear properties can be predicted by quantum mechanical calculations or by chemical intuition. Hyperpolarisability measurements are only strictly applicable for molecules in the dilute gas phase. The hyperpolarisability calculations in this thesis were made from measurements on dilute solutions. Therefore, the hyperpolarisability results presented in this thesis can only be considered as effective and not absolute values of the compounds hyperpolarisability. However, this is not a problem as a material with a high value of β in the liquid phase should in its solid phase have a high χ_2 value, provided that the structure is non-centrosymmetric. In order to devise a process of constructing compounds with high non-linear properties by chemical intuition it will be necessary to analyse a large number of compounds in order to develop a data base of hyperpolarisability measurements, in much the same way

as achieved by Le Fèvre for polarisability measurements. At present there has been a lot of work done on the non-linear properties of crystals but very little consistent work carried out for compounds in the liquid or gas phase. This has made it very difficult to make direct comparisons between hyperpolarisability measurements taken by different research groups and this thesis.

The method of determining the hyperpolarisability of a compound through the temperature dependence of the electro-optic Kerr effect is particularly hampered by the need to extrapolate the molar Kerr constant of a solution to the infinite dilution molar Kerr constant, as errors in the various techniques required to calculate the molar Kerr constant can combine unpredictably. Le Fèvre devised a direct method of determining the infinite dilution molar Kerr constant but this still suffers from the need to make an intuitive guess as to whether to fit the results to a straight line or a polynomial. For instance, the measurements for 2-methyl-4-nitroaniline were fitted to a straight line with concentration whereas the measurements for p-nitroaniline were fitted to a third order polynomial. There is no *a priori* reason why this should have been done, but it is tempting in this instance to postulate that the addition of the CH_3 group to the benzene ring hinders inter molecular interactions. In future it will be necessary to take measurements on more than five different concentrations in order to decide definitively whether to fit the measurements for a particular compound to a straight line or third order

polynomial. At present there is a great deal of time and effort involved in measuring the temperature dependence of the Kerr effect for just five concentrations. Therefore, in order for this process to become practically possible it will be necessary to speed up the process of taking temperature dependent Kerr effect measurements. The easiest way this could be accomplished would be to completely automate the experiment such that it can run independently of the operator's presence.

It is also worth noting that the increase in the dipole moment from p-nitroaniline to 2-methyl-4-nitroaniline is less than would be predicted by straight forward vector addition of the apparent CH_3 dipole moment. It is however possible that there is steric hindrance between the CH_3 group and the NH_2 group, which would force the NH_2 group to rotate, thus reducing the contribution the NH_2 group has to the overall dipole moment of 2-methyl-4-nitroaniline.

Kerr effect measurements made by Le Fèvre have shown that even when the molar Kerr constant is extrapolated to the infinite dilution molar Kerr constant the values obtained for a compound differ according to the solvent used. However, this difference can usually be mainly attributed to an enhanced or decreased dipole moment of the solute caused by the interaction with the solvent. For this reason the dipole moment, Rayleigh depolarisation ratio, and electronic polarisation measurements are conducted using the same solvent for internal consistency. Aniline particularly suffers from

strong solute-solvent interactions in 1,4-dioxane as is evidenced by the considerable change in the dipole moment and in the molar Kerr constant[109] from the values determined using carbon tetrachloride as the solvent. It has been shown that the higher dipole moments observed for aniline in 1,4-dioxane arise through hydrogen bonding between an amino-hydrogen atom and an oxygen atom of the dioxane molecule, and that the increased dipole moment can be related to an increased donation of electron density from the amino-nitrogen atom to the ring.

The accurate measurement of the infinite wavelength refractive index is essential for the accurate determination of the constituents of the polarisability ellipsoid and atomic polarisation of the compound under investigation. The electronic polarisation of a compound should according to theory be invariant with temperature. However, it was found from the measurements taken in this thesis, that there was a marked temperature variation in the electronic polarisation. A possible explanation for this situation is that extrapolating to the infinite wavelength refractive index using the Cauchy dispersion formulae with only two terms is not sufficient.

Rayleigh depolarisation measurements can be affected by the presence of Raman scattering thus giving unreliable results. It would therefore be an advantage to have a narrow band pass (632.8nm) filter positioned in front of the photomultiplier during depolarisation measurements. Unfortunately, this was not possible with the equipment used in this thesis. The $[K_1]$ term in the

Kerr effect equation, which results from the anisotropy of the compound, contributes less than 10% to the overall value of $[K_1]+[K_3]$ for 2-methyl-4-nitroaniline and p-nitroaniline. The Raman effect can therefore be reliably ignored for compounds with a high hyperpolarisability value. However, the Raman effect may be significant for molecules such as aniline and toluene which have a relatively low hyperpolarisability value. Taking into account the experimental errors calculated for the hyperpolarisability of aniline and toluene it would not appear worthwhile to try include any Raman effects for these compounds.

Calculations of the hyperpolarisability are further hampered for compounds in which the dipole moment of the compound is not in the same direction as the maximum polarisability (e.g. aniline). The calculations of the hyperpolarisability not only become more complicated but the question arises as to exactly what is the angle between the plane of the benzene ring and the dipole moment of the substituent. It has already been shown by Le Fèvre[109] that the angle of the dipole moment in aniline apparently varies according to the solvent used, and Le Fèvre claimed that this is a general phenomenon for this type of compound. The angle used in this thesis for the calculation of the hyperpolarisability of aniline was 34°, as recommended by Le Fèvre[109]. If the angle of the dipole moment was varied between 30° and 38° there was an insignificant change in the hyperpolarisability value and a small change in coefficients of the polarisability

ellipsoid. Interestingly, angles above 38° gave imaginary values for the polarisability ellipsoid.

Table 9.1 Variation of the polarisability of aniline in e.s.u.

Angle	$10^{24}\alpha_1$	$10^{24}\alpha_2$	$10^{24}\alpha_3$
30	11	9	14
32	10	10	14
34	10	10	14
36	11	9	14
38	11	9	14

It is worth noting that pure liquid aniline has a negative Kerr constant which is most likely a consequence of molecular aggregation via hydrogen bonding. The Kerr effect for aniline in dilute solutions is positive becoming negative at sufficiently high concentrations.

Levine determined the hyperpolarisability of the compounds studied in this thesis as acting in the direction of the dipole moment whereas the results presented in this thesis indicate that the hyperpolarisability of the compounds acts in the opposite direction to the dipole moment[127]. Levine determined the hyperpolarisability of the compounds using SHG experiments which do not determine the sign of the hyperpolarisability but merely its magnitude. Levine therefore determined the sign of β by measuring the magnitude of the hyperpolarisability produced for a

mixture of quartz and pure liquid nitrobenzene. This was found to be greater than for quartz and in this way he determined that nitrobenzene had a positive hyperpolarisability. The sign of further compounds were then determined by dissolving them in nitrobenzene and determining whether the magnitude of the hyperpolarisability was then increased or decreased. It is well known that for very pure nitrobenzene the dielectric constant increases with the field strength, in contrast to the normal saturation effect. A qualitative explanation of the positive saturation effect for nitrobenzene is based on the formation of molecular pairs in the liquid. The molecular pairs have a net dipole moment, depending on the angle between the molecules constituting the pair. The external electric field influences the average angle between the molecules constituting such a pair in such a way, that the high average dipole moment of the molecular pair is increased at higher field strengths. However, nitrobenzene does not show anomalous saturation in a non-polar solvent, and it therefore seems unreliable to determine the sign of the hyperpolarisability of a nitrobenzene molecule from that of the pure liquid. Further measurements of the hyperpolarisability of nitrobenzene from the dilute gas indicate that the hyperpolarisability of nitrobenzene acts in the opposite direction to the direction of the dipole moment. It is therefore important to only consider the magnitude of the hyperpolarisability of a compound

when comparing the hyperpolarisability results presented in this thesis to those presented by Levine[114,116,119,110].

The polarisability ellipsoids and the infinite dilution molar Kerr constants of the compounds studied in this thesis show good agreement with the values already determined by Le Fèvre, when allowance has been made for the difference in the wavelength. An important point to consider is that when Le Fèvre calculated the polarisability of a compound he did not consider the effects of hyperpolarisability. When the hyperpolarisability is not considered α_3 has an anomalously high value, and the compound is predicted to be more anisotropic than observed.

Although there are significant difficulties in determining the hyperpolarisability of a compound using the temperature dependence of the electro-optic Kerr effect it is gratifying to see that there is a direct relationship between the hyperpolarisabilities calculated in this thesis with the results published by Levine (see Figure 9.1).

With the limited number of compounds studied in this thesis it is not possible to test/formulate any bond addivity model for the hyperpolarisability, neither is it possible to develop a reliable selection criteria for manufacturing materials with higher SHG activity than those currently known.

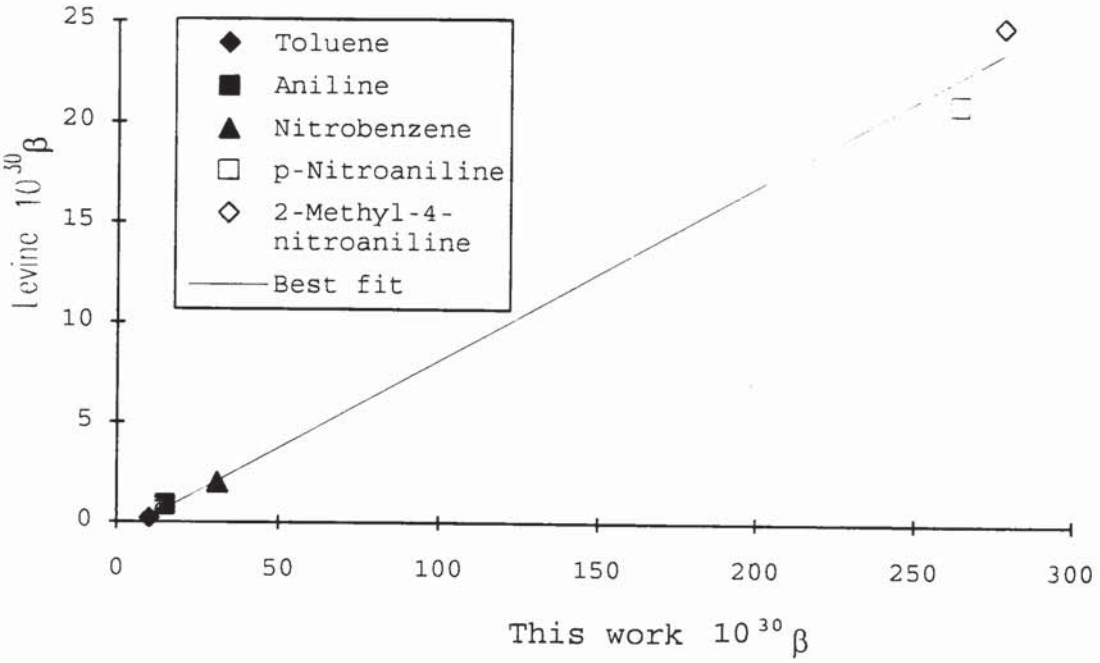

Figure 9.1 First hyperpolarisability for various compounds plotted against literature values

Although there are significant difficulties in measuring the hyperpolarisability of a compound using the temperature dependence of the Kerr effect, the relatively small errors in the hyperpolarisability calculated for 2-methyl-4-nitroaniline and p-nitroaniline are very encouraging. There would, therefore, appear to be no problem in continuing this line of research for compounds where the first hyperpolarisability of the test compound is suspected of being greater or equal to that of p-nitroaniline. However, if a bond addivity model or a data base is required, then the speed and accuracy with which the temperature dependent electro-optic Kerr effect measurements can be taken, would need to be improved.

REFERENCES

1. Kielich, S., 'Optical harmonic generation and laser light frequency mixing processes in nonlinear media', Opto-electronics, **2**, p125-151,(1970).

2. Giordmaine, J.A., 'The interaction of light with light', Scientific American, **210**(4), p38-49,(1964).

3. Bloembergen, N., 'Wave propagation in nonlinear electro-magnetic media', Proc. I.E.E.E., **51**, p124-131, (1963).

4. Franken, P.A. and Ward, J.F., 'Optical harmonics and nonlinear phenomena', Rev. Mod. Phys., **35**, p23-39, (1963).

5. Terhune, R.W., Maker, P.D., and Savage, C.M., 'Measurements of nonlinear light scattering', Physics review letters', **14**, p681-684, (1965).

6. Twieg, R., Azema, A., Jain, K., and Cheng, Y.Y.,'Organic materials for non-linear optics. Nitropyridine derivatives', Chemical Physics letters, **92**, p208-211, (1982).

7. Twieg, R.J. and Jain, K., 'Organic materials for optical second harmonic generation', ACS symposium series, **233**, p57-80, (1983).

8. Kerr, J., 'A new relationship between electricity and light in dielectrified media birefringent', Phil. Mag., **50**(4), p337-348, (1875).

9. Langevin, P., 'Sur les biréfringences électrique et magnétique', Radium, **7**, p249-260, (1910).

10. Born, M., 'Elektronentheorie des natürlichen optischen drehungsvermögens isotroper und anisotroper flüssigkeiten,' Ann. Physik, **55**, p177-240, (1918).

11. Peterlin, A. and Stuart, H.A.,'The determination of the size and shape, as well as the electrical, optical and magnetic anisotropy of sub micro scopic particles with the aid of artificial double refraction and inner viscosity', Z. Phys., **112**, p129-47,(1939).

12. Stuart, H.A., 'Elektrischer Kerr-Effekt.' In: Hand-und Jahrbuch der Chemischen Physik (Ed. A. Eucken and K.L. Wolf), **10**, pt.3. Akademische Verlaggesellschaft, leipzig. (1939)

13. Le Fèvre, C.G. and Le Fèvre, R.J.W., 'The Kerr effect, its measurement and applications in chemistry', Rev. Pure Appl. Chem. (Australia), **5**, p261-318, (1955).

14. Le Fèvre, C.G. and Le Fèvre, R.J.W., In: Technique of Organic Chemistry (ed. A. Weissberger), 3rd edition, **1**, pt. 3, Chap. 36. Interscience, NewYork.

15. Smith, J.W., Sci. Prog., Lond. **48**, p684, (1960).

16. Peterlin, A. and Stuart, H.A., In: Das makromolekülin Lösungen (ed. H.A. Stuart), chap. 12, p. 569. Springer-Verlag, Berlin.

17. Volkenstein, M.V., Configurational statistics of polymer chains. In: High polymers, **17**, chap.7, p432, Interscience, New York, (1963).

18. O'Konski, C.T., In: Encyclopedia of polymer science and technology, (ed. N. Bikales), **9**, p551, Wiley, New York.

19. Yoshioka, K. and Watanabe, H., In: Physical principles and techniques of protein chemistry (ed. S.J. Leach), pt. A, chap 7. Academic Press, New York.

20. Le Fèvre, R.J.W. and Le Fèvre, C.G., 'Molecular polarisability. Its anisotropy in aliphatic and aromatic structures', J. Chem. Soc., p1577-1578, (1954).

21. Smith, R.P. and Mortensen E.M., 'Bond and molecular polarisability tensors. I. Mathematical treatment of bond tensor addivity'., J. Chem. Phys., **32**, p502-507, (1960).

22. Chalam, E.V., 'Application of tensor analysis to molecular anisotropy', Proc. Indian Acad. Sci., **A15**, p190-194, (1942).

23. Orr, B.J., 'Hyperpolarisabilities of halogenated methane molecules. A critical survey', 31st Int. Meet. Soc. Chim. Phys., p227-236, (1978)

24. Buckingham, A.D., 'Theoretical studies of the Kerr effect. The influence of pressure', Proc. Phys. Soc., **A68**, p910-919, (1955)

25. Gentle, I.R. and Ritchie, G.l.D., 'Second hyperpolarisability and static and optical frequency anisotropies of Benzene 1,3,5-Trifluorobenzene and Hexafluorobenzene', J. Phys. Chem., **93**, p7740-7744, (1989)

26. Bogaard, M.P., Orr, B.J., Buckingham, A.D., and Ritchie, G.L.D., ' Temperature dependence of the Kerr effect of chloromethanes', J. Chem. Soc. Faraday Trans., **2**, p1573-1578, (1978).

27. Bogaard, M.P., Buckingham, A.D., and Ritchie, G.L.D., 'Temperature dependence of the Kerr effect of dimethyl ether', J. Chem. Soc. Faraday Trans., **77**, p1547-1551, (1981).

28. Buckingham, A.D., 'The Kerr effect in dilute solutions', Faraday Soc. Trans., **52**, p611-614,(1956)

29. Briegleb, Z., 'Die elektro-optishe Kerr-konstante flüssiger und gelöster substanzen und die art und ursache der gegenseitigen beeinflussung und orientierung der moleküle im flüssigen zustand', Zeitschrift fur Physikalishe Chemie, 14(B), p97-121, (1931).

30. Stuart, H.A. and Volkmann, H., 'The Kerr effect in liquids and solutions and its temperature variation', Z. Physik, **83**, pp444-60, (1933).

31. Otterbein, G., 'The Kerr effect in benzene derivatives', Physik. Z., **35**, pp249-65, (1934).

32. Sachsse, G., 'The Kerr effect of chlorine derivatives of methane ethane and ethylene', Physik. Z., **36**, pp357-67, (1935).

33. Friedrich, H., 'The Kerr effect of nitrobenzene in benzene', Physik. Z., **38**, pp318-29, (1937).

34. Champion, J.V. Meeten, G.H. and Whittle, C.D., 'Temperature dependence of the Kerr effect and depolarisation ratio in liquids', Journal de Chimie Physique et de Physiochimie biologique, **67**(10), p1864-9, (1970).

35. Umegaki, S., 'Organic non-linear optical materials', Oyo Butsuri, **54**(2), p1-13, (1985).

36. Buckingham, A.D. and Pople, J.A., 'Theoretical studies of the Kerr effect. Deviations from a linear polarisation law', Proc. Phys. Soc., **A68**, p905-909, (1955).

37. Gans, R., 'Dielektrizitatskonstante und Elektrische Doppelbrechung', Ann. Physik, **64**, p481-512,(1921).

38. Gans, R., 'Asymmetrie von Gasmolekeln. Ein Beitragzur Bestimmungder-molekularen Form', Annalen der Physik, **65**(10), p97-123, (1921).

39. Meeten, G.H., 'Hyperpolarisability contributions to Kerr effect in liquids', Trans. Faraday Soc., **A64**, pp2267-2272, (1968).

40. Stuart, H.A., 'Molekulstruktur', 3rd. Ed., Springer, Berlin, (1967).

41. Stratton, 'Electromagnetic thoery', McGraw-Hill Book Co., New York, (1941).

42. Le Fèvre, C.G. and Le Fèvre, R.J.W., 'Molecular polarisability. The contributions of terms to the Kerr constant of a substance', J. Chem. Soc., p2670-2675, (1959).

43. Buckingham, A.D. and Pople, J.A., 'Theoretical studies of the Kerr effect. Deviations from a linear polarisation law', Proc. Phys. Soc., **A68**, p905-909, (1955).

44. Beevers, M.S. and Khanarian, G., 'The temperature dependence of the Kerr constant of polar liquids', Aust. J. Chem., **33**, p2585-2595, (1981)

45. Buckingham, A.D. and Raab, R.E., 'A molecular theory of the electro-optical Kerr effect in liquids', J. Chem. Soc., p2341-2351, (1957)

46. Goodbody, A.M., 'Cartesian tensors with applications to mechanics, fluid mechanics and elasticity', Ellis Horwood Ltd. (1982).

47. Buckingham, A.D. and Orr, B.J., 'Molecular hyperpolarisabilities', Chem. Soc. Quart. Rev., **21**, p195-212, (1967).

48. Buckingham, A.D., 'The Kerr effect in dilute solutions', Faraday Soc. Trans., **52**, p611-614, (1956)

49. le Fèvre, C.G. and Le Fèvre R.J.W., 'Molecular polarisability. The measurement of molecular Kerr constants in solution', J. Chem. Soc., p4041-4050, (1953).

50. Specialist Periodic Report, 'Dielectric and related molecular processes, The Chemical Society.

51. Miller, C.K. and Ward J.F., 'Measurements of nonlinear optical polarisabilities for some halogenated methanes. The role of bond-bond interactions', Phys. Rev., **A16**, p1179-1185, (1977).

52. Miller, C.K., orr, B.J., and Ward, J.F., 'An interacting segment model of molecular electric tensor properties. Theory and application to electric dipole moments of the halogenated methanes', J. Chem. Phys., **67**, p2109-2118, (1977).

53. Franken, P.A. and Ward, J.F., 'Optical harmonics and nonlinear phenomena', Rev. Mod. Phys., **35**, p23-39, (1963).

54. Buckingham, A.D. and Orr, B.J., 'Molecular hyperpolarisabilities', Chem. Soc. Quart. Rev., **21**, p195-212, (1967).

55. Orr, B.J., 'Hyperpolarisabilities of halogenated methane molecules. A critical survey', 31st Int. Societe. Chimie. Physiqu., p227-236, (1978)

56. Havelock, T.H., 'The dispersion of double refraction in relation to crystal structure', Proc. Roy. Soc. (London), **A80**, p28-44, (1907).

Havelock, T.H., 'The dispersion of double refraction', physic. Rev., 28, p136-9, (1909)

57. Quarles, G.G., 'The dispersion of the electro-optical effect in carbon dioxide', Phys. Rev., **46**, p692-4, (1934)

58. Powers, J.C. Jr., 'Dispersion of the Kerr constant of the acridine orange-polyglutamic acid complex', J. Amer. Chem. Soc., **89**(8), p1780-5, (1967).

59. Wood, R.W., 'Physical optics', 3rd Edn., Ch. 15, MacMillan, New York, (1934).

60. Le Fèvre, R.J.W. and Solomons, S.C., 'Kerr constant-dispersion measurements on benzene and carbon tetrachloride', Aust. J. Chem., **21**, p1703-10,(1968).

61. O'Konski, C.T. and Zimm, B.H., 'New method for studying electrical orientation and relaxation in aqueous colloids, Science, **111**, p113-116, Feb. (1950).

62. O'Konski, C.T. and Haltner A.J., 'Characterisation of the monomer and dimer of tobacco-mosaic virus by transient electric birefringence', J. Am. Chem. Soc., **78**, p3604-10, (1956).

63. Houssier, C. and Fredericq, E., 'Electro-optical properties of nucleic acids and nucleoproteins. I. Study of the gel-forming deoxyribonucleohistone', Biochim. biophys. Acta., **120**(1), p113-30, (1966).

64. Mumby, S.J., 'Experimental and theoretical investigations of the dielectric and electro-optical properties of polycarbazoles and polysiloxanes', University of Aston in Birmingham, (1983).

65. Beevers, M.S. and Khanarian, G., 'Measurement of Kerr constants of conducting liquids', Australian Journal of Chemistry, **32**, p263-269, (1979)

66. Beevers, M.S., Elliot, D.A., and Williams, G., 'Static and dynamic Kerr effect studies of glycerol in its highly viscous state', J. Chem. Soc., Faraday II, **76**, p112-121, (1980).

67. Rujimethabhas, M. and Crossley, J., 'Temperature dependence of the electro-optic Kerr effect for liquids at 632.8nm., Can. J. Phys., **58**, p1319-1325, (1980)

68. Aroney, M.J., Battaglia, M.R. Ferfoglia, R., Millar, D. and Pierens, R.K., 'The Kerr constant of water and other pure liquids at 633nm', J.C.S., Faraday II, **72**, p724-726, (1976)

69. Anton Paar DMA Digital Density Meter Instruction manual (DMA 602).

70. Le Fèvre, R.J.W., 'Dipole moments', **1**, London, Methuen & Co. ltd, (1953).

71. Mosotti, O.F., Mem. Math. Fis. Modena 24, II (1850)49

72. Clausius, R., Die Mechanishe Wärmetheorie 11 p62 Braunschweig 1879

73. Debye, P., 'Handbuch Radiol', **6**, p597, (1925)

74. Debye, P. and Sack, H., 'Handbuch der Radiologie', **6**, Ch. 2, p69 and p179, (1934).

75. Weast, R.C, 'Handbook of Chemistry and Physics', 52nd Edn., The chemical Rubber Co., 1971-72

76. Hoecker, F.E., 'Dielectric constants of extremely dilute solutions', J. Chem. Phys., **4**, pp 431-4,(1936)

77. Müller, F.H., Phys. Z., 34, p689, (1933)

78. Müller, F.H., Phys. Z., 35, p346, (1934)

79. Guggenheim, E.A., 'A proposed simplification in the procedure for computing electric dipole moments', Trans. Far. Soc., **45**, p714-720, (1949).

80. Onsager, L., 'Electric moments of molecules in liquids', J. Am. Chem. Soc., **58**, p1486-1493, (1936).

81. Cumper, C.W.N. and Singleton, A., 'The electric dipole moments of aniline, aminopyridines, and their n-methyl derivatives in benzene and 1,4 dioxane solutions', J. Chem. Soc., p1096-1099, (1967).

82. Few, A.V. and Smith, J.W., 'Molecular polarisation and molecular interaction. I. The apparent dipole moments of aniline, methylaniline and dimethylaniline in benzene and 1,4-dioxane solutions', J. Chem. Soc., p753-60,(1949).

83. McClellan, A.L., 'Tables of experimental dipole moments', Freeman and Co., San Francisco, (1963).

84. Nelson, D.R., Lide, Jr., and Maryott, A.A., 'Selected values of electric dipole moments for molecules in the gas phase', NSRDS-NBS 10, U.S. Government Printing Office, Washington, D.C., (1967).

85. le Fèvre, C.G. and Le Fèvre R.J.W., 'Molecular polarisability. Its anisotropy in aliphatic and Aromatic Structures', J. Chem. Soc.,p1577-1589, (1954).

86. Levine, B.F. and Bethea, C.G., 'Second and third order hyperpolarisabilities of organic molecules', J. Chem. Phys., **63**, No. 6, (1975).

87. Lap-Tak Cheng, Wilson, T., Stevenson, S.H., and Meredith, G.R., 'Experimental investigations of organic molecular nonlinear optical polarisabilities. 1. Methods and results on benzene and stilbene derivatives', J. Phys. Chem., **95**, p10631-10643, (1991).

88. Levine, B.F. and Bethea, C.G., 'Effects on hyperpolarisabilities of molecular interactions in associating liquid mixtures', J. Chem. Phys., **65**, no. 6, (1976).

89. Chitoku, K and Higasi, K., 'Dielectric relaxation and molecular structure III. Relaxation times of aniline derivatives in benzene and dioxane', bulletin of the chemical society of Japan, **39**, p2160-2168, (1966).

90. Smyth, C.P., 'Dielectric behaviour and structure', McGraw-Hill, (1955)

91. Böttcher, C.J.F. and Bordewijk, P., 'Theory of electric polarisation', 2nd Edn., Vol. II, p288, Elsevier, (1973).

92. Maxwell, J.C., 'Treatise on Electricity and magnetism, **2**, p396, Clarendon press, (1892)

93. Buckingham, A.D. and Stiles, P.J., 'Theory of the solvent effect on the molar refraction, polarisation, Kerr and Cotton-Mouton constants of non-polar solutes', Trans. Far. Soc., **67**, p577-582, (1970).

94. Lorenz, L.K., danske vidensk. Selsk. Skr., (Nat. Math.) [v]8 (1870)230

95. Lorenz, L.K., Ann. Phys., Lpz. II (1880)70

96. Lorentz, H.A., Ann. Phys., Lpz. 9 (1880)641

97. Buckingham, A.D. and Bridge, N.J., 'The polarisation of light scattered by gases', Proc. Roy. Soc., **295**(A), p334-349, (1966).

98. Bogaard, M.P., Buckingam, A.D., Pierens, R.K., and White, A.H., 'Rayleigh scattering depolarisation ratio and molecular polarisability anisotropy for gases', J. Chem. Soc. Trans., **74**, p3008-3015, (1978).

99. Buckingham, A.D. and Stephen, M.J., 'A theory of the depolarisation of light scattered by a dense medium', Trans. Faraday Soc., **53**, p884-893, (1957).

100. Alms, G.R., Burnham, A.K., and Flygare, W.H., 'Measurement of the dispersion in polarisability anisotropies', Chem. Phys., **63**, p3321-3326, (1975).

101. Le Fèvre, R.J., Wand, B., Purnachandra, Rao, 'Molecular Polarisability. The determination of solutes from scattering of light by solutions', Austral. J. Chem., p3644, (1957).

102. Le Fèvre, R.J., Wand, B., Purnachandra, Rao, 'Molecular polarisability. The anisotropies of seven mono-substituted benzenes and of nitromethane as solutes in carbon tetrachloride', Austral. J. Chem., p1465-72, (1958).

103. Bhagavantam, 'Scattering of light and the Raman Effect', Andhra Univ.,Waltair, (1940).

104. Abdel-Azim, A., Abdel-Azim, and Petr Munk, 'Light Scattering of liquids and liquid Mixtures 1. Compressibility of Pure liquids', J. Phys. Chem., **91**, p3910-3914, (1987).

105. Rogerio C.C. leite, Robert S. Moore, and Sergio P.S.Porto, Letters to the Editor, 'Use of a gas laser in studies of the depolarisation of the Rayleigh scattering from simple liquids', J. Chem. Phys., **30**, p3741-3742, (1964).

106. Topping. J., 'Errors of observation and their treatment', Science paperbacks, Chapman and Hall ltd., (1972).

107. Hehre, W.J., Radom, L., and Pople, J.A., 'Molecular orbital theory of the electronic structure of organic compounds. XII. Conformations, stabilities, and charge distributions in monosubstituted benzenes', J. American Chem. Soc., p1496-1497, (1972).

108. Fukuyo, M., Hirotsu, K., and Higuchi, T., 'The structure of aniline at 252K', Acta Cryst., **B38**, p640-643, (1982).

109. Aroney, M.J., Le Fèvre, R.J.W., Radom, L., and Ritchie, G.L.D., 'Molecular Polarisability. The molar Kerr constants of aniline and of three substituted anilines in a variety of non-polar media', J. Chem. Soc. (B), p507-512, (1968).

110. Levine, B.F., and Bethea, C.G., 'Second and third order hyperpolarisabilities of organic molecules', J. Chem. Phys., **63**, No. 6., p2666-2682, (1975).

111. Mendicuti, F., Saiz, E., 'Dependence of the Kerr constants of benzene, p-dioxane and poly(oxydiethylene terephthalate) on temperature', Makromol. Chem., **187**, p2483-2488, (1986).

112. Stuart, H.A. and Volkmann, H.,'Experimentelle untersuchungen des elektrischen Kerreffekts an gasen und dämpfen bei höheren temperaturen', Annalen der Physik, **18**, p121-149, (1933).

113. Pugh, D., Sherwood, J.N., 'Organic crystals for nonlinear optics', Chemistry in Britain, p544-548, June (1988).

114. Levine, B.F., and Bethea, C.G., 'Effects on hyperpolarisability of molecular interactions in associating liquid mixtures', J. Chem. Phys., **65**, No. 6., p2429-2438, (1976).

115. Dulcic, A., and Sauteret, C., 'The regularities observed in the second order hyperpolarisability of variously disubstituted benzenes', J. Chem. Phys., **69**(8), p3453-3457, (1978).

116. Cheng, L., Tam, W., Stevenson, S.H., Meredith, G.R., Rikken, G., and Marder S.R, 'Experimental investigations of organic molecular nonlinear optical polarisabilities. 1. Methods and results on benzene and stilbene derivatives', J. Phys. Chem., **95**, p10631-10643, (1991).

117. Cardelino, B.H., Moore, C.E., and Stickel, R.E., 'Static second-order polarisability calculations for large molecular systems', J. Phys. Chem., **95**, p8645-8652, (1991).

118. Bordewijk, P., 'On the determination of molecular hyperpolarisabilities by combining data from the Kerr effect and from the electrically induced NMR line splitting', Chemical Physics Letters, **39**, No. 2, p342-346, (1976).

119. Levine, B.F., 'Donor-acceptor charge transfer contributions to the second order hyperpolarisability', Chemical Physics Letters, **37**, No. 3, p516-520, (1976).

120. Hermann, J.P. and Ducuing, J., 'Third-order polarisabilities of long-chain molecules,' J. Appl. Phys., **45**, p5100-5102, (1974).

121. Dulcic, A. and Flytzanis, C., 'A new class of conjugated molecules with large second-order polarisability,' Opt. Commun., **25**, p402-406, (1978).

122. Oudar, J.L. and Hierle, R., 'An efficient organic crystal for non-linear optics: Methyl-(2,4-dinitrophenyl)-aminopropanoate,' J. Appl. Phys., **48**, p2699-2704, (1977).

123. Halbout, J.M. Blit, S. Donaldson, W., and Tang, C.L., 'Efficient phase-matched second-harmonic generation and sum-frequency mixing in urea', IEEE J. Quantum Electron., **QE-15**, p1176-1180, (1979).

124. Davies, P.L., 'Polarisabilities of long chain conjugated molecules,' Trans. Faraday Soc., **48**, p789-795, (1952).

125. Rustagi, K.C., and Ducuing, J., 'Third-order optical polarisability of conjugated organic molecules,' Opt. Commun., **13**, p164-168, (1975).

126. Levine, B.F., Bethea, C.G., Thurmond, C.D., and Lynch, R.T., 'An organic crystal with an exceptionally large optical second-harmonic coefficient: 2-methyl-4-nitroaniline,' J. Appl. Phys., **50**, p2523-2527, (1979)

127. Levine, B.F., Bethea, C.G., 'Absolute signs of hyperpolarisabilities in the liquid state,' J. Chem. Phys., **60**(10), p3856-3858, (1974).

APPENDIX A

COMPUTER CONNECTIONS

A1.1 XCALIBUR COMPUTERS XVIA BOARD

As far as the Apple IIe computer microprocessor is concerned the VIA board exists at 16 consecutive memory addresses. At each address there exists an 8 bit register which may be read from or written to. From BASIC a register is written to by using POKE and read using PEEK. The double VIA has 4x8 bit bi-directional data lines which form the 4 ports A1, B1, A2, and B2 (see Figure A1).

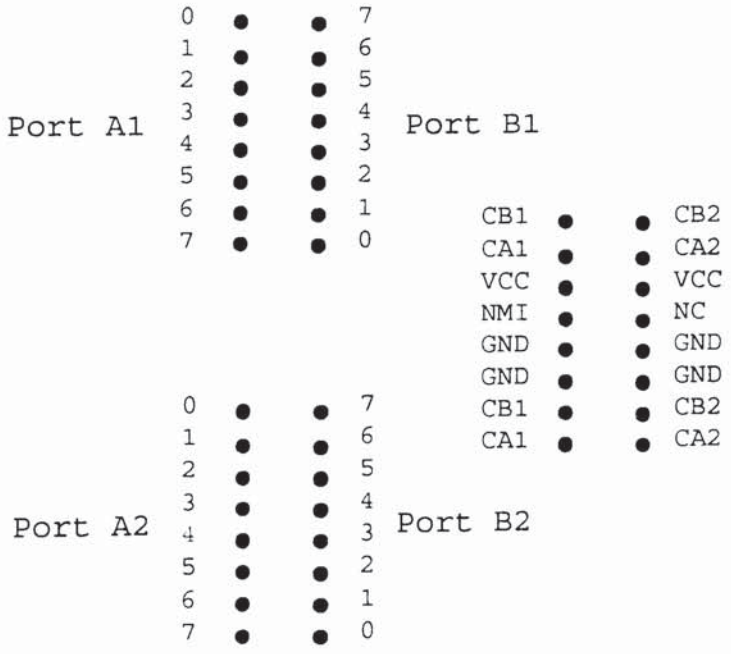

Figure A1 Connections for the VIA board

For the Apple IIe the addresses of the four VIA ports are given by:-

Address = 49280 + (Slot*16) + Register

and

Address = 49152 + (Slot*256) + Register

where Register = 0 to 15. Port A has a register value of 1 and port B has a register value of 0.
Each bit of each port can be individually defined as an input or output by setting the Data Direction Registers DDRA and DDRB. A 1 in a bit position in the DDR defines the corresponding I/O bit to be an output; a 0 defines an input bit. The VIA board was inserted into slot 5 of the Apple IIe computer; the corresponding addresses of the ports and the DDR can be seen in Table A1

Table A1 Addresses of the VIA ports and the Data Directional Registers (DDR).

Remarks	Address
Port B1	50432
Port A1	50433
DDRB1	50434
DDRA1	50435
Port B2	49360
Port A2	49361
DDRB2	49362
DDRA2	49363

Table A2 Examples of programming the VIA and data direction register (DDR).

BASIC commands	Result
Poke 50434,0	Set all 8 bit lines on port B1 to input
Peek 50532	Yields data on port B1
Poke 50435,253	Set Port A1 pin 1 to input rest of pins to output

A1.2 DL905 TRANSIENT RECORDER

The digital output interface enables the 1024 words stored in the memory of the DL905 transient recorder to be read out in sequence to the Apple IIe computer. The transfer process is completely controlled by the Apple IIe computer.

Each word is represented as 8 parallel, binary digits B8-B1 (J1/4-J1/11) B8 being the most significant bit. The code is pure binary with a number range extending from 00000000 (decimal 000) representing -ve full scale, to 11111111 (decimal 255) representing +ve full scale. This coding is not changed by Input Amplifier gain offset settings. If the +UP/-UP control is set to - then the notation is inverted.

The control signals used in this interface are Digital Output Enable (J1/19), Digital Output Request (J1/24), Digital Output Flag (J1/18), Word Request (J1/23) and Data Ready (J1/17). These and the data

signals are accessible at the 24 way rear panel connector J1; mating plug Amphenol 57-30240.

The control and data signals used in this interface are TTL/DTL compatible and positive true notation is used throughout; logic 1=+2.5v to +5.0v, logic 0=0v to 0.8v. The connecting cables from the computer to the interface are kept as short as possible to ensure spurious signals or noise do not occur.

A1.2.1 DL905 TRANSIENT RECORDER CONTROL SEQUENCE

The DL905 must be in the single trigger mode and in the quiescent display state (Cycle (J1/20)=0, Plot Flag (J1/15=0) for the interface to operate. An armed condition will be cancelled when the output starts.
To enable the initiation of output, Digital Output Enable (J1/19) should be put to 0. The signal is used as a device present signal and may either be activated by the computer when it is ready e.g. power on; or,more simply, by a link to 0v in the interconnecting cable.

Once the Digital Output Enable is 0 then digital readout is initiated by applying a 1 to 0 transition of Digital Output Request (J1/24). The output sequence will then start, indicated by a 0 to 1 transition of Digital Output Flag. Digital Output Flag remains at 1 for the whole of the readout period. The first word is automatically placed on the output lines of Digital Output Flag going to 1; a 0 to 1 transition by Data Ready

indicates valid data. To read out further words the Word Request Signal (J1/23) is used; a positive pulse of greater than 100ns causes Data Ready to go to 0 indicating that the Word Request was received. The readout continues until all 1024 words have been output, whereupon the next Word Request automatically terminates the Output mode and Digital Output Flag makes a 1/0 transition to indicate this.

Table A3 Relevant DL905 Transient Recorder J1 connections.

Pin	Signal	Use
2	Digital arm	1/0 transition
4	Binary data bit 8	Most significant bit 2^7
5	Binary data bit 7	
6	Binary data bit 6	
7	Binary data bit 5	
8	Binary data bit 4	
9	Binary data bit 3	
10	Binary data bit 2	
11	Binary data bit 1	Least significant bit 2^0
17	Data ready	1 indicates valid data
19	Digital output enable	Apply 0 to enable initiation of digital output sequence
23	Word request	0/1 transition requests new data in digital output mode.
24	Digital output request	1/0 transition initiates digital output mode.

Table A4 Connections between Xcalibur Via board and DL905 Transient Recorder.

VIA Board	905 Interface
Port B2 pin 0	24
Port B2 pin 1	23
Port A1 pin 3	19
Port A1 pin 1	17
Port B1 pin 7	4
Port B1 pin 6	5
Port B1 pin 5	6
Port B1 pin 4	7
Port B1 pin 3	8
Port B1 pin 2	9
Port B1 pin 1	10
Port B1 pin 0	11
Port A2 pin 4	2

Table A5 Connection between the Xcalibur VIA board and other devices.

Via Board	Other devices
Port A2 pin 3	Move stepper motor
Port A2 pin 2	Trigger pulse generator

APPENDIX B

THE USE OF A QUARTER WAVE RETARDER

Figure B1 illustrates the use of a quarter-wave plate by showing the electric vectors of the light before entering, and after leaving, the various optical components. The parallel beam of incident light emitted by the laser is plane polarised at an angle of 45° to the applied electric field, E. The electric vector,

$$V_{45} = a \sin \omega t \qquad \text{B1}$$

may be resolved into the parallel and perpendicular components

$$V_s = a \sin \omega t \sin 45^\circ \qquad \text{B2}$$

and

$$V_p = a \sin \omega t \cos 45^\circ \qquad \text{B3}$$

respectively. On passing through a birefringent sample the parallel component is retarded relative to the perpendicular component by a phase difference, δ, and the resultant waveform becomes

$$V_p' = a \sin(\omega t - \delta) \sin 45^\circ \qquad \text{B4}$$

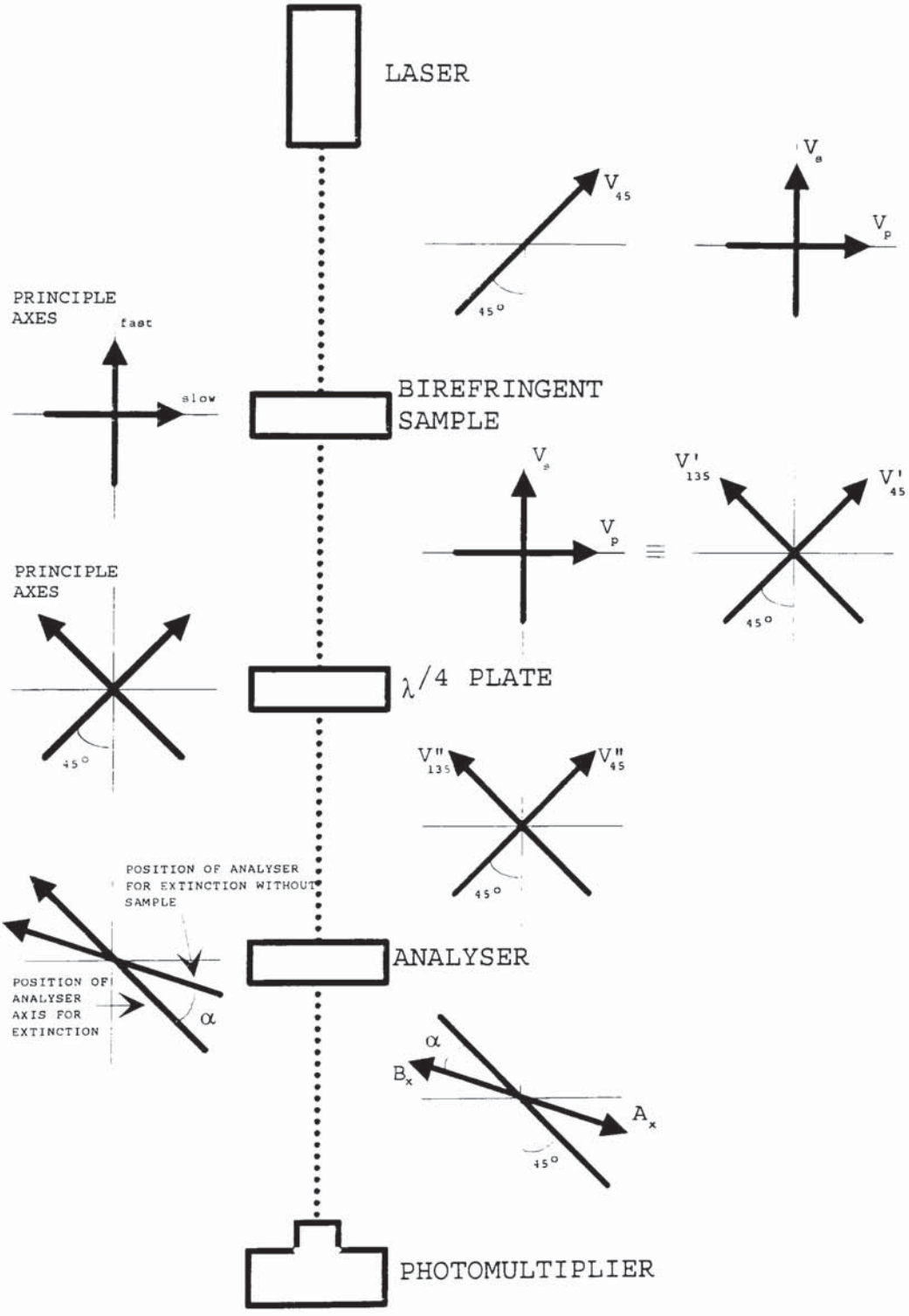

Figure B1 Electric vectors of light before entering, and after leaving, the various optical components of the electro-optical Kerr effect apparatus.

The parallel and perpendicular components of the electric vector may each be further resolved into two components at 45° to the direction of the applied electric field. these components are

$$V'_{45} = a \sin \omega t \cos^2 45^\circ + a \sin(\omega t - \delta) \sin^2 45^\circ \qquad \text{B5}$$

and

$$V'_{135} = a \sin \omega t \cos^2 45^\circ \sin 45^\circ - a \sin(\omega t - \delta) \sin 45^\circ \cos 45^\circ \qquad \text{B6}$$

respectively. The component, V'_{45}, suffers a relative phase retardation of $\pi/2$ (90°) on passing through the quarter wave plate. The waveform emerging from the quarter wave plate may now be represented by the following orthogonal vectors

$$V''_{45} = a \sin(\omega t - \pi/2) \cos^2 45^\circ + a \sin(\omega t - \delta - \pi/2) \sin^2 45^\circ \qquad \text{B7}$$

$$V''_{135} = a \sin \omega t \cos 45^\circ \sin 45^\circ - a \sin(\omega t - \delta) \sin 45^\circ \cos 45^\circ \qquad \text{B8}$$

Since,

$$\sin 45^\circ = \cos 45^\circ \qquad \text{B9}$$

then the two components may be simplified to give

$$V''_{45} = a \cos^2 45^\circ \left[\sin(\omega t - \pi/2) + \sin(\omega t - \delta - \pi/2) \right] \qquad \text{B10}$$

and

$$V''_{135} = a\cos^2 45^\circ\left[\sin\omega t - \sin(\omega t - \delta)\right] \qquad \text{B11}$$

By applying the identity,

$$\sin x \pm \sin y = 2\sin\tfrac{1}{2}(x \pm y)\cos\tfrac{1}{2}(x \mp y) \qquad \text{B12}$$

equations B11 and B12 may be rewritten in the form

$$V''_{45} = 2a\cos^2 45^\circ\left[\sin\tfrac{1}{2}(\omega t - \pi/2 + \omega t - \delta - \pi/2)\right. \qquad \text{B13}$$
$$\left.\cos\tfrac{1}{2}(\omega t - \pi/2 - \omega t + \delta + \pi/2)\right]$$

and

$$V''_{135} = 2a\cos^2 45^\circ\left[\sin\tfrac{1}{2}(\omega t - \omega t + \delta)\right. \qquad \text{B14}$$
$$\left.\cos\tfrac{1}{2}(\omega t + \omega t - \delta)\right]$$

These further simplify to give

$$V''_{45} = 2a\cos^2 45^\circ\cos\delta/2\sin(\omega t - \pi/2 - \pi/2) \qquad \text{B15}$$

and

$$V''_{135} = 2a\cos^2 45^\circ\sin\delta/2\cos(\omega t - \delta/2) \qquad \text{B16}$$

Since,

$$\sin(x - \pi/2) = -\cos x \qquad \text{B17}$$

equation B15 may then be written in the form

$$V''_{45} = -2a\cos^2 45^\circ\cos\delta/2\cos(\omega t - \delta/2) \qquad \text{B18}$$

Thus, it can be seen that the two orthogonal components,

$$V''_{45} = -2a\cos^2 45^\circ \cos\delta/2 \cos(\omega t - \delta/2) \qquad \text{B19}$$

and

$$V''_{135} = 2a\cos^2 45^\circ \sin\delta/2 \cos(\omega t - \delta/2) \qquad \text{B20}$$

have the same phase relationship, and differ only in their relative amplitudes. Therefore, the light emerging from the quarter wave plate is plane polarised and may thus be completely extinguished by the analyser when the latter is rotated by an angle α_s from its normally crossed (E=0) position.

APPENDIX C

MEASUREMENT OF THE PHASE DIFFERENCE, δ, USING PULSED ELECTRIC FIELDS

The relationship between the transmitted intensity, I, of a plane polarised beam of light, the initial intensity, I_o, and the rotation, α, of the analyser with respect to the nulled position is known as Malus' Law and may be expressed as

$$I = I_o \sin^2 \alpha \qquad C1$$

Applying Malus' Law, the intensity of light transmitted by the analyser, when the electric field, E, is zero, is given by

$$I_{E=0} = I_o \sin^2 \alpha \qquad C2$$

However, upon application of an electric field to the sample, the light transmitted by the sample becomes

$$I_{E\neq 0} = I_o \sin^2(\alpha + \delta/2) \qquad C3$$

If the electronically-induced pulse of light is nulled, by rotating the analyser, to the quiescent level then

intensities $I_{E=0}$ and $I_{E\neq0}$ become equal. Thus, from equations C2 and C3 we may write

$$I_o \sin^2 \alpha_1 = I_o \sin^2(\alpha_1 + \delta/2) \qquad C4$$

Thus,

$$\sin^2 \alpha_1 = \sin^2(\alpha_1 + \delta/2), \qquad C5$$

and for arguments corresponding to less than 20° a satisfactory approximation is given by

$$\alpha_1 = (\alpha_1 + \delta/2)^2 \qquad C6$$

Expanding and rearranging equation C6 gives

$$\alpha_1 = -\frac{\delta}{4} \qquad C7$$

Thus, for the pulsed mode of operation, expression C7 describes the relationship between the angular rotation of the analyser, required to null the optical signal, and the electronically-induced phase retardation, δ.

APPENDIX D

SOLUTION OF THE NULL POINT, α_1, FOR VARIOUS ROTATIONS OF THE ANALYSER.

According to Malus' law

$$I = I_o\left[\sin^2(\alpha) - \sin^2(\alpha + \delta/2)\right] \qquad \text{D1}$$

where I is the difference between the light intensity transmitted for E=0 and E≠0. By applying

$$2\sin^2(\alpha) = 1 - \cos(2\alpha) \qquad \text{D2}$$

then

$$\begin{aligned} 2I/I_o &= \cos(2\alpha + \delta) - \cos(2\alpha) \\ &= \cos(2\alpha)\cos(\delta) - \sin(2\alpha)\sin(\delta) - \cos(2\alpha) \\ &= \left(\cos(\delta) - 1\right)\cos(2\delta) - \sin(\delta)\sin(2\alpha) \end{aligned} \qquad \text{D3}$$

If $K_1 = \cos(\delta) - 1$ and $K_2 = -\sin(\delta)$ then

$$2I/I_o = K_1\cos(2\alpha) + K_2\sin(2\alpha) \qquad \text{D4}$$

Expression D1.4 expresses the difference in the light intensity detected by the photomultiplier between the conditions E=0 and E≠0 as the analyser is rotated by an angle, α, from the crossed position. If a set of

observations of (α_i, Y_i) is considered where $Y_i = 2I/I_o$ then in order to determine the null-point, α_1, it is desirable to fit the observations to the relation

$$Y_i = K_1 \cos(2\alpha_i) + K_2 \sin(2\alpha_i) \qquad \text{D5}$$

It is assumed that the α values are precise such that all the uncertainty is contained in the Y values and that the weights of the Y values are equal. It follows that the differences, whose sum of squares it is desired to minimise, are of the form

$$\Delta Y_i = Y_i - \left(K_1 \cos(2\alpha_i) + K_2 \sin(2\alpha_i)\right) \qquad \text{D6}$$

therefore,

$$\begin{aligned} \Delta Y_i^2 &= \left[Y_i - \left(K_1 \cos(2\alpha_i) + K_2 \sin(2\alpha_i)\right)\right] \\ &= Y_i^2 - 2Y_iK_1 \cos(2\alpha_i) - 2Y_iK_2 \sin(2\alpha_i) + K_1^2 \cos^2(2\alpha_i) \\ &\quad + K_2^2 \sin^2(2\alpha_i) + 2K_1K_2 \cos(2\alpha_i)\sin(2\alpha_i) \end{aligned} \qquad \text{D7}$$

If there are n pairs of observations the sum is

$$\begin{aligned} S = \Delta Y_i^2 &- 2K_1Y_i \cos(2\alpha_i) - 2K_2Y_i \sin(2\alpha_i) - K_1^2 \cos^2(2\alpha_i) \\ &+ K_2^2 \sin^2(2\alpha_i) + 2K_1K_2 \cos(2\alpha_i)\sin(2\alpha_i) \end{aligned} \qquad \text{D8}$$

The condition for the best choice of K_1 and K_2 is that ΔY_i^2 should be a minimum i.e.

$$\frac{\partial S}{\partial K_1} = 0 \qquad \text{and} \qquad \frac{\partial S}{\partial K_2} = 0$$

D9

The first condition gives

$$2K_1 \cos^2(2\alpha_i) + 2K_2 \cos(2\alpha_i)\sin(2\alpha_i) - 2Y_i \cos(2\alpha_i) = 0 \quad \text{D10}$$

The second gives

$$2K_1 \cos(2\alpha_i)\sin(2\alpha_i) + 2K_2 \sin^2(2\alpha_i) - 2Y_i \sin(2\alpha_i) = 0 \quad \text{D11}$$

The solution of these simultaneous equations gives K_1 and K_2. It can easily seen that the solution of α_1 when I=0 is then given by

$$\alpha_1 = \tan^{-1}\left(\frac{K_2}{K_1}\right) \quad \text{D12}$$

APPENDIX E

APPLE IIE COMPUTER PROGRAM

E1.1 INTRODUCTION

The following computer program was used to determine the Kerr constant of the solutions and solvents used throughout this thesis and was written in Apple IIe basic. The computer program calculates the angle, α, required to solve for the condition $I_{E=0} = I_{E\neq0}$ (see Chapter 3). The gradient and 68% confidence limit of α versus E^2 is then calculated. The gradient can then be manually converted to the Kerr constant of the sample using the method outlined in section 3.6. The output of the results can be printed to the computer screen and/or a printer. It is also possible to perform relaxation experiments using this program.

E1.2 Computer program listing

```
10      REM SHIFT PROGRAM LOCATION IN MEMORY
20      :
30      LOC=17913+1:IF PEEK(103)+PEEK(104)*256<>LOC THEN
        POKE LOC-1,0:POKE 103,LOC-INT(LOC/256)*256:POKE
        104,INT(LOC/256):PRINT CHR$(4);"RUN KERR PROGRAM"
40      :
```

```
100     REM LOAD IN MACHINE CODE PROGRAM
110     PRINT CHR$(4);"BLOAD FASTDAT6,D2"
120     POKE 49363,255
130     POKE 49361,0
140     :
150     REM CLEAR SCREEN AND DEFINE VARIABLES
160     DIM PULSE(1025):DIM COUNT(3)
170     DIM WINDOW(4):DIM ITENSITY(2)
180     DIM R1(30):DIM R2(30)
190     DIM R3(30):DIM R4(30)
200     DIM R5(30):DIM R6(30)
210     WINDOW(1)=2078
220     WINDOW(2)=2316
230     WINDOW(3)=2511
240     WINDOW(4)=2816
250     HOME
260     FOR F=1 TO 1025
270          PULSE(F)=0
280     NEXT F
290     AVERAGE=1:ITENSITY(1)=0:CHANGE=0
300     COUNT(1)=0:ITENSITY(2)=0:COUNT(2)=0
310     :
320     REM COUNT(1)=TOTAL NUMBER OF PULSES TRANSFERRED
330     REM COUNT(2)=NUMBER OF PULSES TRANSFERRED FOR A
340                  SET VOLTAGE
350     REM COUNT(3)=MECHANICAL COUNTER NUMBER
360     REM JUMP=COUNTER INCREMENT
370     :


1000    REM MAIN PROGRAM
1005    :
1010    GOSUB 2000:INPUT K$
1020    GOSUB 2500:REM MAIN MENU/RETURN VALUE OF K$
1030    IF K$="R" THEN GOTO 1010:REM RESTART PROGRAM
1040    IF K$="Q" THEN GOTO 1090:REM DETERMINE PULSE QUALITY
1050    IF K$="N" THEN GOTO 1090:REM FIND NULL-POINT
1060    IF K$="W" THEN GOTO 1320:REM FIND WINDOW POSITIONS
```

```
1070    GOTO 1020:REM INCORRECT RESPONSE TO MENU
1080    :
1090    REM DETERMINE PULSE QUALITY AND NULL-POINT
1100    GOSUB 3000:REM INPUT VARIABLES
1110    GOSUB 3500:REM CLEAR SCREEN AND DISPLAY MESSAGE
1120    GOSUB 4000:REM TRANSFER PULSE AND AVERAGE
1130    GOSUB 4500
1140    IF K$<>"Q" THEN FLAG=0
1150    IF FLAG=1 THEN GOTO 1120
1160    IF K$="Q" THEN GOTO 1020:REM REPEAT MENU
1170    K$="":REM RESET K$
1180    IF ITENSITY(2)=0 THEN GOTO 1200
1190    IF ITENSITY(1)>ITENSITY(2) THEN GOTO 1230
1200    ITENSITY(2)=ITENSITY(1)
1210    GOSUB 5000:REM MOVE ANALYSER
1220    GOTO 1120: REM GET NEXT PULSE
1230    REM NULL-POINT FOUND - DISPLAY MESSAGE
1240    HOME:VTAB 16:HTAB 12
1250    PRINT "NULL-POINT FOUND"
1260    VTAB 18:HTAB 6
1270    PRINT "RESET THE MECHANICAL COUNTER"
1280    VTAB 20:HTAB 1
1290    INPUT "R-TO REPEAT , RETURN TO CONTINUE:";K$
1300    IF K$="R" THEN GOTO 210:REM RESTART PROGRAM
1310    :
1320    REM FIND WINDOW POSITIONS
1330
1340    GOSUB 5200:REM DISPLAY FIND WINDOWS MENU K$(D,T)
1350    IF K$="T" THEN GOTO 1380
1360    IF K$<>"D" THEN GOTO 1340
1370    GOSUB 5400:REM DISPLAY PULSE ON OSCILLOSCOPE
1375    GOTO 1340
1380    GOSUB 5600:REM TRANSFER PULSE TO COMPUTER
1390    GOSUB 5800:REM DISPLAY PULSE ON COMPUTER
1400    GOSUB 6000:REM DISPLAY AND MOVE POINTER
1410    :
1420    REM TAKE KERR EFFECT READINGS
1430    :
1440    GOSUB 6500:REM INPUT RELEVANT DATA FOR KERR MEASURMENTS
```

```
1450    GOSUB 6600:REM INITIALISE VARIABLES
1460    GOSUB 6700:REM INPUT HT VOLTAGE VALUE
1470    IF V1<>0 THEN GOTO 1510
1480    GOSUB 7000:REM END SESSION AND RETURN ANALYSER TO NULL POINT
1490    GOSUB 10000:REM CALCULATE KERR GRADIENT
1500    HOME:GOTO 260:REM RESTART PROGRAM
1510    :
1520    COUNT(1)=COUNT(1)+1
1530    GOSUB 8000:REM GET COUNTER INCREMENT
1540    GOSUB 8600:REM TRANSFER PULSE AND AVERAGE IF NESCESSARY
1550    GOSUB 9500:REM CHECK IF PULSE HAS INVERTED
1560    IF TEST<>1 THEN GOTO 1600
1570    GOSUB 9000:REM ANALYSE DATA
1580    COUNT(2)=0
1590    GOTO 1460
1600    :
1610    GOSUB 5000:REM MOVE ANALYSER POSITION
1620    GOTO 1490
1630    STOP


2000    REM DISPLAY INTRODUCTION SCREEN
2005    :
2010    HOME:VTAB 2:HTAB 10
2020    PRINT "KERR EFFECT PROGRAM"
2030    VTAB 3: HTAB 8
2040    PRINT "WRITTEN BY J.H.ROBSON"
2050    :
2060    VTAB 8:HTAB 7
2070    INPUT "PRESS 'RETURN' TO START :";K$
2080    RETURN


2500    REM DISPLAY MAIN MENU
2510    :
2520    HOME:VTAB 2:HTAB 15:PRINT "MAIN MENU"
2530    VTAB 10:HTAB 6
2540    PRINT "N-TO FIND NULL-POINT"
2560    VTAB 12:HTAB 6
```

```
2570      PRINT "Q-TO FIND PULSE QUALITY"
2580      VTAB 14:HTAB 6
2590      PRINT "R-TO RESTART THE PROGRAM"
2600      VTAB 16:HTAB 6
2610      PRINT "W-TO FIND THE WINDOW POSITION"
2620      VTAB 19:HTAB 6
2630      INPUT "ENTER SELECTION : ";K$
2640      :
2650      RETURN


3000      REM INPUT MEASUREMENT VARIABLE VALUES
3010      :
3020      ITENSITY(1)=0:ITENSITY(2)=0:COUNT(3)=0
3030      :
3040      IF K$="Q" THEN GOTO 3070
3050      HOME:VTAB 12:HTAB 1
3060      INPUT "NUMBER OF COUNTER MOVEMENTS PER STEP=";JUMP
3070      VTAB 13:HTAB 1
3080      INPUT "NUMBER OF PULSES TO AVERAGE OVER = ";AVERAGE
3090      VTAB 16:HTAB 6
3100      INPUT "PRESS 'RETURN' WHEN READY";TEST$
3110      RETURN

3500      REM CLEAR SCREEN AND DISPLAY MESSAGE
3510      :
3520      IF K$="Q" THEN GOTO 3570
3530      HOME:VTAB 10:HTAB 5
3540      PRINT "FINDING NULL POINT PLEASE WAIT"
3550      GOTO 3590
3560      :
3570      HOME:VTAB 10:HTAB 2
3580      PRINT "FINDING PULSE QUALITY PLEASE WAIT"
3590      RETURN

4000      REM TRANSFER PULSES AND AVERAGE IF REQUIRED
4010      :
4020      ITENSITY(1)=0:CHANGE=0:FLAG=0
4030      FOR F=1 TO 1025
```

```
4040          PULSE(F)=0
4050       NEXT
4060       :
4070       FOR G=1 TO AVERAGE
4080            POKE 49361,16
4090            FOR F=1 TO 50:NEXT
4100            POKE 49361,0
4110            :
4120            POKE 49361,4
4130            FOR F=1 TO 50:NEXT
4140            POKE 49361,0
4150            :
4160            POKE 7800,12
4170            POKE 7802,0
4180            CALL 7000
4190            POKE 50433,8
4200            :
4210            FOR F=2049 TO 3049
4220               ITENSITY(1)=ITENSITY(1)+PEEK(F)
4230            NEXT F
4240            :
4250            FOR F=2049 TO 3049
4260               PULSE(F-2048)=PEEK(F)+PULSE(F-2048)
4270            NEXT F
4280            :
4290       NEXT G
4300       RETURN

4500       REM CALCULATE AND DISPLAY AVERAGE INTENSITY LEVEL
4510       :
4520       CHANGE=0
4530       ITENSITY(1)=ITENSITY(1)/(1000*AVERAGE)
4540       :
4550       FOR F=1 TO 1000
4560            CRAP=((PULSE(F)/AVERAGE)-ITENSITY(1))^2
4570            CHANGE=CHANGE+CRAP
4580       NEXT F
4590       SDEVN=(CHANGE/1000)^0.5
4600       MESSAGE$="CLEAN PULSE":REM DEFAULT MESSAGE
```

```
4610    IF 100*(SDEVN/ITENSITY(1))>3 THEN MESSAGE$="NOISY PULSE"
4620    VTAB 14:HTAB 1
4630    ITENSITY(1)=INT(ITENSITY(1))
4640    PRINT "INTENSITY LEVEL = ";ITENSITY(1);"    ";MESSAGE$
4650    VTAB 16:HTAB 1
4660    PRINT "COUNTER = ";COUNT(3);"  ";"ERROR =
        ";INT(100*(SDEVN/ITENSITY(1)));"%"
4670    :
4680    IF K$<>"Q" THEN RETURN
4690    :
4700    VTAB 19:HTAB 4
4710    KEY=PEEK(49152)
4720    IF KEY<128 THEN FLAG=1
4730    POKE 49168,0
4740    RETURN

5000    REM MOVE THE ANALYSER
5010    :
5020    FOR H=1 TO JUMP
5030         POKE 49361,8
5040         FOR F=1 TO 100:NEXT
5050         POKE 49361,0
5060         FOR F=1 TO 100:NEXT
5070    NEXT H
5080    COUNT(3)=COUNT(3)+JUMP:REM CORRECT COUNTER LEVEL
5090    RETURN

5200    REM DISPLAY FIND WINDOW POSITION MENU
5210    :
5220    TEXT:HOME:VTAB 10:HTAB 2
5230    PRINT "D-DISPLAY PULSE ON OSCILLOSCOPE"
5240    VTAB 12:HTAB 4
5250    PRINT "T-TRANSFER PULSE TO COMPUTER"
5260    VTAB 15:HTAB 7
5270    INPUT "ENTER SELECTION:";K$
5280    RETURN

5400    REM DISPLAY PULSE ON OSCILLOSCOPE
5410    :
```

```
5420      POKE 49361,16
5430      FOR F=1 TO 50:NEXT
5440      POKE 49361,0
5450      FOR F=1 TO 50:NEXT
5460      POKE 49361,4
5470      FOR F=1 TO 50:NEXT
5480      POKE 49361,0
5490      FOR F=1 TO 50:NEXT
5500      RETURN

5600      REM TRANSFER PULSE TO COMPUTER
5610      :
5620      POKE 49361,16
5630      FOR F=1 TO 200:NEXT
5640      POKE 49361,4
5650      FOR F=1 TO 200:NEXT
5660      POKE 49361,4
5670      FOR F=1 TO 200:NEXT
5680      POKE 49361,0
5690      POKE 7800,12
5700      POKE 7802,2
5710      CALL 7000:REM CALL MACHINE CODE PROGRAM
5720      POKE 50433,8
5730      RETURN

5800      REM DISPLAY PULSE ON COMPUTER SCREEN
5810      :
5820      HOME:HGR:HCOLOR=3
5830      HPLOT 0,0 TO 279,0
5840      HPLOT 279,0 TO 279,159
5850      HPLOT 279,159 TO 0,159
5860      HPLOT 0,159 TO 0,0
5870      :
5880      VTAB 24:HTAB 1
5890      PRINT "ADVANCE-ANYKEY, S-SET, Q-QUIT";
5900      :
5910      FOR F=2049 TO 3068
5920           HPLOT (F-2049)/3.685,159-PEEK(F)/1.6
5930      NEXT
```

```
5940      RETURN

6000      REM DISPLAY AND MOVE POINTER
6010      :
6020      NUMBER=0:REM LOCAL VARIABLE
6030      :
6040      FOR F=5 TO 275
6050           HCOLOR=3
6060           HPLOT F,5 TO F,154
6070           TIME=PEEK(3079)
6080           TIME=(TIME*F)/279
6090           TIME=INT(TIME*1000)/1000
6100           ITENSITY(1)=PEEK(F*3.685+2049)
6110           VTAB 22:HTAB 25
6120           PRINT "              ";
6130           VTAB 22:HTAB 25
6140           PRINT "INTENSITY=";ITENSITY(1)
6150           GET K$:PRINT CHR$(4)
6160           IF K$="Q" THEN GOTO 5200:REM WINDOW MENU
6170           IF K$="S" THEN NUMBER=NUMBER+1
6180           IF K$="S" THEN WINDOW(NUMBER)=INT(2049+F*3.685)
6190           VTAB 22:HTAB 1
6200           PRINT "WINDOW(";NUMBER;") = ";WINDOW(NUMBER);
6210           IF K$="S" THEN GOTO 6280
6220           :
6230           HCOLOR=0
6240           HPLOT F,5 TO F,154
6250           HCOLOR=3
6260           HPLOT F,159-PEEK(2049+F*3.685)/1.6
6270           :
6280           IF NUMBER=4 THEN RETURN:REM ALL POSTIONS FOUND
6290      NEXT F
6300      RETURN

6500      REM INPUT RELEVANT DATA FOR KERR MEASUREMENTS
6510      :
6520      TEXT:HOME:HTAB 15:FLASH
6530      PRINT "TAKE READINGS":NORMAL
6540      VTAB 9:HTAB 3
```

```
6550      INPUT "CELL TEMPERATURE:";TMP
6560      VTAB 13:HTAB 3
6570      INPUT "NUMBER OF READINGS TO AVERAGE:";AVERAGE
6580      RETURN

6600      REM INITIALISE VARIABLE VALUES
6610      :
6620      COUNT(3)=0:V2=0:V1=0:ALPHA=0
6630      COUNT(2)=0:AVERAGE=1:SUGGEST=2
6640      RETURN

6700      REM INPUT VOLTAGE VALUE
6710      :
6720      COUNT(2)=0
6730      IF V1<>0 THEN C=COUNT(3)/V1^2
6740      HOME:FLASH:VTAB 2:HTAB 5
6750      PRINT "ENTER '0' TO END THIS SESSION"
6760      NORMAL:VTAB 9:HTAB 3
6770      INPUT "HT VOLTAGE SETTING = ";V1
6780      C1=C*V1^2
6790      SUGGEST=INT((C1-COUNT(3))/20 +0.5)
6800      IF SUGGEST<1 THEN SUGGEST=1
6810      RETURN

7000      REM END SESSION AND RETURN ANALYSER TO NULL POINT
7010      :
7020      IF COUNT(3)=0 THEN GOTO 250:REM RESTART PROGRAM
7030      HOME:FLASH:VTAB 9:HTAB 3
7040      PRINT "PLEASE REVERSE"
7050      PRINT "THE DIRECTION OF THE STEPPER MOTOR"
7060      NORMAL:VTAB 11:HTAB 3
7070      INPUT "PRESS 'RETURN' WHEN READY:";K$
7075      HOME
7080      FOR F=1 TO COUNT(3)+30
7090           POKE 49361,8
7100           FOR G=1 TO 100:NEXT
7110           POKE 49361,0
7120           FOR G=1 TO 100:NEXT
7130      NEXT F
```

```
7140    HOME:FLASH:VTAB 11:HTAB 13
7150    PRINT "PLEASE REVERSE"
7160    PRINT "THE DIRECTION OF THE STEPPER MOTOR"
7170    NORMAL:VTAB 15:HTAB 3
7180    INPUT "PRESS 'RETURN' WHEN READY:";K$
7190    HOME
7200    FOR F=1 TO 30
7210         POKE 49361,8
7220         FOR G=1 TO 100:NEXT
7230         POKE 49361,0
7240         FOR G=1 TO 100:NEXT
7250    NEXT F
7260    HOME:FLASH:VTAB 9:HTAB 3
7270    PRINT "ANALYSER RETURNED TO NULL POINT"
7280    VTAB 11:HTAB 4
7290    PRINT "RESET THE MECHANICAL COUNTER"
7300    HOME:VTAB 15:HTAB 10
7310    INPUT "PRESS 'RETURN TO CONTINUE:";K$
7320    RETURN

7500    REM CHECK PULSE IS WITHIN WINDOW LIMITS
7510    :
7520    REM TRANSFER PULSE TO COMPUTER
7530    POKE 49361,8
7540    FOR F=1 TO 100:NEXT
7550    POKE 49361,0
7560    FOR F=1 TO 100:NEXT
7570    POKE 49361,4
7580    FOR F=1 TO 100:NEXT
7590    POKE 49361,0
7600    POKE 7800,12
7610    POKE 7802,0
7620    CALL 7000:REM CALL MACHINE CODE PROGRAM
7630    POKE 50433,8
7640    :
7650    REM CHECK PULSE LIMITS
7660    FLAG=0
7670    IF PEEK(7805)<>0 THEN FLAG=1
7680    IF FLAG<>1 THEN GOTO 7780
```

```
7690    HOME:FLASH:VTAB 7:HTAB 3
7700    PRINT "PULSE EXCEEDS SCALE LIMITS-PLEASE ADJUST THE"
7710    VTAB 9:HTAB 3
7720    PRINT "TRANSIENT RECORDER SCALE OR LOWER THE VOLTAGE"
7730    VTAB 11:HTAB 9
7740    PRINT "TO THE PHOTO-MULTIPLIER"
7750    VTAB 15:HTAB 6
7760    INPUT "PRESS 'RETURN' WHEN READY:";K$
7770    GOTO 7500:REM GET A NEW PULSE
7780    RETURN

8000    REM GET COUNTER INCREMENT (JUMP)
8010    :
8020    ER=0:HOME:NORMAL:VTAB 9:HTAB 5
8030    IF COUNT(3)=0 THEN SUGGEST=1
8040    JUMP=SUGGEST:REM DEFAULT VALUE
8050    PRINT "COUNTER INCREMENT <";SUGGEST;">";
8060    INPUT CI$
8070    IF CI$="" THEN GOTO 8100
8080    JUMP=VAL(CI$)
8090    :
8100    REM INPUT VARIABLE VALUES
8110    :
8120    HOME:INVERSE:VTAB 1:HTAB 3
8130    PRINT "PRESS 'ENTER' TO ACCEPT DEFAULT VALUES"
8140    PRINT "CHANGE VOLT<VS=0>,AVERAGE<RA=RETURN>"
8150    NORMAL:VTAB 6:HTAB 10
8160    PRINT "VOLTAGE SETTING <";V1;">"
8170    VTAB 8:HTAB 10
8180    PRINT "ROTATION NUMBER <";INT(ALPHA/0.0045+0.05);">"
8190    VTAB 12:HTAB 10
8200    PRINT "AVERAGING NUMBER <";AVERAGE;">"
8210    VTAB 16:HTAB 10
8220    PRINT "TAKE READING: <Y>";
8230    :
8240    VTAB 10:HTAB 33
8250    INPUT K$
8260    IF K$="" THEN GOTO 8310
8270    COUNT(3)=VAL(K$)
```

```
8280    ALPHA=0.0045*VAL(K$)
8290    VTAB 10:HTAB 10
8300    PRINT "ROTATION NUMBER <";INT(ALPHA/0.0045+0.05);">";
8310    VTAB 12:HTAB 33
8320    INPUT K$
8330    IF K$="" THEN GOTO 8370
8340    AVERAGE=VAL(K$)
8350    VTAB 12:HTAB 10
8360    PRINT "AVERAGE NUMBER <";AVERAGE;">";
8370    VTAB 16:HTAB 33
8380    INPUT K$
8390    IF K$="N" THEN V2=0
8400    IF K$="N" THEN RETURN: REM GOTO VOLTAGE CHANGE MENU
8410    :
8420    VTAB 18:HTAB 7:FLASH
8430    PRINT "COLLECTING DATA FROM RECORDER"
8440    VTAB 20:HTAB 16
8450    PRINT "PLEASE WAIT":NORMAL
8460    :
8470    REM MOVE ANALYSER POSTION
8480    :
8490    FOR F=1 TO JUMP
8500         POKE 49361,8
8510         FOR G=1 TO 100:NEXT
8520         POKE 49361,0
8530         FOR G=1 TO 100:NEXT
8540    NEXT F
8550    COUNT(3)=COUNT(3)+JUMP
8560    ALPHA=0.0045*COUNT(3)
8570    RETURN

8600    REM TRANSFER PULSE AND AVERAGE IF NESCESSARY
8610    :
8620    NUMBER=0:REM LOCAL VARIABLE
8630    FOR F=1 TO AVERAGE
8640         POKE 49361,16
8650         FOR G=1 TO 100:NEXT
8660         POKE 49361,0
8670         POKE 49361,4
```

```
8680          FOR G=1 TO 100:NEXT
8690          POKE 49361,0
8700          FOR G=1 TO 100:NEXT
8710          POKE 7800,12
8720          POKE 7802,0
8730          CALL 7000
8740          POKE 50433,8
8750          IF PEEK(7805)=0 THEN GOTO 8670: REM PULSE OK
8760          NUMBER=NUMBER+1
8770          IF NUMBER<5 THEN GOTO 8630
8780          FLASH:VTAB 23:HTAB 1
8790          PRINT "PULSE HAS EXCEEDED WINDOW LIMITS FOR 5TH TIME-"
8800          PRINT "PLEASE ADJUST SCALE-PRESS 'RETURN' WHEN READY:";
8810          INPUT TEST$
8820          NORMAL:VTAB 23:HTAB 1
8830          PRINT "                                                  "
8840          PRINT "                                                  "
8650          GOTO 8630
8660          :
8670          IF AVERAGE=1 THEN RETURN
8680          FOR G=0 TO 1025
8690             PULSE(G)=PULSE(G)+PEEK(G+2049)
8700          NEXT G
8710     NEXT F
8720     :
8730     FOR F=0 TO 1025
8740          PULSE(F)=PULSE(F)/AVERAGE
8750     NEXT F
8760     RETURN

9000     REM ANALYSE DATA
9010     :
9020     A=0:B=0:C=0:D=0:E=0:F=0:H=0:I=0
9030     IF V1>0 THEN COUNT(2)=COUNT(2)-1
9040     :
9050     FOR G=1 TO COUNT(2)
9060          A=R3(G)*R1(G)*R1(G)+A
9070          C=R3(G)*R1(G)*R2(G)+C
9080          D=R3(G)*R1(G)+D
```

```
9090          E=R3(G)+E
9100          F=R3(G)*R2(G)+F
9110      NEXT G
9120      :
9130      AG=(E*C-D*F)/(E*A-D^2)
9140      B=(F*A-D*C)/(E*A-D^2)
9150      :
9160      FOR G=1 TO COUNT(2)
9170          H=R2(G)-(AG*R1(G)+B)
9180          I=I+R3(G)*H*H
9190      NEXT G
9200      :
9210      AE=((E*I)/((COUNT(2)-2)*(E*A-D^2)))^.5
9220      IF V1=0 THEN GOTO 9320
9230      BE = ((A*I)/(COUNT(2)-2)*(E*A-D^2)))^.5
9240      B=ATN(B/SQR(-B*B+1)
9250      BH=ATN((B+BE)/SQR(-1*(B+BE)^2+1))
9260      BL=ATN((B-BE)/SQR(-1*(B-BE)^2+1))
9270      BE=(ABS(BH-B)+ABS(B-BL))/2
9280      B=(180*B)/(2*0.0045*3.141592654)
9290      BE=(180*BE)/(2*0.0045*3.141592654)
9300      R5(COUNT(1))=B
9310      R6(COUNT(1))=BE
9320      RETURN

9500      REM CHECK TO SEE IF PULSE HAS BEEN INVERTED
9510      :
9520      A=0:B=0:C=0:REM LOCAL VARIABLES
9530      FOR F=WINDOW(1) TO WINDOW(2)
9540          A=A+PEEK(F)
9550      NEXT
9560      FOR F=WINDOW(3) TO WINDOW(4)
9570          B=B+PEEK(F)
9580      NEXT
9590      A=A/(WINDOW(2)-WINDOW(1))
9600      B=B/(WINDOW(4)-WINDOW(3))
9610      AE=0:BE=0
9620      FOR F=WINDOW(1) TO WINDOW(2)
9630          AE=AE+(PEEK(F)-A)^2
```

```
9640      NEXT
9650      AE=(AE/((WINDOW(2)-WINDOW(1))-2))^0.5
9660      FOR F=WINDOW(3) TO WINDOW(4)
9670           BE=BE+(PEEK(F)-B)^2
9680      NEXT
9690      BE=(BE/((WINDOW(4)-WINDOW(3))-2))^0.5
9700      R1(COUNT(2))=(B-A)
9710      R2(COUNT(2))=SIN((2*3.141592654*ALPHA/180)
9720      R3(COUNT(2))=AE+BE
9730      R4(COUNT(1))=V1
9740      IF A>B THEN TEST=1
9750      COUNT(2)=COUNT(2)+1
9760      IF COUNT(2)<3 THEN TEST=0
9770      IF COUNT(2)=30 THEN TEST=1
9780      RETURN

10000     REM CALCULATE GRADIENT
10010     :
10020     FOR F=1 TO COUNT(1)
10030          R1(F)=R4(F)^2
10040          R2(F)=R5(F)
10050          R3(F)=R6(F)
10060     NEXT
10070     COUNT(2)=COUNT(1)
10080     GOSUB 9000:REM ANALYSE DATA
10090     HOME:VTAB 12:HTAB 4
10100     INPUT "RESULTS TO S-SCREEN,P-PRINTER : ";K$
10110     IF K$<>"P" THEN GOTO 10130
10120     PRINT CHR$(4);"PR#1"
10130     HOME
10140     PRINT "VOLTAGE","NULL","ERROR"
10150     PRINT
10160     FOR F=1 TO COUNT(1)
10170          PRINT R4(F),INT(100*R5(F))/100,INT(100*R6(F))/100
10180     NEXT
10190     PRINT:PRINT
10200     AG=INT(AG*1000)/1000
10210     AE=INT(AE*1000)/1000
10220     PRINT "GRADIENT = ";AG
```

```
10230     PRINT "ERROR     = ";AE
10240     PRINT "TEMPERATURE = ";TMP
10250     :
10260     PRINT CHR$(4);"PR#0"
10270     PRINT:PRINT
10280     INPUT "PRESS 'RETURN' TO CONTINUE : ";K$
10290     RETURN
```

E3.3 MACHINE CODE PROGRAM

E3.3.1 Introduction

In order to speed up the transmission rate from the transient recorder to the Apple IIe computer a short machine code was written. This program transfers the optical data pulse captured by the transient recorder directly into the Apple memory by using the Xcalibur Via board. The program is activated from the previous basic program by the "CALL" statement.

E3.3.2 Machine code program listing

```
1B58 - A9 01     LDA  #$01    REM -  INITIALISE CONDITIONS FOR THE
1B5A             STA  #CODO   REM -  XCALIBUR VIA BOARD
1B5D             LDA  #$00    REM
1B5F             STA  $C502   REM
1B62             STA  $1E7D   REM
1B65             LDA  #$03    REM
1B67             STA  $C0D2   REM
1B6A             LDA  #$FD    REM
1B6C             STA  $C503   REM
1B6F             LDA  #$00    REM
1B71             STA  $C501   REM
1B74             STA  $C0D0   REM
1B77             STA  $A0     REM
1B79             LDA  #$08    REM
```

```
1B7B            STA  $A1     REM
1B7D            LDX  #$00    REM - CLEAR X COUNTER
1B7F            LDY  #$00    REM - CLEAR Y COUNTER
1B81            LDA  #$02
1B83            STA  $CODO   REM - SET REQUEST DATA HIGH
1B86            LDA  $1E78   REM - DELAY SUBROUTINE
1B89            JSR  $1E78   REM - DELAY ROUTINE
1B8C            LDA  #$00
1B8E            STA  $CODO   REM - SET REQUEST DATA LOW
1B91            LDA  $1E78
1B94            JSR  $FCA8
1B97            LDA  $C501
1B9A            CMP  #$00    REM - CHECK TRANSIENT STATUS
1B9C            BEQ  $1BCC   REM - BRANCH IF EQUAL
1B9E            CMP  #$06    REM - CHECK TRANSIENT STATUS
1BA0            BNE  $1BB1   REM - BRANCH IF NOT EQUAL
1BA2            LDA  $1E7A
1BA5            CMP  #$FF
1BA7            BNE  $1BAC
1BA9            JMP  $0303
1BAC            LDA  $C500
1BAF            STA  ($A0),Y
1BB1            JSR  $1BCE
1BB4            INY
1BB5            CPY  #$CD
1BB7            BNE  $1B81
1BB9            CLD          REM - INCREASE MEMORY LOCATION 1
1BBA            CLC
1BBB            LDA  $A0
1BBD            ADC  #$CD
1BBF            STA  $A0
1BC1            LDA  $A1
1BC3            ADC  #$00
1BC5            STA  $A1
1BC7            INX
1BC8            CPX  #$05
1BCA            BNE  $1B7F
1BCC            RTS
1BCD            RTS
1BCE            CMP  #$00
1BD0            BNE  $1BDA
1BD2            LDA  #$FF
1BD4            STA  $1E7D
1BD7            LDA  $C500
1BDA            CMP  #$FF
1BDC            BNE  $1BE6
1BDE            LDA  #$FF
1BE0            STA  $1E7D
1BE3            LDA  $C500
1BE6            RTS
1BE7            RTS
1BE8            LDA  $C500
1BEB            CLC
1BEC            CLD
1BED            TXA
1BEE            STA  $1C3F
1BF1            LDA  ($A0),Y
1BF3            STA  $1C35
1BF6            LDA  $00
```

```
1BF8            STA  $1C38
1BFB            LDA  #$02
1BFD            STA  $1C3C
1C00            LDA  $1C38
1C03            LDX  #$08
1C05            SEC
1C06            SBC  $1C3C
1C09            PHP
1C0A            ROL  $1C3B
1C0D            ASL  $1C35
1C10            ROL
1C11            PLP
1C12            BCC  $1C1A
1C14            SBS  $1C3C
1C17            JMP  $1C1D
1C1A            ADC  $1C3C
1C1D            DEX
1C1E            BNE  $1C11
1C20            BCS  $1C26
1C22            ADC  $1C3C
1C25            CLC
1C26            ROL $1C3B
1C29            STA  ($A0),Y
1C2B            LDX  $1C3F
1C2E            JMP  $1BB4
1C32            ASL  $B14C,X
1C35            TAX
1C37            BRK
```

APPENDIX F

KERR CONSTANT RESULTS

F1.1 INTRODUCTION

This appendix contains all of the Kerr constant data for the compounds and solutions used throughout this thesis. The Kerr constant was measured according to the method outlined in Chapter 3. The molar Kerr constant of 1,4-dioxane is also presented. The error in the Kerr constant measurments is approximately ±1%. The concentration of the solutions are all weight per volume (i.e. a 5% solution refers to 2.5g of solute made up to $50cm^3$ with the solvent).

F1.1.1 Tables of Kerr constant results

Table F1 Kerr constants for solutions of 2-methyl-4-nitroaniline in 1,4-dioxane.

Temp. °C	Kerr Const. $10^{16}B$ (5%)	Kerr Const. $10^{16}B$ (4%)	Kerr Const. $10^{16}B$ (3%)	Kerr Const. $10^{16}B$ (2%)	Kerr Const. $10^{16}B$ (1%)
15	1690	1411	1039	696	333
20	1620	1294	987	659	317
25	1545	1229	943	629	304
30	1464	1166	903	601	290
35	1397	1116	857	576	278
40	1324	1069	816	550	263
45	1244	1015	780	526	254
50	1179	964	746	504	243
55	1120	928	709	488	232
60	1067	885	679	465	223
65	1005	833	641	463	215
70	954	793	614	440	206

Temp. = Temperature, Const. = Constant

Table F2 Kerr constants for solutions of p-nitroaniline in 1,4-dioxane.

Temp. °C	Kerr Const. $10^{16}B$ (5%)	Kerr Const. $10^{16}B$ (4%)	Kerr Const. $10^{16}B$ (3%)	Kerr Const. $10^{16}B$ (2%)	Kerr Const. $10^{16}B$ (1%)
15	1628	1300	897	605	303
20	1561	1221	824	572	293
25	1472	1124	783	545	275
30	1368	1066	749	489	268
35	1282	1016	706	485	254
40	1201	954	677	479	244
45	1150	909	639	449	228
50	1102	824	609	399	217
55	1033	799	574	387	200
60	985	748	545	372	195
65	942	692	514	357	187
70	860	655	493	348	176

Temp. = Temperature, Const. = Constant

Table F3 Kerr constants for solutions of nitrobenzene in 1,4-dioxane.

Temp. °C	Kerr Const. $10^{16}B$ (5%)	Kerr Const. $10^{16}B$ (4%)	Kerr Const. $10^{16}B$ (3%)	Kerr Const. $10^{16}B$ (2%)	Kerr Const. $10^{16}B$ (1%)
15	245	191	140	104	58
20	236	175	134	97	52
25	204	181	129	94	51
30	201	161	122	89	49
35	202	155	117	86	47
40	183	150	112	82	45
45	174	144	108	79	43
50	171	139	104	76	42
55	166	133	100	73	40
60	161	128	96	70	39
65	154	123	93	68	38
70	147	119	90	63	36

Temp. = Temperature, Const. = Constant

Table F4 Kerr constants for solutions of aniline in 1,4-dioxane.

Temp. °C	Kerr Const. $10^{16}B$ (5%)	Kerr Const. $10^{16}B$ (4%)	Kerr Const. $10^{16}B$ (3%)	Kerr Const. $10^{16}B$ (2%)	Kerr Const. $10^{16}B$ (1%)
15	29.6	25.6	19.6	16.3	12.3
20	26.1	23.7	18.1	12.8	11.4
25	26.2	22.0	17.7	14.0	10.5
30	25.6	20.3	17.2	13.6	10.1
35	24.6	20.9	16.5	13.1	9.9
40	23.7	20.5	16.4	13.1	10.0
45	22.5	19.8	15.7	12.9	9.5
50	21.9	19.5	15.2	12.9	9.5
55	21.1	18.6	14.8	11.7	8.5
60	20.7	18.4	14.4	11.8	9.2
65	19.5	17.6	13.6	11.2	8.3
70	19.2	16.7	13.2	10.8	7.9

Temp. = Temperature, Const. = Constant

Table F5 Kerr constants for HPLC grade toluene, 1,4-dioxane, and the molar Kerr constants for 1,4-dioxane.

Temp. °C	Kerr Const. $10^{16}B$ Toluene	Kerr Const. $10^{16}B$ Toluene◊	Kerr Const. $10^{16}B$ 1,4-dioxane	Kerr Const. $10^{16}B$ Best Fit* 1,4-dioxane	Molar Kerr Const. $10^{27}{}_{m}K$ 1,4-dioxane
15	79.0	-	6.73	6.64	1.04
20	79.8	-	6.49	6.58	1.05
25	81.7	78.7	6.40	6.53	1.05
30	78.3	78.1	6.52	6.47	1.05
35	77.9	76.9	6.53	6.42	1.06
40	74.1	76.3	6.37	6.37	1.06
45	73.6	73.3	6.28	6.33	1.07
50	73.2	72.8	6.36	6.28	1.07
55	70.6	69.0	6.09	6.23	1.08
60	71.0	68.2	6.15	6.19	1.08
65	69.3	67.4	6.09	6.15	1.09
70	65.9	-	6.04	6.11	1.09

Temp. = Temperature, Const. = Constant

◊ = Repeated set of measurements

* = Kerr constant for 1,4-dioxane fitted to a line according to $y = a + b/T$

APPENDIX G

DENSITY MEASUREMENT RESULTS

G1.1 INTRODUCTION

This appendix contains all of the density data for the compounds and solutions used throughout this thesis. The error in the density measurements is less than ±1%. The concentration of the solutions are all weight per volume (i.e. a 5% solution refers to 2.5g of solute made up to $50cm^3$ with the solvent).

G1.1.1 Tables of density measurements

Table G1 Densities for solutions of 2-methyl-4-nitroaniline in 1,4-dioxane.

Temp. °C ±0.05	Density kgm^{-3} 5% Soln.	Density kgm^{-3} 4% Soln.	Density kgm^{-3} 3% Soln.	Density kgm^{-3} 2% Soln.	Density kgm^{-3} 1% Soln.
20	1044.(79)	1042.(58)	1041.(20)	1038.(91)	1036.(76)
25	1039.(47)	1037.(28)	1035.(27)	1032.(99)	1031.(18)
30	1033.(77)	1031.(58)	1029.(75)	1027.(48)	1025.(44)
35	1027.(67)	1025.(46)	1023.(72)	1021.(46)	1019.(35)
40	1022.(01)	1019.(81)	1018.(01)	1015.(77)	1013.(66)
45	1016.(09)	1014.(05)	1011.(89)	1009.(78)	1007.(81)
50	1011.(03)	1008.(91)	1006.(15)	1003.(96)	1002.(35)
55	1005.(16)	1003.(06)	1000.(32)	998.(17)	996.(35)
60	1000.(08)	998.(02)	994.(77)	992.(68)	991.(10)
65	994.(21)	992.(02)	988.(79)	986.(57)	985.(11)

Temp. = Temperature

Table G2 Densities for solutions of p-nitroaniline in 1,4-dioxane.

Temp. °C ±0.05	Density kgm^{-3} 5% Soln.	Density kgm^{-3} 4% Soln.	Density kgm^{-3} 3% Soln.	Density kgm^{-3} 2% Soln.	Density kgm^{-3} 1% Soln.
20	1045.(89)	1043.(05)	1040.(71)	1038.(36)	1036.(73)
25	1040.(56)	1037.(76)	1035.(36)	1032.(97)	1031.(41)
30	1034.(98)	1032.(18)	1029.(75)	1027.(32)	1025.(84)
35	1029.(40)	1026.(62)	1024.(15)	1021.(68)	1019.(30)
40	1023.(89)	1021.(14)	1018.(64)	1016.(13)	1013.(07)
45	1018.(41)	1015.(83)	1013.(31)	1010.(62)	1007.(66)
50	1012.(98)	1010.(32)	1007.(77)	1005.(11)	1002.(09)
55	1007.(55)	1004.(99)	1002.(46)	999.(71)	996.(72)
60	1002.(07)	999.(56)	996.(88)	994.(11)	991.(17)
65	996.(74)	994.(06)	991.(35)	988.(66)	985.(53)

Temp. = Temperature

Table G3 Densities for solutions of nitrobenzene in 1,4-dioxane.

Temp. °C ±0.05	Density kgm^{-3} 5% Soln.	Density kgm^{-3} 4% Soln.	Density kgm^{-3} 3% Soln.	Density kgm^{-3} 2% Soln.	Density kgm^{-3} 1% Soln.
20	1042.(18)	1040.(56)	1039.(39)	1037.(50)	1036.(22)
25	1036.(72)	1035.(14)	1033.(92)	1032.(08)	1030.(77)
30	1031.(07)	1029.(50)	1028.(24)	1026.(41)	1025.(07)
35	1025.(42)	1023.(85)	1022.(56)	1020.(73)	1019.(35)
40	1019.(85)	1018.(28)	1016.(92)	1015.(13)	1013.(72)
45	1014.(26)	1012.(90)	1011.(34)	1009.(74)	1008.(11)
50	1008.(75)	1007.(30)	1005.(79)	1004.(08)	1002.(55)
55	1003.(22)	1001.(85)	1000.(21)	998.(68)	997.(06)
60	997.(66)	996.(30)	994.(62)	993.(08)	991.(42)
65	992.(14)	990.(74)	989.(16)	987.(51)	985.(95)

Temp. = Temperature

Table G4 Densities for solutions of aniline in 1,4-dioxane.

Temp. °C ±0.05	Density kgm^{-3} 5% Soln.	Density kgm^{-3} 4% Soln.	Density kgm^{-3} 3% Soln.	Density kgm^{-3} 2% Soln.	Density kgm^{-3} 1% Soln.
20	1034.(99)	1034.(94)	1034.(90)	1034.(82)	1034.(71)
25	1029.(65)	1029.(54)	1029.(48)	1029.(40)	1029.(25)
30	1024.(04)	1023.(97)	1023.(89)	1023.(81)	1023.(63)
35	1018.(30)	1018.(17)	1018.(06)	1017.(99)	1017.(77)
40	1012.(83)	1012.(73)	1012.(57)	1012.(52)	1012.(24)
45	1007.(08)	1007.(23)	1006.(87)	1007.(00)	1006.(50)
50	1001.(89)	1001.(77)	1001.(48)	1001.(52)	1001.(07)
55	996.(16)	996.(22)	995.(85)	995.(94)	995.(41)
60	990.(94)	990.(86)	990.(48)	990.(56)	990.(01)
65	985.(39)	985.(15)	984.(91)	984.(83)	984.(40)

Temp. = Temperature

Table G5 Densities of 1,4-dioxane and toluene.

Temp. °C ±0.05	Density kgm^{-3} 1,4-Dioxane	Density kgm^{-3} Toluene
20	1034.(76)	867.(63)
25	1029.(12)	862.(96)
30	1023.(30)	858.(18)
35	1017.(26)	853.(11)
40	1011.(54)	848.(34)
45	1005.(61)	843.(25)
50	1000.(00)	838.(84)
55	994.(15)	833.(76)
60	988.(56)	829.(35)
65	982.(77)	824.(49)

Temp. = Temperature

APPENDIX H

DETERMINATION OF THE DIELECTRIC CONSTANT

If the stray capacitance of the dielectric cell, ΔC, remains constant upon filling the empty cell then the capacitance of the dielectric cell, when empty (C_a), when filled with the standard liquid (C_s), and when filled with the test liquid (C_t) can be expressed by equations H1, H2, and H3.

$$C_a = \varepsilon_o \frac{A}{d} + \Delta C \qquad \text{H1}$$

$$C_s = \varepsilon_o \varepsilon_s \frac{A}{d} + \Delta C \qquad \text{H2}$$

$$C_t = \varepsilon_o \varepsilon \frac{A}{d} + \Delta C \qquad \text{H3}$$

where ε_o is the permittivity of free space, ε_s is the dielectric constant of the standard, ε is the dielectric constant of the test sample, A is the surface area of the cell electrodes, and d is the distance between the cell electrodes. The dielectric constant of the test sample can therefore be determined as follows:

Equation H2-H1

$$C_s - C_a = \varepsilon_o \frac{A}{d} (\varepsilon_s - 1) \qquad \text{H4}$$

Equation H3-H1

$$C_t - C_a = \varepsilon_o \frac{A}{d}(\varepsilon - 1) \qquad \text{H5}$$

Equation H5÷H4

$$\frac{C_t - C_a}{C_s - C_a} = \frac{\varepsilon - 1}{\varepsilon_s - 1} \qquad \text{H6}$$

Rearranging equation H6 then gives

$$\varepsilon = 1 + \frac{(C_t - C_a)}{(C_s - C_a)}(\varepsilon_s - 1) \qquad \text{H7}$$

APPENDIX I

DIELECTRIC RESULTS

I1.1 INTRODUCTION

This appendix contains all of the static dielectric data for the compounds and solutions used throughout this thesis. The error in the dielectric results is less than 1%. The concentration of the solutions are all weight per volume (i.e. a 5% solution refers to 2.5g of solute made up to $50cm^3$ with the solvent).

I1.1.1 Tables of static dielectric constant

Table I1 Dielectric constants for solutions of 2-methyl-4-nitroaniline in 1,4-dioxane.

Temp. °C ±0.05	ε Conc.5%	ε Conc.4%	ε Conc.3%	ε Conc.2%	ε Conc.1%
25	4.31(7)	3.75(7)	3.38(3)	2.96(8)	2.57(1)
30	4.25(6)	3.70(2)	3.33(9)	2.93(9)	2.55(1)
35	4.19(8)	3.65(5)	3.30(4)	2.90(8)	2.53(1)
40	4.14(2)	3.60(8)	3.26(5)	2.88(5)	2.51(5)
45	4.08(4)	3.56(1)	3.22(9)	2.85(3)	2.49(5)
50	4.03(2)	3.51(7)	3.19(4)	2.82(1)	2.47(9)
55	3.97(7)	3.46(9)	3.16(0)	2.78(8)	2.45(8)
60	3.92(2)	3.42(8)	3.12(4)	2.76(4)	2.44(1)
65	3.87(4)	3.38(4)	3.08(8)	2.73(9)	2.42(5)

Temp. = Temperature ε = Dielectric constant
Conc. = Concentration

Table I2 Dielectric constants for solutions of p-nitroaniline in 1,4-dioxane.

Temp. °C ±0.05	ε Conc.5%	ε Conc.4%	ε Conc.3%	ε Conc.2%	ε Conc.1%
25	4.34(4)	3.92(4)	3.42(3)	3.05(1)	2.66(9)
30	4.27(2)	3.86(8)	3.38(1)	3.01(9)	2.64(6)
35	4.20(8)	3.81(2)	3.33(9)	2.98(8)	2.62(7)
40	4.14(5)	3.76(1)	3.29(9)	2.96(0)	2.60(7)
45	4.08(5)	3.70(9)	3.26(1)	2.93(0)	2.58(7)
50	4.02(5)	3.66(1)	3.22(4)	2.90(1)	2.56(8)
55	3.96(6)	3.61(2)	3.18(5)	2.87(3)	2.54(7)
60	3.90(7)	3.56(3)	3.14(9)	2.84(5)	2.52(9)
65	3.85(1)	3.51(9)	3.11(3)	2.81(8)	2.51(0)

Temp. = Temperature ε = Dielectric constant
Conc. = Concentration

Table I3 Dielectric constants for solutions of nitrobenzene in 1,4-dioxane.

Temp. °C ±0.05	ε Conc.5%	ε Conc.4%	ε Conc.3%	ε Conc.2%	ε Conc.1%
25	3.07(2)	2.90(9)	2.74(3)	2.55(2)	2.41(0)
30	3.04(2)	2.88(1)	2.72(2)	2.54(1)	2.39(7)
35	3.01(4)	2.85(6)	2.70(1)	2.52(5)	2.38(2)
40	2.98(7)	2.83(3)	2.68(1)	2.50(8)	2.36(9)
45	2.95(9)	2.80(9)	2.66(1)	2.49(2)	2.35(6)
50	2.93(1)	2.78(5)	2.64(1)	2.47(6)	2.34(2)
55	2.90(6)	2.76(3)	2.62(1)	2.45(9)	2.32(9)
60	2.88(0)	2.73(9)	2.60(1)	2.44(3)	2.31(6)
65	2.85(5)	2.71(7)	2.58(2)	2.42(8)	2.30(3)

Temp. = Temperature ε = Dielectric constant
Conc. = Concentration

Table I4 Dielectric constants for solutions of aniline in 1,4-dioxane.

Temp. °C ±0.05	ε Conc.5%	ε Conc.4%	ε Conc.3%	ε Conc.2%	ε Conc.1%
25	2.44(0)	2.39(7)	2.35(2)	2.30(6)	2.26(9)
30	2.42(5)	2.38(3)	2.33(8)	2.29(5)	2.26(0)
35	2.41(2)	2.37(2)	2.32(7)	2.28(4)	2.24(8)
40	2.39(8)	2.35(9)	2.31(5)	2.27(4)	2.23(8)
45	2.38(4)	2.34(6)	2.30(3)	2.26(3)	2.22(6)
50	2.37(0)	2.33(3)	2.29(1)	2.25(1)	2.21(5)
55	2.35(5)	2.31(9)	2.27(8)	2.24(0)	2.20(4)
60	2.34(2)	2.30(5)	2.26(7)	2.22(9)	2.19(1)
65	2.32(8)	2.29(4)	2.25(5)	2.21(8)	2.18(0)

Temp. = Temperature ε = Dielectric constant
Conc. = Concentration

Table I5 Dielectric constants for pure HPLC grade 1,4-dioxane and toluene.

Temp. °C ±0.05	ε 1,4-Dioxane	ε Toluene
25	2.22(4)	2.38(9)
30	2.21(6)	2.37(8)
35	2.20(6)	2.36(6)
40	2.19(3)	2.35(4)
45	2.18(4)	2.34(1)
50	2.17(5)	2.32(9)
55	2.16(6)	2.31(6)
60	2.15(8)	2.30(4)
65	2.14(9)	2.29(3)

Temp. = Temperature
ε = Dielectric constant

APPENDIX J

REFRACTIVE INDEX RESULTS

J1.1 INTRODUCTION

This appendix contains all of the refractive index data for the compounds and solutions used throughout this thesis. The infinite wavelength refractive index was calculated using the Cauchy dispersion theory as outlined in chapter 5. The concentration of the solutions are all weight per volume (i.e. a 5% solution refers to 2.5g of solute made up to $50cm^3$ with the solvent).

J1.1.1 Tables of refractive index

Table J1 Refractive indices for 2-methyl-4-nitroaniline in 1,4-dioxane, 5%.

Conc. %	Temperature °C ±0.1°C	Refractive index at 589.3nm	Refractive index at 632.8nm	Refractive index at infinite λ
5	25	1.429(9)	1.427(4)	1.41(23)
	30	1.427(8)	1.425(8)	1.41(14)
	35	1.425(7)	1.423(6)	1.41(04)
	40	1.423(2)	1.421(7)	1.40(95)
	45	1.420(9)	1.419(1)	1.40(86)
	50	1.418(6)	1.417(3)	1.40(77)
	55	1.416(2)	1.415(2)	1.40(68)
	60	1.414(3)	1.412(8)	1.40(58)

Conc. = concentration

Table J2 Refractive indices for 2-methyl-4-nitroaniline in 1,4-dioxane, 4%.

Conc. %	Temperature °C ±0.1°C	Refractive index at 589.3nm	Refractive index at 632.8nm	Refractive index at infinite λ
4	25	1.427(7)	1.425(8)	1.40(99)
	30	1.425(5)	1.423(2)	1.40(89)
	35	1.423(6)	1.421(6)	1.40(78)
	40	1.421(3)	1.419(0)	1.40(68)
	45	1.419(2)	1.416(9)	1.40(58)
	50	1.416(5)	1.415(2)	1.40(47)
	55	1.414(1)	1.413(2)	1.40(37)
	60	1.411(9)	1.410(6)	1.40(26)

Conc. = concentration

Table J3 Refractive indices for 2-methyl-4-nitroaniline in 1,4-dioxane, 3%.

Conc. %	Temperature °C ±0.1°C	Refractive index at 589.3nm	Refractive index at 632.8nm	Refractive index at infinite λ
3	25	1.425(4)	1.423(2)	1.40(92)
	30	1.423(3)	1.421(0)	1.40(80)
	35	1.421(1)	1.418(9)	1.40(68)
	40	1.417(3)	1.416(7)	1.40(57)
	45	1.416(0)	1.414(5)	1.40(45)
	50	1.414(2)	1.412(7)	1.40(33)
	55	1.411(7)	1.410(4)	1.40(21)
	60	1.409(7)	1.408(3)	1.40(09)

Conc. = concentration

Table J4 Refractive indices for 2-methyl-4-nitroaniline in 1,4-dioxane, 2%.

Conc. %	Temperature °C ±0.1°C	Refractive index at 589.3nm	Refractive index at 632.8nm	Refractive index at infinite λ
2	25	1.423(6)	1.421(6)	1.40(77)
	30	1.421(3)	1.419(4)	1.40(63)
	35	1.419(2)	1.417(4)	1.40(49)
	40	1.416(9)	1.414(9)	1.40(35)
	45	1.414(5)	1.412(7)	1.40(21)
	50	1.412(3)	1.410(9)	1.40(07)
	55	1.409(5)	1.408(3)	1.39(93)
	60	1.407(8)	1.406(5)	1.39(79)

Conc. = concentration

Table J5 Refractive indices for 2-methyl-4-nitroaniline in 1,4-dioxane, 1%.

Conc. %	Temperature °C ±0.1°C	Refractive index at 589.3nm	Refractive index at 632.8nm	Refractive index at infinite λ
1	25	1.421(1)	1.419(1)	1.40(59)
	30	1.418(7)	1.416(8)	1.40(40)
	35	1.416(8)	1.414(7)	1.40(22)
	40	1.413(9)	1.412(1)	1.40(03)
	45	1.411(8)	1.410(0)	1.39(85)
	50	1.409(6)	1.407(8)	1.39(67)
	55	1.407(0)	1.405(6)	1.39(48)
	60	1.404(9)	1.403(2)	1.39(30)

Conc. = concentration

Table J6 Refractive indices for p-nitroaniline in 1,4-dioxane, 5%.

Conc. %	Temperature °C ±0.1°C	Refractive index at 589.3nm	Refractive index at 632.8nm	Refractive index at infinite λ
5	25	1.424(8)	1.422(7)	1.40(66)
	30	1.422(5)	1.420(4)	1.40(55)
	35	1.420(5)	1.418(3)	1.40(44)
	40	1.418(4)	1.416(0)	1.40(33)
	45	1.416(1)	1.414(1)	1.40(23)
	50	1.413(9)	1.411(5)	1.40(12)
	55	1.411(0)	1.409(7)	1.40(01)
	60	1.408(5)	1.407(9)	1.39(90)

Conc. = concentration

Table J7 Refractive indices for p-nitroaniline in 1,4-dioxane, 4%.

Conc. %	Temperature °C ±0.1°C	Refractive index at 589.3nm	Refractive index at 632.8nm	Refractive index at infinite λ
4	25	1.423(7)	1.421(7)	1.40(70)
	30	1.421(5)	1.419(3)	1.40(56)
	35	1.419(4)	1.417(3)	1.40(42)
	40	1.417(1)	1.415(2)	1.40(27)
	45	1.414(9)	1.413(0)	1.40(13)
	50	1.412(6)	1.410(5)	1.39(99)
	55	1.410(0)	1.408(6)	1.39(85)
	60	1.407(7)	1.406(5)	1.39(71)

Conc. = concentration

Table J8 Refractive indices for p-nitroaniline in 1,4-dioxane, 3%.

Conc. %	Temperature °C ±0.1°C	Refractive index at 589.3nm	Refractive index at 632.8nm	Refractive index at infinite λ
3	25	1.422(5)	1.420(6)	1.40(46)
	30	1.420(7)	1.418(1)	1.40(30)
	35	1.418(4)	1.416(0)	1.40(14)
	40	1.416(2)	1.413(8)	1.39(99)
	45	1.413(7)	1.411(9)	1.39(83)
	50	1.411(3)	1.409(2)	1.39(67)
	55	1.408(9)	1.407(4)	1.39(52)
	60	1.406(9)	1.405(1)	1.39(36)

Conc. = concentration

Table J9 Refractive indices for p-nitroaniline in 1,4-dioxane, 2%.

Conc. %	Temperature °C ±0.1°C	Refractive index at 589.3nm	Refractive index at 632.8nm	Refractive index at infinite λ
2	25	1.421(4)	1.419(5)	1.40(48)
	30	1.419(3)	1.417(0)	1.40(33)
	35	1.417(0)	1.415(0)	1.40(17)
	40	1.414(8)	1.412(8)	1.40(01)
	45	1.412(3)	1.410(4)	1.39(86)
	50	1.410(0)	1.408(2)	1.39(70)
	55	1.407(7)	1.406(0)	1.39(55)
	60	1.405(1)	1.403(9)	1.39(39)

Conc. = concentration

Table J10 Refractive indices for p-nitroaniline in 1,4-dioxane, 1%.

Conc. %	Temperature °C ±0.1°C	Refractive index at 589.3nm	Refractive index at 632.8nm	Refractive index at infinite λ
1	25	1.420(5)	1.418(6)	1.40(84)
	30	1.418(0)	1.416(3)	1.40(58)
	35	1.415(8)	1.413(9)	1.40(32)
	40	1.411(8)	1.411(5)	1.40(06)
	45	1.410(8)	1.409(1)	1.39(80)
	50	1.408(9)	1.406(9)	1.39(54)
	55	1.406(3)	1.404(5)	1.39(28)
	60	1.404(1)	1.402(0)	1.39(02)

Conc. = concentration

Table J11 Refractive indices for aniline in 1,4-dioxane, 5%.

Conc. %	Temperature °C ±0.1°C	Refractive index at 589.3nm	Refractive index at 632.8nm	Refractive index at infinite λ
5	25	1.427(5)	1.422(5)	1.38(76)
	30	1.425(4)	1.420(3)	1.38(55)
	35	1.423(1)	1.417(9)	1.38(34)
	40	1.421(1)	1.415(6)	1.38(13)
	45	1.418(6)	1.413(1)	1.37(91)
	50	1.416(3)	1.411(0)	1.37(70)
	55	1.413(9)	1.409(0)	1.37(49)
	60	1.411(4)	1.406(5)	1.37(28)

Conc. = concentration

Table J12 Refractive indices for aniline in 1,4-dioxane, 4%.

Conc. %	Temperature °C ±0.1°C	Refractive index at 589.3nm	Refractive index at 632.8nm	Refractive index at infinite λ
4	25	1.425(9)	1.420(8)	1.38(69)
	30	1.423(7)	1.418(6)	1.38(46)
	35	1.421(2)	1.416(1)	1.38(23)
	40	1.419(0)	1.414(1)	1.38(00)
	45	1.416(9)	1.411(6)	1.37(77)
	50	1.414(6)	1.409(2)	1.37(55)
	55	1.412(2)	1.407(1)	1.37(32)
	60	1.409(5)	1.404(6)	1.37(09)

Conc. = concentration

Table J13 Refractive indices for aniline in 1,4-dioxane, 3%.

Conc. %	Temperature °C ±0.1°C	Refractive index at 589.3nm	Refractive index at 632.8nm	Refractive index at infinite λ
3	25	1.424(4)	1.419(0)	1.38(41)
	30	1.422(1)	1.416(8)	1.38(21)
	35	1.419(5)	1.414(6)	1.38(00)
	40	1.417(4)	1.412(1)	1.37(80)
	45	1.415(1)	1.409(9)	1.37(59)
	50	1.412(9)	1.407(7)	1.37(39)
	55	1.410(3)	1.405(3)	1.37(19)
	60	1.408(0)	1.403(0)	1.36(98)

Conc. = concentration

Table J14 Refractive indices for aniline in 1,4-dioxane, 2%.

Conc. %	Temperature °C ±0.1°C	Refractive index at 589.3nm	Refractive index at 632.8nm	Refractive index at infinite λ
2	25	1.422(7)	1.417(5)	1.38(38)
	30	1.420(2)	1.415(2)	1.38(15)
	35	1.417(8)	1.412(8)	1.37(93)
	40	1.415(7)	1.410(6)	1.37(70)
	45	1.413(5)	1.408(3)	1.37(48)
	50	1.411(1)	1.405(9)	1.37(25)
	55	1.408(6)	1.403(6)	1.37(03)
	60	1.406(3)	1.401(4)	1.36(80)

Conc. = concentration

Table J15 Refractive indices for aniline in 1,4-dioxane, 1%.

Conc. %	Temperature °C ±0.1°C	Refractive index at 589.3nm	Refractive index at 632.8nm	Refractive index at infinite λ
1	25	1.420(8)	1.415(7)	1.38(21)
	30	1.418(6)	1.413(5)	1.37(97)
	35	1.416(1)	1.411(1)	1.37(73)
	40	1.413(7)	1.408(8)	1.37(49)
	45	1.411(9)	1.406(4)	1.37(25)
	50	1.409(4)	1.404(0)	1.37(01)
	55	1.406(9)	1.401(7)	1.36(77)
	60	1.404(9)	1.399(9)	1.36(54)

Conc. = concentration

Table J16 Refractive indices for nitrobenzene in 1,4-dioxane, 5%.

Conc. %	Temperature °C ±0.1°C	Refractive index at 589.3nm	Refractive index at 632.8nm	Refractive index at infinite λ
5	25	1.424(8)	1.422(7)	1.40(66)
	30	1.422(5)	1.420(4)	1.40(55)
	35	1.420(5)	1.418(3)	1.40(44)
	40	1.418(4)	1.416(0)	1.40(33)
	45	1.416(1)	1.414(1)	1.40(23)
	50	1.413(9)	1.411(5)	1.40(12)
	55	1.411(0)	1.409(7)	1.40(01)
	60	1.408(5)	1.407(9)	1.39(90)

Conc. = concentration

Table J17 Refractive indices for nitrobenzene in 1,4-dioxane, 4%.

Conc. %	Temperature °C ±0.1°C	Refractive index at 589.3nm	Refractive index at 632.8nm	Refractive index at infinite λ
4	25	1.423(7)	1.421(7)	1.40(70)
	30	1.421(5)	1.419(3)	1.40(56)
	35	1.419(4)	1.417(3)	1.40(42)
	40	1.417(1)	1.415(2)	1.40(27)
	45	1.414(9)	1.413(0)	1.40(13)
	50	1.412(6)	1.410(5)	1.39(99)
	55	1.410(0)	1.408(6)	1.39(85)
	60	1.407(7)	1.406(5)	1.39(71)

Conc. = concentration

Table J18 Refractive indices for nitrobenzene in 1,4-dioxane, 3%.

Conc. %	Temperature °C ±0.1°C	Refractive index at 589.3nm	Refractive index at 632.8nm	Refractive index at infinite λ
3	25	1.422(5)	1.420(6)	1.40(46)
	30	1.420(7)	1.418(1)	1.40(30)
	35	1.418(4)	1.416(0)	1.40(14)
	40	1.416(2)	1.413(8)	1.39(99)
	45	1.413(7)	1.411(9)	1.39(83)
	50	1.411(3)	1.409(2)	1.39(67)
	55	1.408(9)	1.407(4)	1.39(52)
	60	1.406(9)	1.405(1)	1.39(36)

Conc. = concentration

Table J19 Refractive indices for nitrobenzene in 1,4-dioxane, 2%.

Conc. %	Temperature °C ±0.1°C	Refractive index at 589.3nm	Refractive index at 632.8nm	Refractive index at infinite λ
2	25	1.421(4)	1.419(5)	1.40(48)
	30	1.419(3)	1.417(0)	1.40(33)
	35	1.417(0)	1.415(0)	1.40(17)
	40	1.414(8)	1.412(8)	1.40(01)
	45	1.412(3)	1.410(4)	1.39(86)
	50	1.410(0)	1.408(2)	1.39(70)
	55	1.407(7)	1.406(0)	1.39(55)
	60	1.405(1)	1.403(9)	1.39(39)

Conc. = concentration

Table J20 Refractive indices for nitrobenzene in 1,4-dioxane, 1%.

Conc. %	Temperature °C ±0.1°C	Refractive index at 589.3nm	Refractive index at 632.8nm	Refractive index at infinite λ
2	25	1.420(5)	1.418(6)	1.40(84)
	30	1.418(0)	1.416(3)	1.40(58)
	35	1.415(8)	1.413(9)	1.40(32)
	40	1.411(8)	1.411(5)	1.40(06)
	45	1.410(8)	1.409(1)	1.39(80)
	50	1.408(9)	1.406(9)	1.39(54)
	55	1.406(3)	1.404(5)	1.39(28)
	60	1.404(1)	1.402(0)	1.39(02)

Conc. = concentration

Table J21 Refractive indices for 1,4-dioxane.

Temperature °C ±0.1°C	Refractive index at 589.3nm	Refractive index at 632.8nm	Refractive index at infinite λ
25	1.419(5)	1.414(2)	1.37(86)
30	1.417(1)	1.411(8)	1.37(70)
35	1.415(0)	1.409(7)	1.37(53)
40	1.412(4)	1.407(2)	1.37(37)
45	1.409(8)	1.405(0)	1.37(21)
50	1.407(7)	1.402(7)	1.37(04)
55	1.405(3)	1.400(5)	1.36(88)
60	1.403(1)	1.398(4)	1.36(72)

Table J22 Refractive indices for toluene.

Temperature °C ±0.1°C	Refractive index at 589.3nm	Refractive index at 632.8nm	Refractive index at infinite λ
25	1.493(4)	1.490(5)	1.47(10)
30	1.490(3)	1.488(1)	1.47(35)
35	1.487(7)	1.486(3)	1.47(67)
40	1.484(7)	1.483(4)	1.47(50)
45	1.482(1)	1.480(5)	1.47(04)
50	1.479(3)	1.477(6)	1.46(65)
55	1.476(2)	1.474(4)	1.46(31)
60	1.473(5)	1.472(1)	1.46(34)

APPENDIX K

RAYLEIGH DEPOLARISATION RESULTS

K1.1 INTRODUCTION

This appendix contains all of the Rayleigh depolarisation ratio data at 20°C for the compounds and solutions used throughout this thesis. All solutions were made using 1,4-dioxane as the solvent. Toluene and 1,4-dioxane were measured as the pure liquids. For more information see chapter 7. The concentration of the solutions are all weight per volume (i.e. a 5% solution refers to 2.5g of solute made up to 50cm^3 with the solvent).

K1.2 Tables of Rayleigh Depolarisation ratios

Table K1 Rayleigh depolarisation ratios

Compound	$\Delta_{12}-\Delta_1$ conc. 5%	$\Delta_{12}-\Delta_1$ conc. 4%	$\Delta_{12}-\Delta_1$ conc. 3%	$\Delta_{12}-\Delta_1$ conc. 2%	$\Delta_{12}-\Delta_1$ conc. 1%	Δ_1 Solvent
2-Methyl-4-nitroaniline	0.075(2)	0.064(4)	0.056(3)	0.039(9)	0.012(5)	0.064(5)
p-Nitro-aniline	0.052(4)	0.046(3)	0.034(9)	0.026(6)	0.016(6)	0.064(5)
Nitrobenzene	0.036(4)	0.035(4)	0.022(7)	0.017(1)	0.007(3)	0.064(5)
Aniline	0.012(0)	0.007(8)	0.009(0)	0.009(6)	0.003(4)	0.064(5)
Toluene	-	-	-	-	-	0.323(4)
1,4-Dioxane	-	-	-	-	-	0.064(5)

APPENDIX L

TABLES OF CONVERSION FACTORS AND SYMBOLS USED

Table L1.1 Symbols and meanings used in this thesis

Symbol	Meaning
μ	Dipole moment
α	Polarisability
M	Molecular weight
k	Boltzmann constant
${}_mK$	Molar Kerr constant
${}_sK$	Specific Kerr constant
β	First Hyperpolarisability
γ	Second Hyperpolarisability
δ	Anisotropy parameter
n	Refractive index
ε	Dielectric constant
P_E	Electronic polarisation
P_D	Dispersion polarisation
P_A	Atomic polarisation
P_μ	Orientation polarisation
d	Density
${}_\infty K_2$	Infinite dilution molar Kerr constant
${}_sK_2$	Specific Kerr constant
B	Kerr constant
${}_mK$	Molar Kerr constant
f	Molar fraction
w	Weight fraction
N	Avogadros' number
ε_o	Permittivity of free space

Table L1.2 Conversion table for e.s.u to SI units

SI	Conversion factor	Typical esu values
$\mu =$	$(3.3357 \times 10^{-30}) \times$ (debye)	
$\mu =$	$(3.3357 \times 10^{-12}) \times$ (esu)	10^{-18}
$\alpha =$	$(1.11265 \times 10^{-16}) \times$ (esu)	10^{-24}
d =	kgm^{-3}	gcm^{-3}
M =	Kilograms	grams
k =	$(1 \times 10^{-7}) \times$ (esu)	1.380622×10^{-16}
${}_mK$ =	$(1.11265 \times 10^{-15}) \times$ (esu)	10^{-12}
${}_sK$ =	$(1.11265 \times 10^{-12}) \times$ (esu)	
$\beta =$	$(0.3711 \times 10^{-20}) \times$ (esu)	
$\gamma =$	$(0.1238 \times 10^{-24}) \times$ (esu)	